1964-01

Installation and test of a rectilinear cascade

Rose, Charles C.; Guttormson, Darold L.

Monterey, California: U.S. Naval Postgraduate School

INSTALLATION AND TEST OF A RECTILINEAR CASCADE

CHARLES C. ROSE
DAROLD L. GUTTORMSON

INSTALLATION AND TEST
OF A
RECTILINEAR CASCADE

by

Charles C. Rose, Jr.

Lieutenant Commander, United States Navy

and

Darold L. Guttormson

Captain, United States Marine Corps

Submitted in partial fulfillment of
the requirements for the degree of

MASTER OF SCIENCE
IN
AERONAUTICAL ENGINEERING

United States Naval Postgraduate School
Monterey, California

1964

INSTALLATION AND TEST OF A RECTILINEAR CASCADE

by

Charles C. Rose, Jr.

and

Darold L. Guttormson

This work is accepted as fulfilling
the thesis requirements for the degree of
MASTER OF SCIENCE
IN
AERONAUTICAL ENGINEERING
from the
United States Naval Postgraduate School

ABSTRACT

The purpose of this thesis is to investigate the capabilities of the rectilinear cascade and its associated equipment as installed in the new Propulsion Laboratory of the U. S. Naval Postgraduate School, Monterey, California. The various parameters are developed from the momentum theorem and results are compared with NACA data. Computer programming is included to rapidly evaluate future test data obtained from various blade configurations. The purpose of these tests is to gain more precise knowledge of the physical nature of the flow through cascades and to establish design data for the accurate prediction of the performance of axial-flow turbomachines, turbines as well as pumps and compressors. These efforts, it is hoped, will result eventually in more efficient machines for many applications.

ACKNOWLEDGMENT

The writers wish to express their appreciation to Professor M. H. Vavra for his assistance in this investigation.

TABLE OF CONTENTS

Section	Title	Page
1.	Introduction	1
2.	Description of Cascade Rig	5
3.	Description of Measuring and Recording Equipment	18
4.	Static Pressure Distribution	31
5.	Evaluation of Test Data	39
6.	Discussion of Results	50
7.	General Discussion	60
8.	Conclusions	62
9.	Recommedations	63
10.	References	65
11.	Appendix A	66
12.	Appendix B	86

LIST OF ILLUSTRATIONS

Figure		Page
1.	The Rectilinear Cascade Rig.	3
2.	Cascade Laboratory of the Department of Aeronautics, U. S. Naval Postgraduate School.	4
3.	Schematic of Cascade Laboratory.	6
4.	Schematic of Sound Baffles.	8
5.	Angle Notation.	9
6.	View of Inlet Guide Vanes, Test Blades, & End Walls.	11
7.	Inlet Guide Vanes and Three Speed Motor.	14
8.	Cross Section of a Conventional Cascade Rig.	15
9.	Schematic of Circular Cascade Configuration.	17
10.	Static Taps on North Side Wall.	19
11.	Multi-tube Manometer Board.	20
12.	Pitot Tube Traverse Assembly.	22
13.	View of South Wall Showing Transducer and Power Leads.	23
14.	Automatic Data Logging Console.	24
15.	Right Side of Console.	27
16.	Left Side of Console.	28
17.	Friden Paper Tape Punch.	29
18.	Initial Static Pressure Survey, IGV's set at 45°.	33
19.	Static Pressure Survey, IGV's set at 40°.	35
20.	Static Pressure Survey, IGV's set at 42° and Fine Mesh Wire Screen at Exit of Bell Mouth.	36
21.	Static Pressure Survey, IGV's set at 42° Without Wire Screen.	38
22.	Final Static Pressure Survey.	40
23.	Dynamic Pressure Lower Traverse.	42

Figure Page

24. Dynamic Pressure Upper Traverse. 43

25. Vector Diagram 48

26. Static Pressure Variation. 57

27. Flow Angle Variation. 58

TABLE OF SYMBOLS

C_D	drag coefficient, dimensionless
C_L	lift coefficient, dimensionless
D	drag force, lb./ft.
$\vec{dR}$	force exerted by fluid on test blade, lb./ft.
J	conversion unit, ft.lb./B.T.U.
L	lift force, lb./ft.
M	Mach number, dimensionless
N	integer number of blade spacings, dimensionless
P	absolute total pressure, lb./ft.^{2}
R	gas constant, ft./^oR.
T	temperature, ^oR.
$\vec{V}$	velocity of fluid, ft./sec.
a	speed of sound, ft./sec.
c	chord of test blade, ft.
c_p	specific heat at constant pressure, B.T.U./lb.^oR.
c_v	specific heat at constant volume, B.T.U./lb.^oR.
dm_s	mass flow rate, lb.sec./ft.
g	gravitational constant, ft./sec.^{2}
h	test blade height, ft.
$\vec{i}$	unit vector in tangential direction, dimensionless
$\vec{j}$	unit vector in axial direction, dimensionless
$\vec{n}$	unit vector normal to control surface, dimensionless
o	blade opening or throat, ft.
p	absolute static pressure, lb./ft.^{2}
q	dynamic pressure, lb./ft.^{2}
s	blade spacing, ft.

$\vec{t}$ unit vector orthogonal to $\vec{n}$ in direction of shear stress, dimensionless

x distance in tangential direction, ft.

y distance along blade height, ft.

α gas flow angle, deg.

β angle between $\vec{i}$ and $\vec{V}$, deg.

γ ratio of specific heats, dimensionless

ζ loss coefficient, dimensionless

Θ (subscripted) angle between $\vec{j}$ and $\vec{V}$, deg.

Θ (non-subscripted) angle between $\vec{i}$ and $\vec{dR}$, deg.

ξ x/Ns distance in tangential direction/blade spacing, dimensionless

ρ density, lb.-sec. ^{2}/ft.^{4}

σ solidity of cascade, c/s, dimensionless

τ shear stress, lb./ft.^{2}

ϕ stagger angle, angle between chord line and axial direction, deg.

ψ velocity coefficient, dimensionless

Subscripts:

a axial direction

p plenum

s static conditions

t total

u tangential direction

0 station 0, far ahead of cascade

1 station 1, measuring plane ahead of cascade

2 station 2, measuring plane after cascade

3 station 3, far aft of cascade

∞ station ∞, vectorial mean of conditions at stations 0 & 3

1. Introduction

There are many steps in the design of axial-flow turbomachinery and these steps should be performed in a systematic, orderly manner in order to arrive at a method of design which is based on a proper understanding of the flow phenomena that occur in turbomachines. As a first analysis one is concerned with the two-dimensional flow of an ideal fluid; that is a fluid which is homogeneous, continuous, imcompressible, and nonviscous. There are presently several analytical methods of determining the solution of such conditions. When finite blade spacing is considered, these analytical solutions become extremely laborious except for trivial blade shapes, such as flat plates. Therefore with the assumption of an ideal fluid it becomes advantageous to use a more direct approach such as the electrical analogy method described by F. R. Fahland and L. L. Hawkins, Ref. 1.

The introduction of the compressibility and viscosity of the working fluid requires experimental methods of flow analysis since there do not exist analytical methods to evaluate these conditions. The first step in this direction is the use of a rectilinear cascade as described by J. R. Eshman, Ref. 2.

Eshman's investigation was conducted on a small working model of the present large cascade rig which is the subject of this thesis. As might be expected the results obtained from the model cascade were rather poor and limited in value.

The large rectilinear cascade rig is located in the Cascade Laboratory of the new Propulsion Laboratories of the Department of Aeronautics, U. S. Naval Postgraduate School, Monterey, California. The cascade rig, shown in Fig. 1, was designed by Professor M. H. Varva of the Department of Aeronautics, at the U. S. Naval Postgraduate School. An overall view of the Cascade Laboratory is shown in Fig. 2.

Construction of the new Propulsion Laboratories started in the summer of 1962. Fruin-Colnon of San Mateo, California was the general contractor for this construction. The Cascade Laboratory and the cascade rig were accepted in December, 1963. The cascade rig was built by Kenney Engineering Corporation of Pasadena, California. The intrumentation was by General Electric of Ontario, California and Coleman Electronic Systems of Santa Ana, California. These companies were subcontractors to Fruin-Colnon.

The purpose of this cascade test rig is to determine the performance of various blade shapes under conditions of different solidities, inlet angles and incidence angles. This rig makes it possible to undertake systematic tests of cascades for various applications with the aim to evaluate and improve different blade shapes which will lead to the design of improved turbines, compressors, and pumps.

The purpose of this thesis was to investigate whether the cascade rig would perform its designed function. This was accomplished by determining flow deflection and the lift and drag coefficients of a known blade shape and comparing

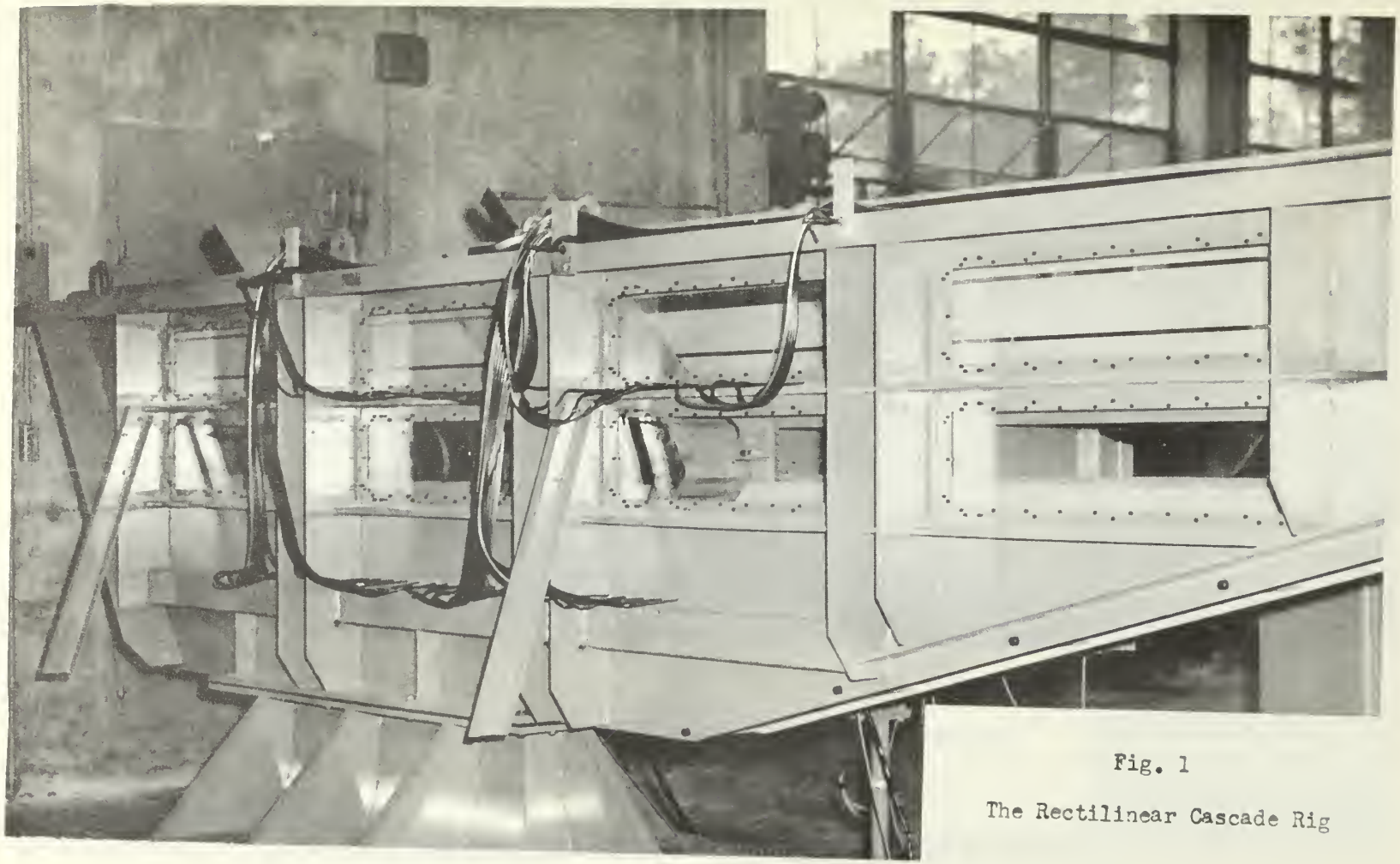

Fig. 1

The Rectilinear Cascade Rig

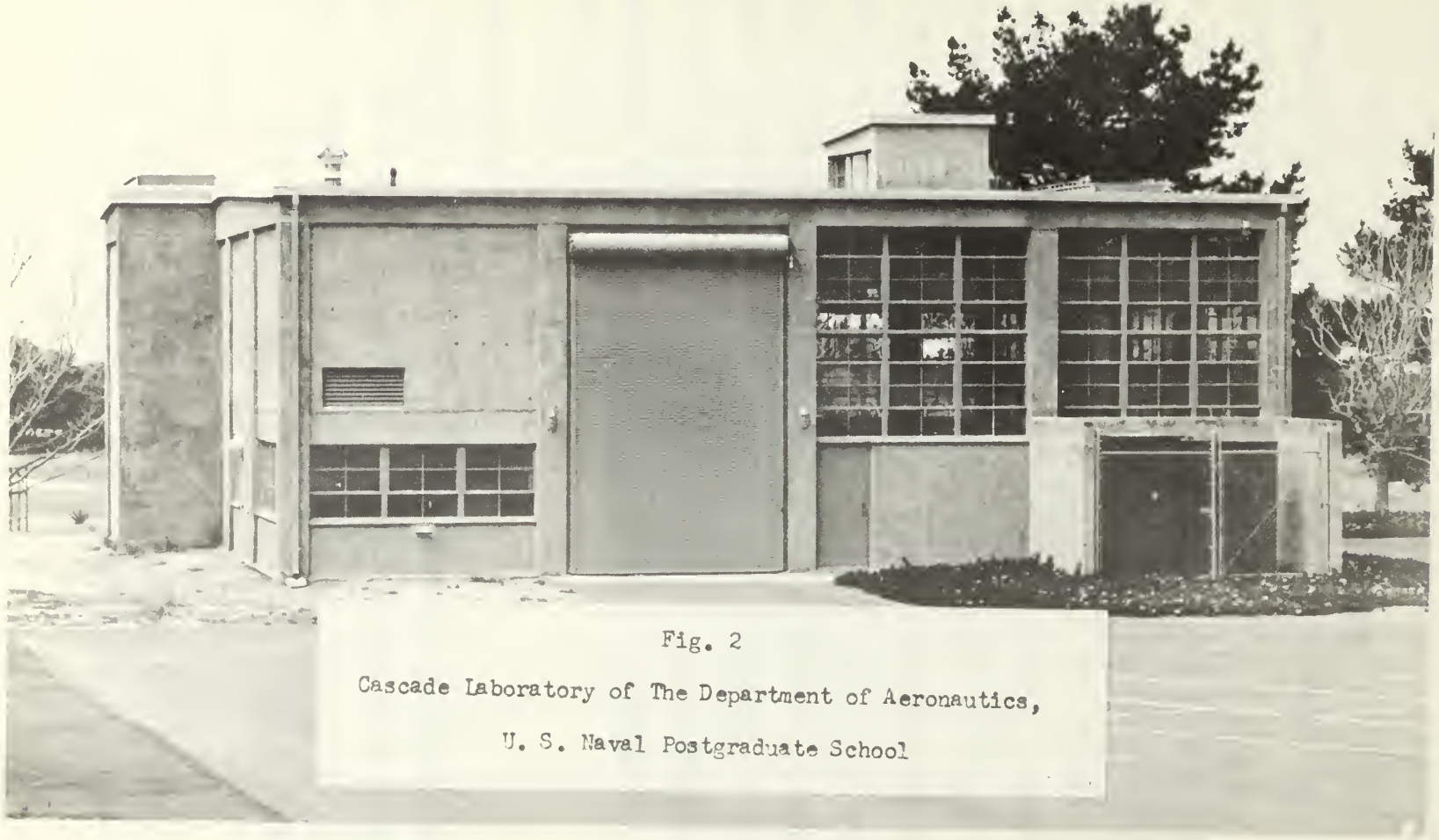

Fig. 2

Cascade Laboratory of The Department of Aeronautics,

U. S. Naval Postgraduate School

these values with those published by NACA in Ref. 3. At the same time, parameters more useful to the turbomachinery engineer, such as loss coefficient, will be presented.

A further purpose of this thesis was to indicate improvements and modifications in order to bring the test rig into operating order.

Coupled with the above work, was the testing and utilization of an automatic data logging system. The purpose of this system is to eliminate, or to avoid the laborious task of collecting and transcribing the data into a form compatible with a computer solution. This system utilizes transducers to transform pressure inputs into electrical signals, which are then collected along with other data and punched on paper tape available as input to a computer program. Without the use of this automatic data logging system along with computer solutions the rig could not be utilized to its capabilities because of the long periods required to evaluate the data.

2. Description of Cascade Rig

A general overall view of the cascade is shown in Fig. 3. The rig is essentially an open cycle wind tunnel. Air is brought from the outside down through a 5 by 12 ft. stack into the blower room. The air then enters a double-entry blower.

The blower is a Turbovane Fan, number 470997, size 1001, design 2, manufactured by B. F. Sturtevant Co. of

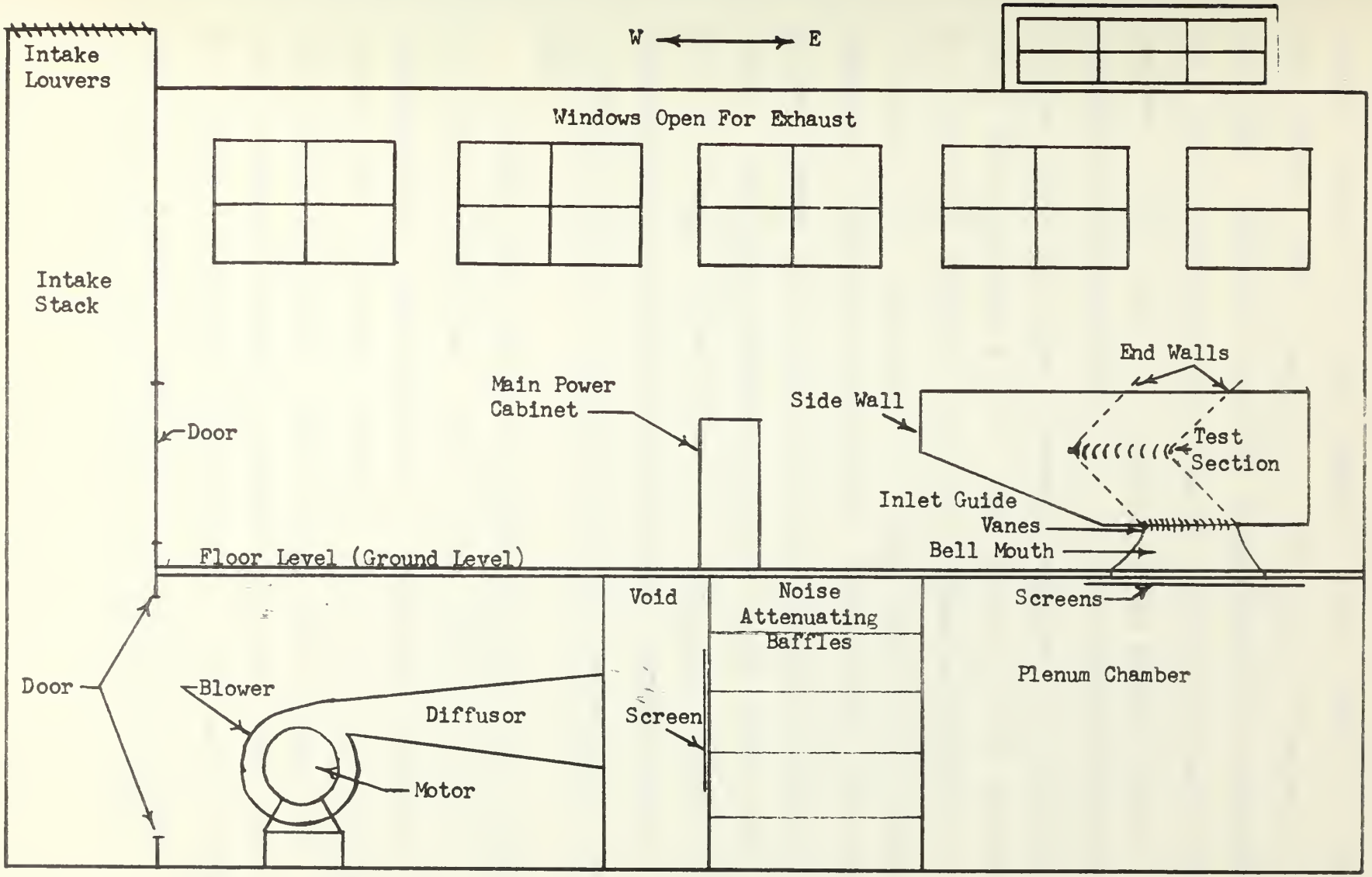

Fig. 3 Schematic Of Cascade Laboratory

Boston, Massachusetts. This blower is driven by a 60 cycle General Electric Tri-Clad Induction Motor, number 5 M 6346 AA1, rated at 700 horsepower at 4160 volts, 86 amperes, and 1780 RPM. The motor has three speeds which are controlled by a three position switch located on the main power control cabinet. This cabinet is located on the ground floor of the Laboratory as shown in Fig. 3. The air exhausts through the diffusor into the noise attenuator section. The diffusor is 11 feet long with a 2 ft. 2 in. by 3 ft. 5 in. inlet and 5 ft. by 5 ft. outlet. The noise attenuator section is 14.5 ft. high, 7 ft. long and 12 ft. wide. Fig. 4 is a schematic drawing of the noise attenuators. The air then enters the plenum chamber from which the air is supplied to the bell mouth. The plenum chamber is 14.5 ft. high, 12 ft. wide and 21.5 ft. long. The bell mouth is a nine foot by five foot rectangle at the entrance and the sides converge along a hyperbolic curve to a 60 inch by 10 inch rectangle at the exit.

At this point the air is guided into the test section by 29 inlet guide vanes. These IGV's are constructed of aluminum with a blade height of 10 inches and a chord of approximately $5\frac{1}{4}$ inches. Presently there are five different blade shapes available. These blades have an angle of 0, ± 30 and ± 60 degrees between the tangents from the camber line at the leading and trailing edges, Fig. 5. When mounted these blades may be rotated individually to produce the desired flow exit angle. For this thesis the positive 60 degree

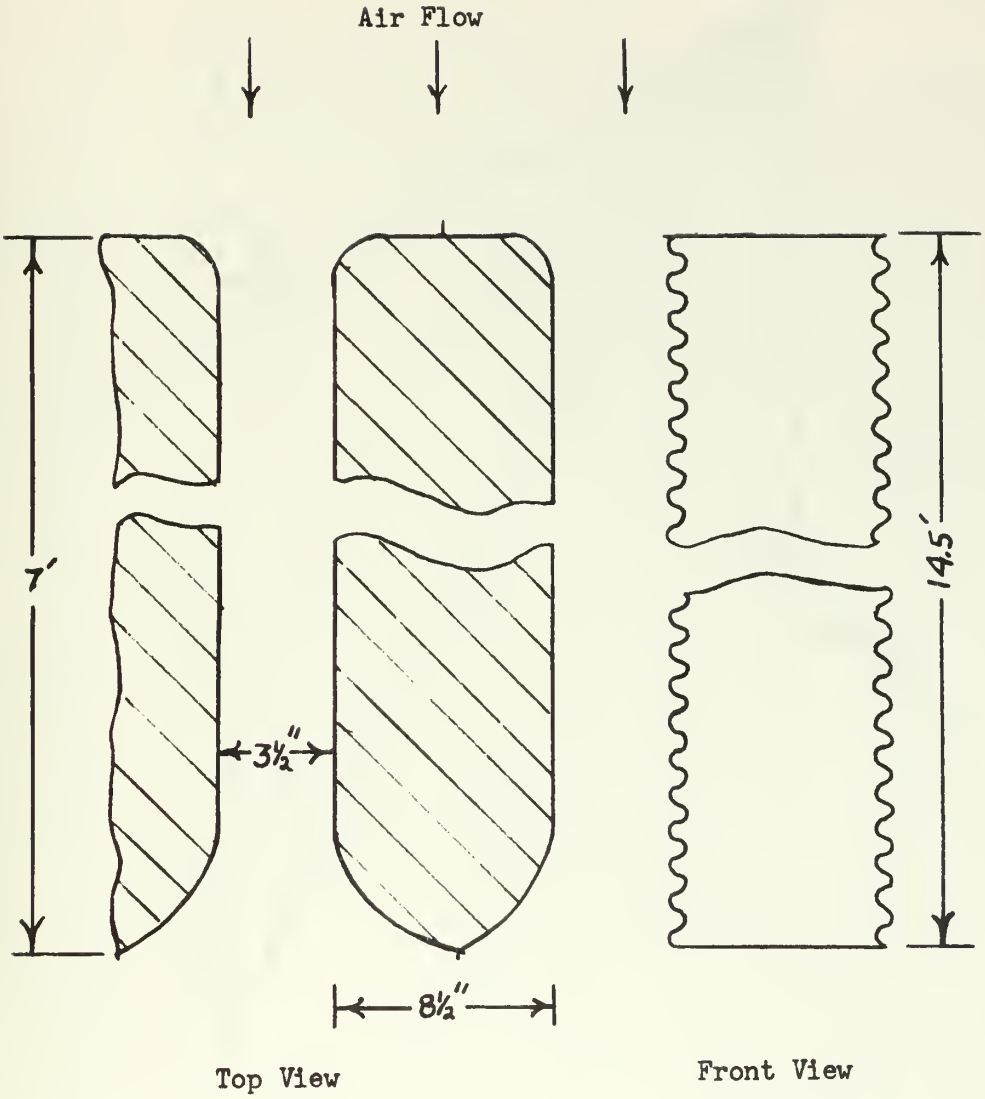

Fig. 4 Schematic Of Sound Baffles

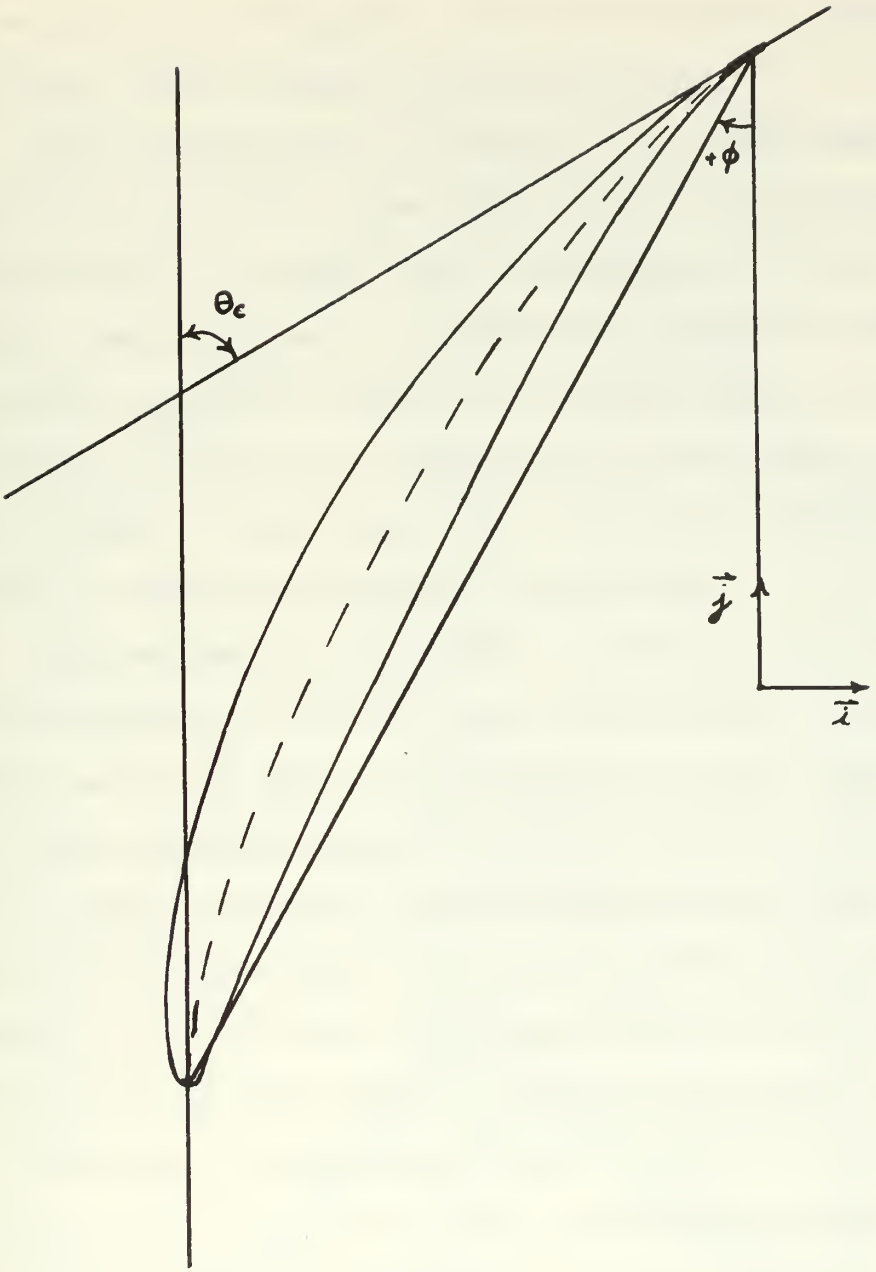

Fig. 5

Angle Notation

ϕ = Stagger Angle

blades were used with the trailing edges set at angles of between 40 and 45 degrees from the vertical depending on the run. Fig. 6 shows a typical setting.

The test section is bounded on the long side by two parallel side walls. One wall acts as the structural support and all blades and attachments are affixed to this wall. The other wall is removable in order to change the position of the end walls or to change blades or blade position. A three ton over-head electric crane is used for the removal of this wall. The removable wall is located by means of dowels to simplify the assembly.

The end walls which bound the short side of the working section guide the flow to the cascade which is to be tested. These walls may be set independently of each other and therefore may not necessarily be parallel. These walls may be set at any angle in order to provide the proper flow direction. Each wall has an upper and a lower portion which are hinged together. This allows the upper portion to be independently set at an arbitrary angle. For testing turbine blades, as in this work, the upper portions are "folded" back in the opposite direction of the lower portions depending on the test blade shape and setting. For this thesis the lower walls were set at 45 degrees and the upper walls were set at -49 degrees. These conditions are also shown in Fig. 6. The lower walls telescope so that the hinge points may be adjusted to various vertical positions.

For testing compressor blades the upper portion of the

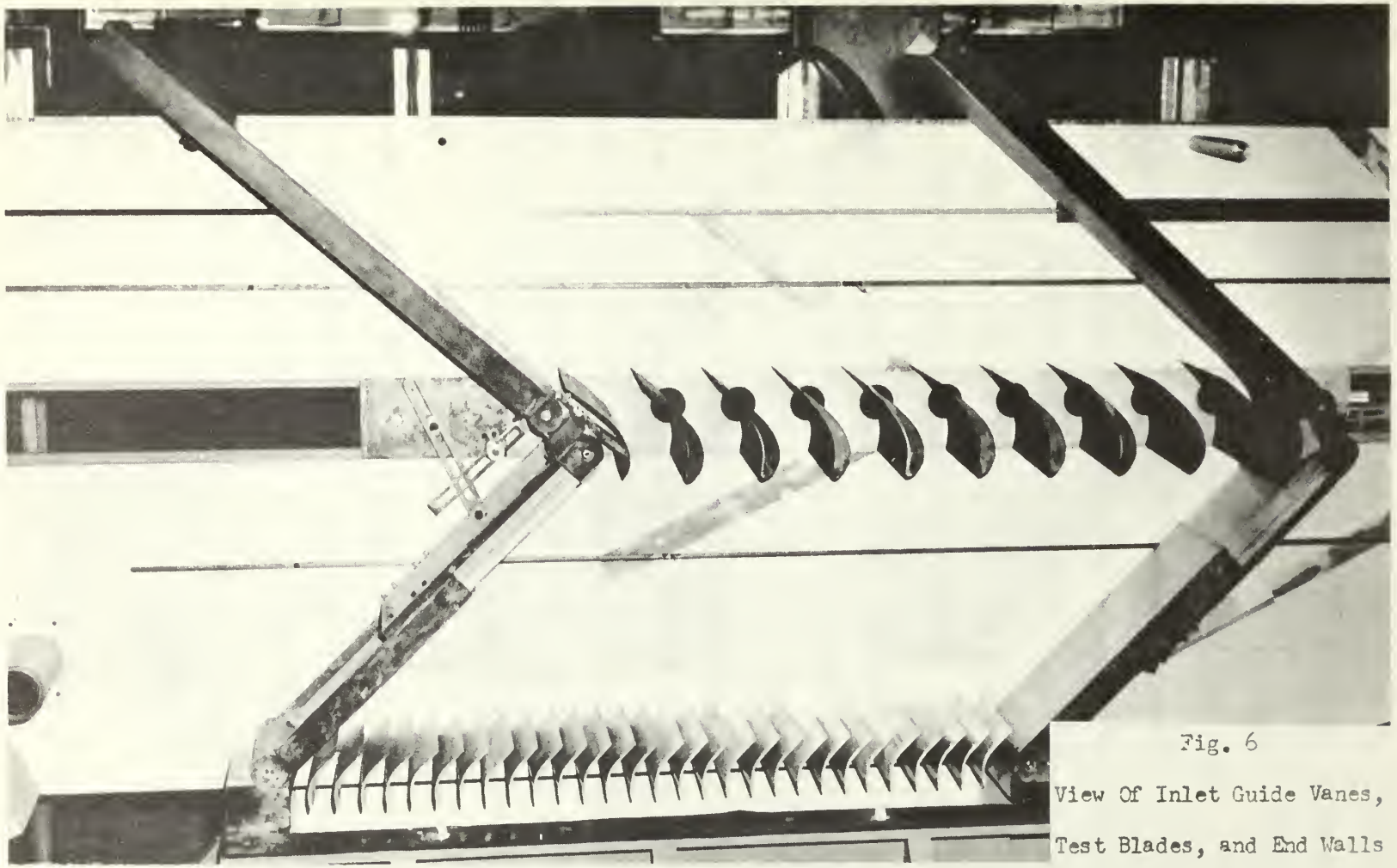

Fig. 6

View Of Inlet Guide Vanes, Test Blades, and End Walls

end walls would be nearly parallel to the lower portion. The air flow would be deflected between 15 to 25 degrees in a compressor blade test instead of the 30 to 110 degrees as in a turbine blade test. The test blade shape used for these tests was a reaction turbine blade with a camber angle of 95 degrees and a maximum thickness of 15 per cent. This type of blade was established by NACA and used for tests in the cascade investigation conducted by Dunavant and Erwin at the Langley Aeronautical Laboratory, Langley Field, Virginia, Ref. 3. The blades tested at the present cascade rig were cast of epoxy and nickel plated. They are 10 inches high and have a chord of 8.5 inches.

The blades are mounted into a sliding blade holder. This sliding blade holder is required since the blades must be located between the adjustable end walls. For this investigation the test blades were set with a stagger angle as defined in Fig. 5, of -25 degrees and with a spacing of six inches. The spacing is dictated by the blade holder used. Holders with four and ten inch spacings are also available.

The air, after passing through the test section, exhausts into the laboratory. The air can then either exhaust through open windows or be recirculated. In order to recirculate the air, the louvers in the intake stack would be closed and the doors between the laboratory and stack opened.

Inlet guide vanes mounted on the blower are controlled

pneumatically from the laboratory. These vanes are shown in Fig. 7 along with the three speed motor used to drive the blower. By running the blower at one of its three speeds and properly adjusting the inlet guide vanes many volume flow rates may be obtained up to approximately 100,000 cubic feet per minute.

Table I shows the range of pressures, velocities and Reynolds numbers available for the various inlet guide vane positions and motor speeds. Reynolds number is based on a chord of 8.5 inches.

TABLE I

Performance Range

of The Cascade Rig

Pressure			Motor Speed	Blower Vanes	Velocity (ft/sec)	Reynolds Number x 10^{-6}
Total	Static	Dynamic				
5.6	1.1	4.5	slow	closed	140	.63
10.3	2.0	8.3	slow	open	191	.855
11.5	2.0	9.5	med.	closed	204	.916
26.6	4.0	22.6	med.	open	314	1.41
16.6	2.7	13.9	fast	closed	247	1.11
46.7	8.7	38.0	fast	open	407	1.83

Pressures - inches of water gage

This cascade rig is unique in many respects. This is due to its advantages and versatility as compared to conventional cascade rigs.

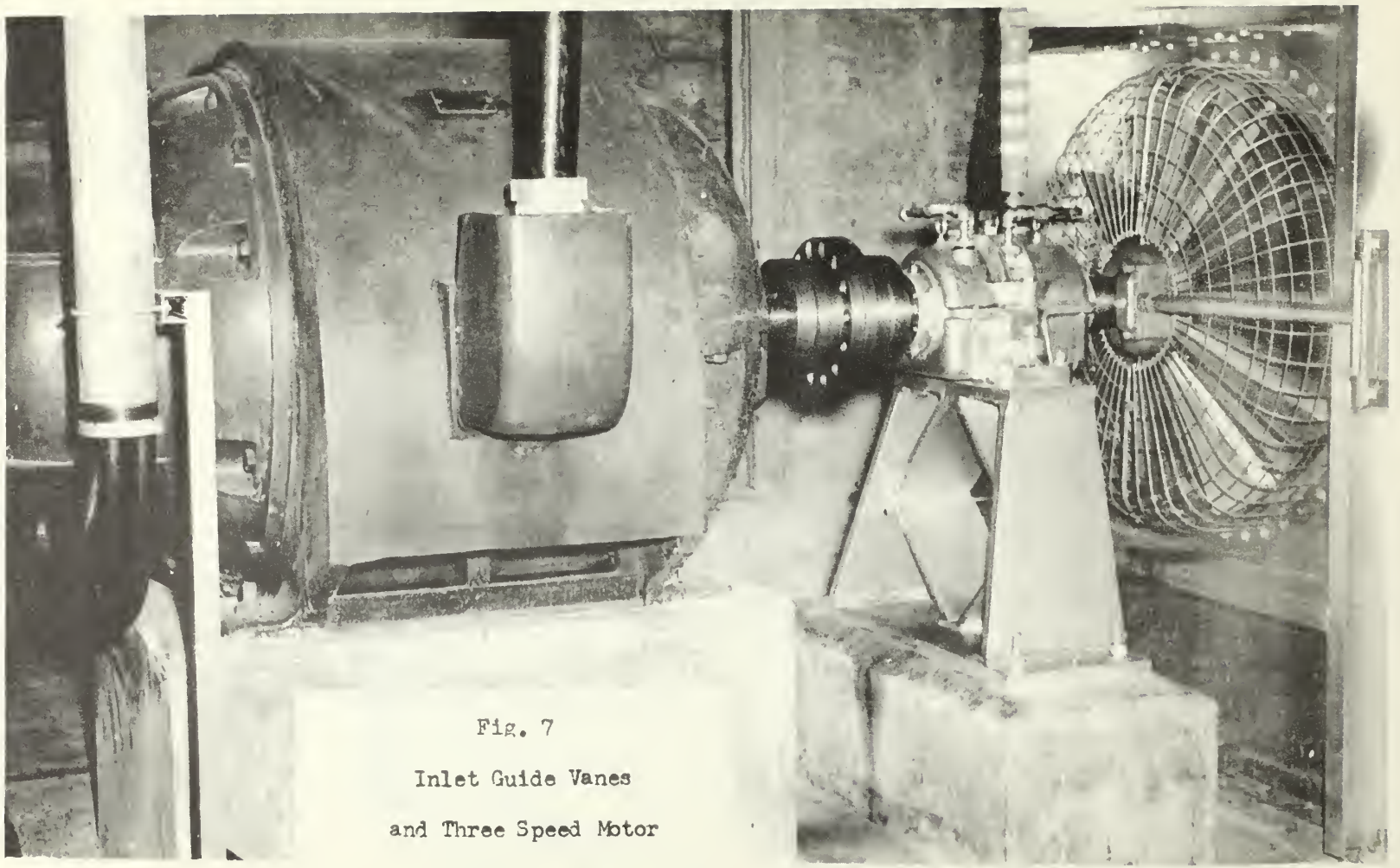

Fig. 7

Inlet Guide Vanes

and Three Speed Motor

Fig. 8 shows the cross section of a conventional cascade rig. One of the difficulties encountered in this type of cascade rig is the control of the boundary layer ahead of the cascade. Fig. 8 shows that the air passing along the lower wall of the channel must travel a greater distance before reaching the blades than the air passing along the upper wall. Since the thickness of the boundary layer increases with the distance traveled along a wall, the thickness of the boundary layer is greater at the lower blades than at the upper blades. Hence boundary layer removal is required. In the present cascade rig the distance along each wall to the test section is equal. This eliminates the dissimilarity in boundary layer thickness and therefore the need for boundary layer removal.

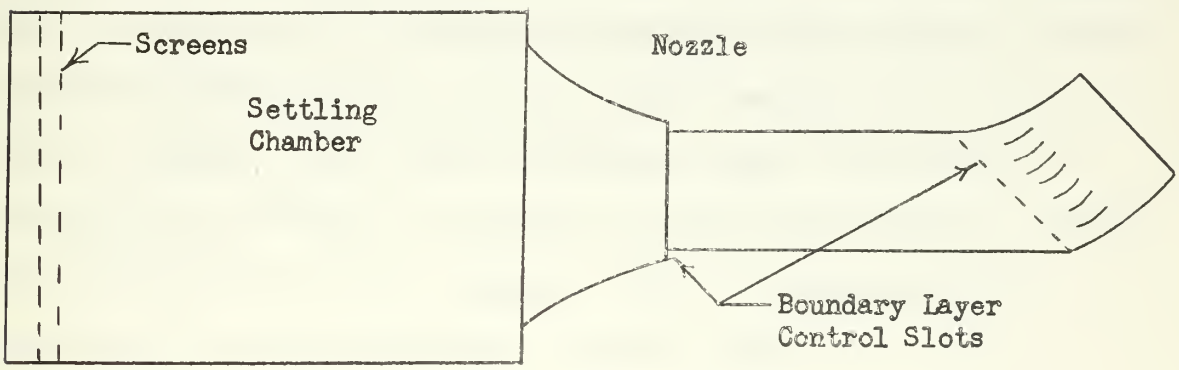

Fig. 8 Cross Section Of A Conventional Cascade Rig.

This cascade, however, has provisions for removing the boundary layer along the side walls. By conducting tests with and without boundary layer removal, studies can be

made concerning the effects of boundary layer on cascades. Hence information can be obtained on the effects of boundary layer in turbomachines.

In all conventional cascade rigs, the air flow is idealized in that conditions of static and total pressure, velocity and flow angle are constant at the entrance of the test section. Thus the effects of inlet guide vanes or preceding rows of blades, as encountered in turbomachinery, are not considered. Due to the inlet guide vane section incorporated in the present cascade, the flow entering the test section approximates the flow in turbomachines.

Any axial flow compressor or turbine blade shape can be tested in this cascade rig. This is accomplished by positioning the inlet guide vanes and the lower and upper portions of the end walls to achieve the proper flow angles. The solidity may be varied by changing blade holders. The present blade holders provide blade spacings of 4, 6, 8, and 10 inches. The blade incidence angle can easily be changed by rotating the blades in the blade holder. All of these factors give the cascade rig a versatility not attained by any conventional cascade rig.

The blower used with the rectilinear cascade rig can also be used for testing circular cascades. Referring to Fig. 9, the doors between the intake stack and the blower room would be closed and the doors between the plenum and the discharge stack would be opened. Doors at the entrance to the bell mouth of the rectilinear cascade rig would also

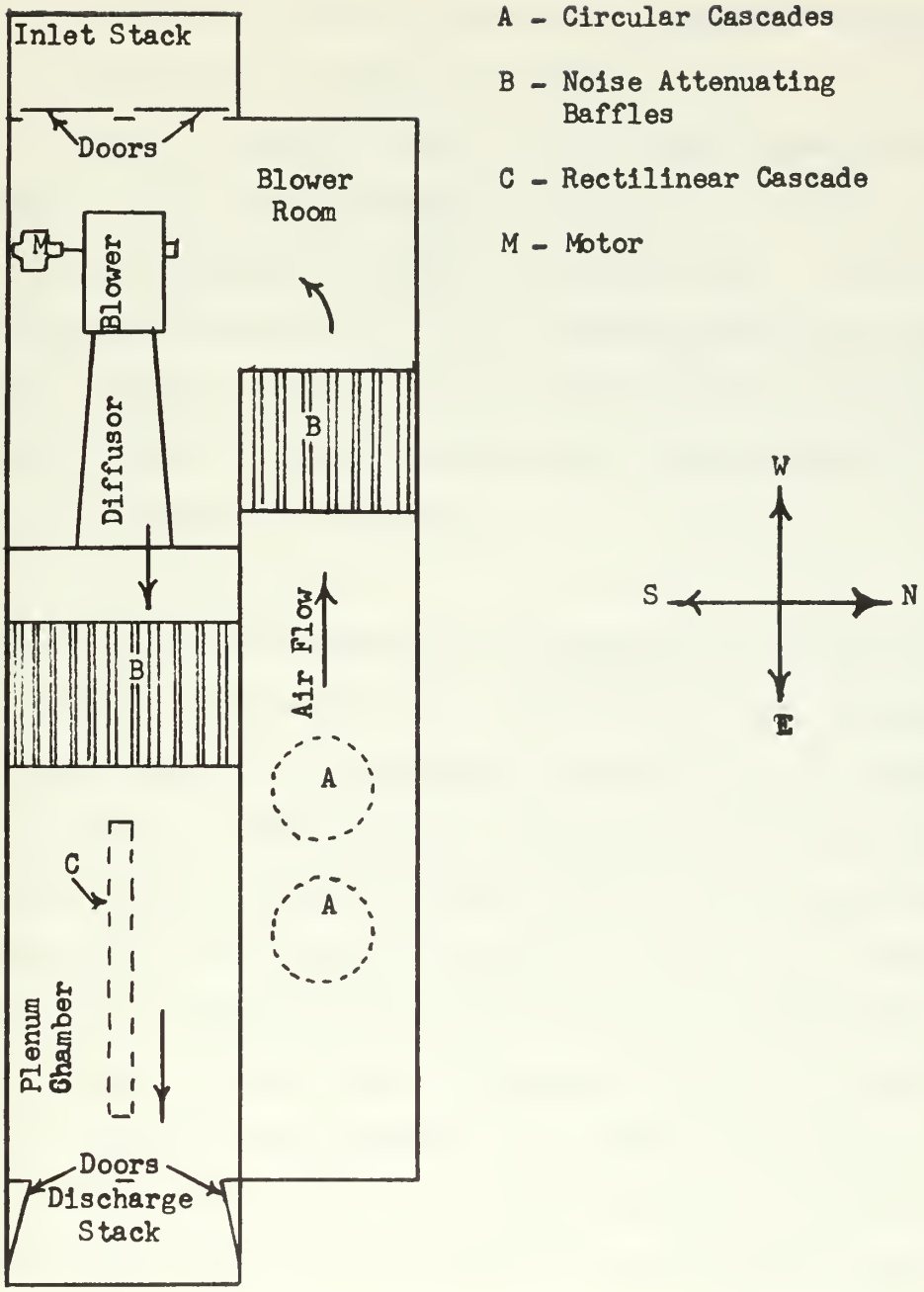

Fig. 9 Schematic Of Circular Cascade Configuration

be closed. Air would then be drawn through the circular cascade by the blower and exhausted out the discharge stack. In this case the blower could provide negative pressures up to approximately 46 inches of water.

Circular cascades with 5.5 ft. outer diameters can be tested at the locations shown on Fig. 9. A unique feature of this arrangement is that the ground level portion of the Cascade Laboratory acts as the plenum chamber for the circular cascades. Hence the flow entering the circular cascades would be more uniform than flow obtained by blowing the air through the cascades.

3. Description of Measuring and Recording Equipment

Static taps in the two side walls of the cascade give an indication of the uniformity of the air flow through the test section. These taps are approximately three inches apart and are located 13 inches ahead of the blades and three inches aft of the blades, as shown in Fig. 10. Plastic tubes connect the static ports with water-filled multitube manometer banks. These banks, as shown in Fig. 11, are 96 inches high and are graduated in tenths of an inch. Green colored water was used in the manometers in order that photographs can be taken during a run for later interpretation.

Two pitot-static probes traverse the test section; one ahead and the other after the blades. The lower probe traverses the test section 13 inches ahead of the center of the test blades. The upper probe can traverse the test

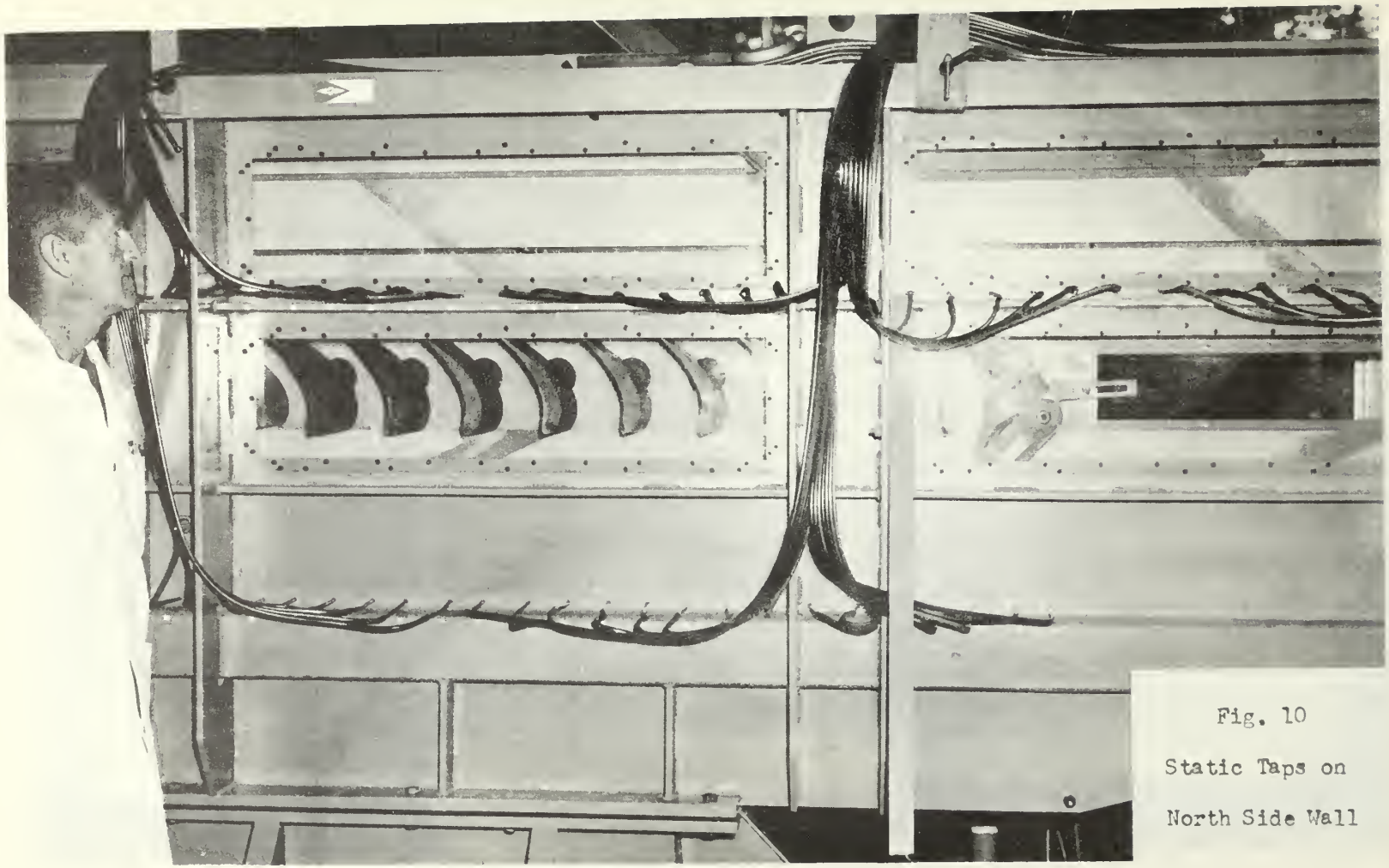

Fig. 10

Static Taps on

North Side Wall

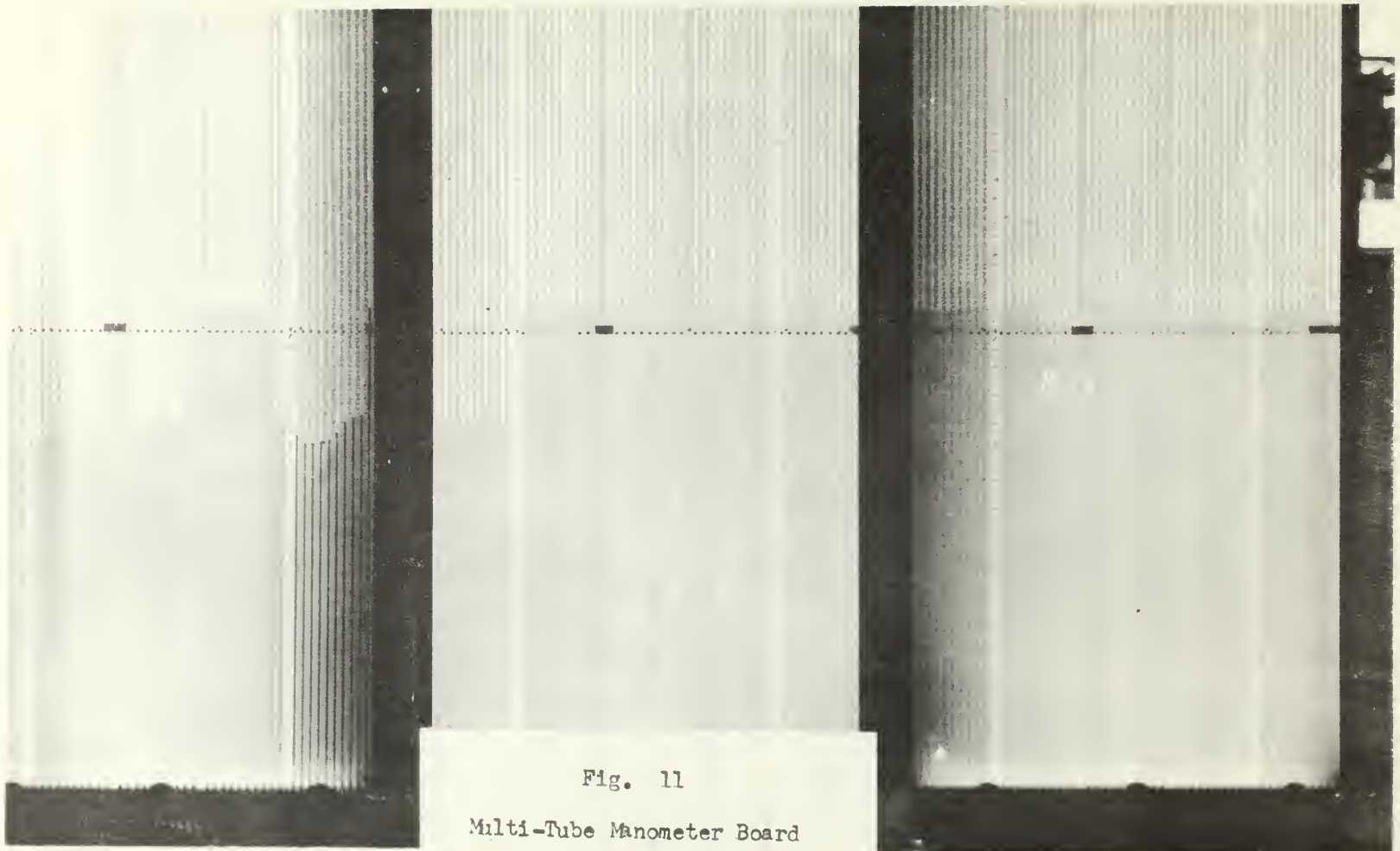

Fig. 11

Multi-Tube Manometer Board

section either 10 or 16 inches behind the center of the test blades. These two upper positions for the probe provide a means by which mixing losses can be determined. This would be accomplished by comparing the results of two succeeding tests differing only in the position of the upper probe. Mixing losses are discussed in section 5 of this thesis.

These United Sensor, YC-120, probes have a three-hole, prism shaped measuring section. The probes measure total and static pressure and yaw angle. They are insensitive to pitch angle up to 20° and are usable up to Mach 0.7. These probes were supplied by United Sensor and Control Corporation of East Hartford, Connecticut. Each probe is mounted in a traverse, Fig. 12, which is located on the stationary side wall of the cascade rig as shown on Fig. 13. The traverse is electrically controlled from an operating and measuring console shown in Fig. 14. The probe extends into the test section through a metal runner and a 1/2 inch slot. This metal runner moves with the traverse and seals the slot in order to prevent air leakage.

Each probe is mounted in a carriage, which moves the probe in and out of the test section (y-direction). The probe can be rotated 90 degrees, in either direction, automatically or manually. This is accomplished manually by switches on the console. The number of degrees rotated are indicated on the console. When on automatic the probe is rotated by a servo.

Also mounted on each traverse are four transducers,

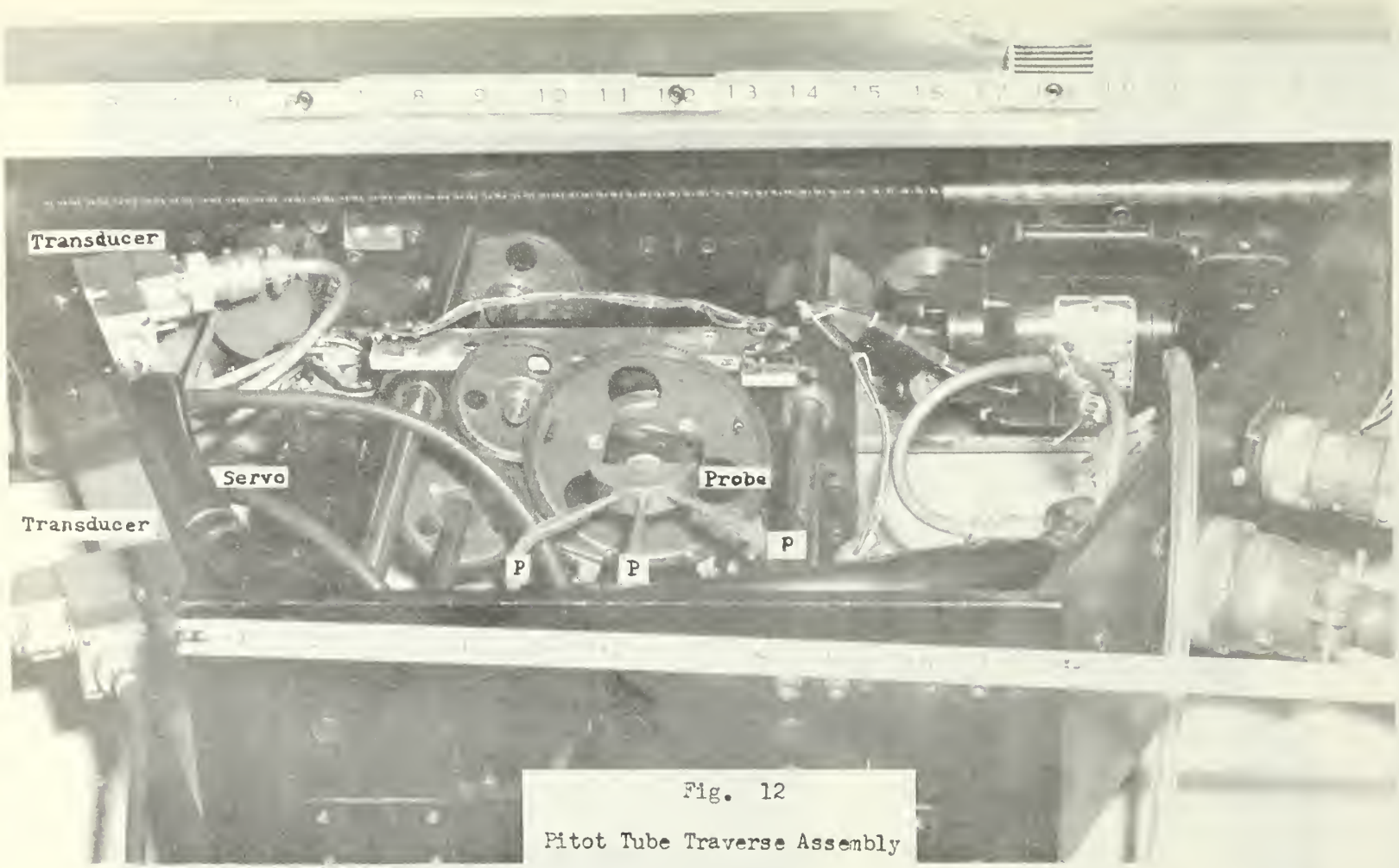

Fig. 12

Pitot Tube Traverse Assembly

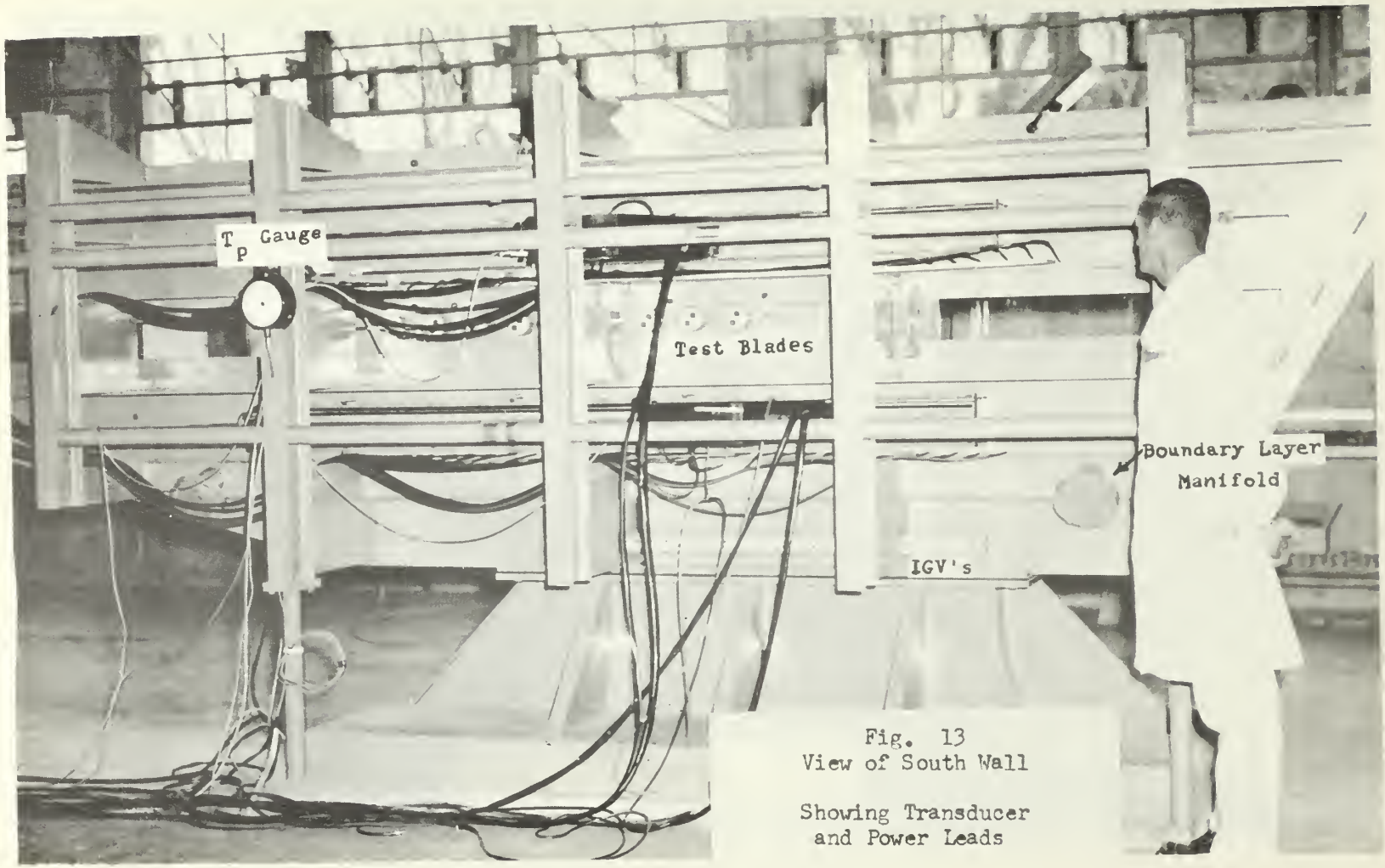

Fig. 13
View of South Wall

Showing Transducer
and Power Leads

Fig. 14

Automatic Data Logging Console

which convert the pressures obtained from the probes into electrical signals. One transducer is used for the total pressure and two for the static pressure. Positive static pressures are transmitted from one of the transducers and negative pressures from the other.

The fourth transducer is used to supply power to a servo which rotates the pitot tube into the flow. This differential transducer measures the difference between the two static pressures obtained from the probe and converts this difference into an electrical signal. This signal drives the servo, which rotates the probe in a direction depending on the sign of the signal. When the pressures become equal no power is supplied to the servo by the differential transducer. With this condition the probe is directed exactly into the air flow and measures the actual total and static guage pressures.

This unique system was designed by Professor M. H. Vavra as an improvement to the tedious and time consuming conventional methods. Conventional methods require the probe to be rotated manually until the difference in static pressures are zero as measured on a differential micromanometer. Due to the inertia of the fluid columns in the micromanometer, this is a very insensitive system and therefore time consuming. This method would require five to ten minutes to locate the flow direction whereas this would be accomplished within five to ten seconds using the electrical system. Fig. 13 shows the electrical leads that connect the console with the upper and lower traverses.

All controls for positioning and monitoring the probes are contained on the right side of the console shown in Fig. 14. A view of the right side only is found in Fig. 15. Only one of the probes can be controlled and monitored at any one time. Two sets of rotating counters indicate the probe's position in the x and y directions to one hundredth of an inch. The angle that the probe is rotated from the vertical position is indicated by a voltmeter graduated every five degrees clockwise and counter-clockwise. The monitoring system is a separate and distinct system from that used for recording.

The left side of the console as shown in Fig. 16, contains all controls for recording the data. All data received from the probes and the carriages are recorded automatically on punched and printed tapes. Fig. 17 shows the Friden paper tape punch. This machine is installed in a drawer that is closed during normal operations in order to protect the punched tape.

The console uses a digitizer to convert the signals received from the measuring equipment into a certain number of counts. There are 1000 counts (000-999) available for indicating measured values. Each of the six measured quantities (x, y, θ, P, p positive and p negative) for both upper and lower traverses have gain controls so that the counts may indicate in any dimension. Normally for the pressures, the counts will indicate 0.1 inches of water pressure. An example would be 131 counts which would be

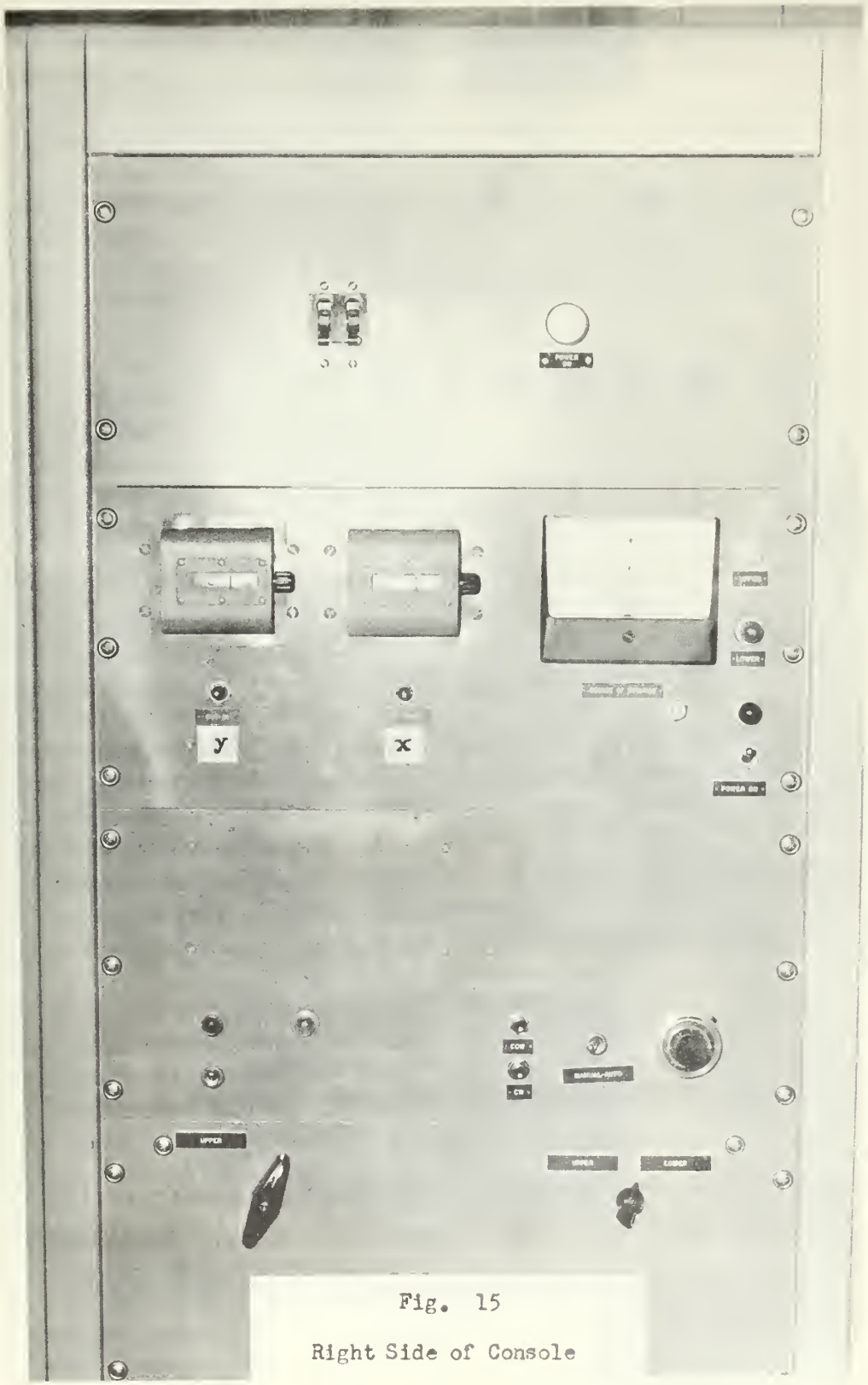

Fig. 15

Right Side of Console

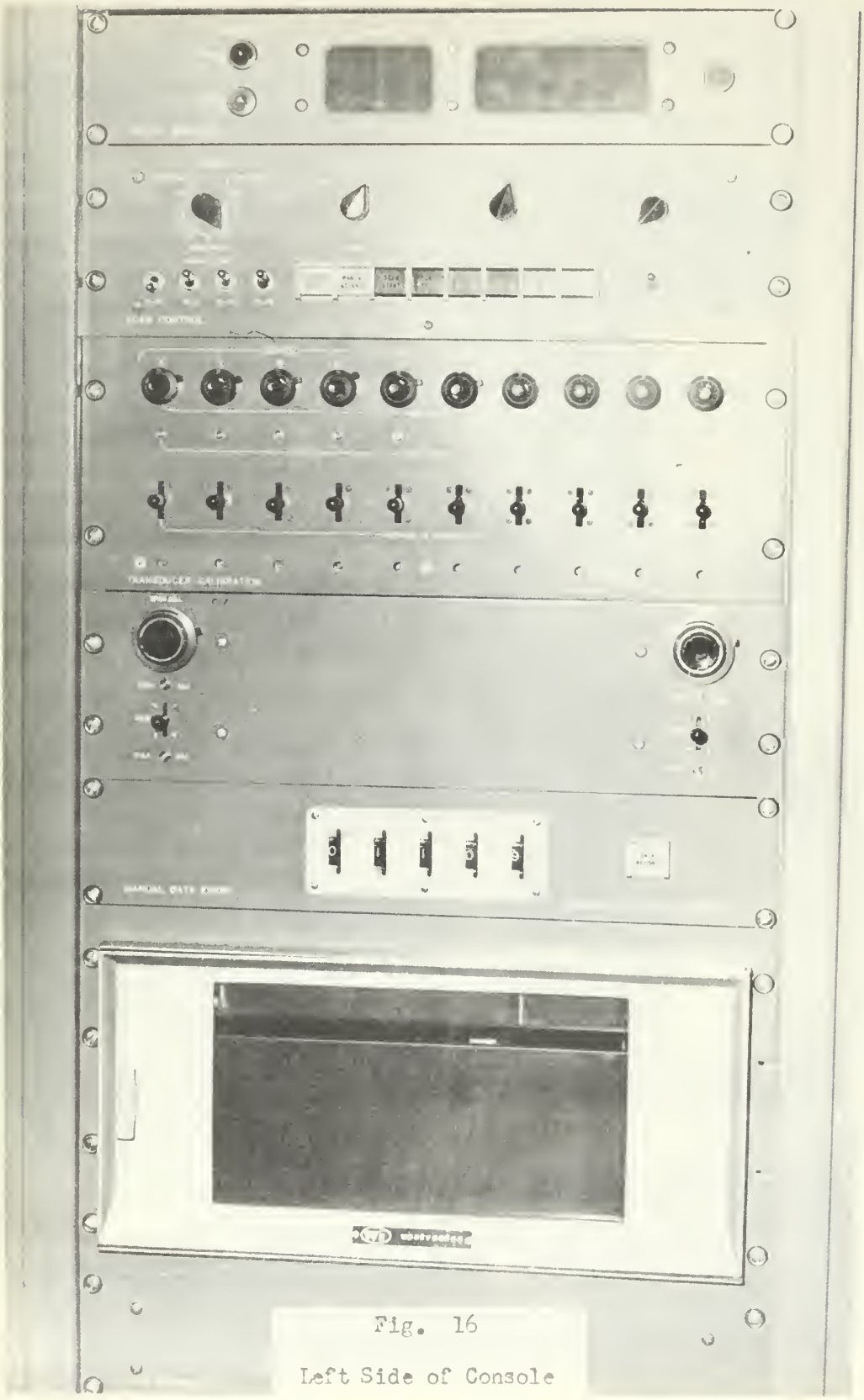

Fig. 16

Left Side of Console

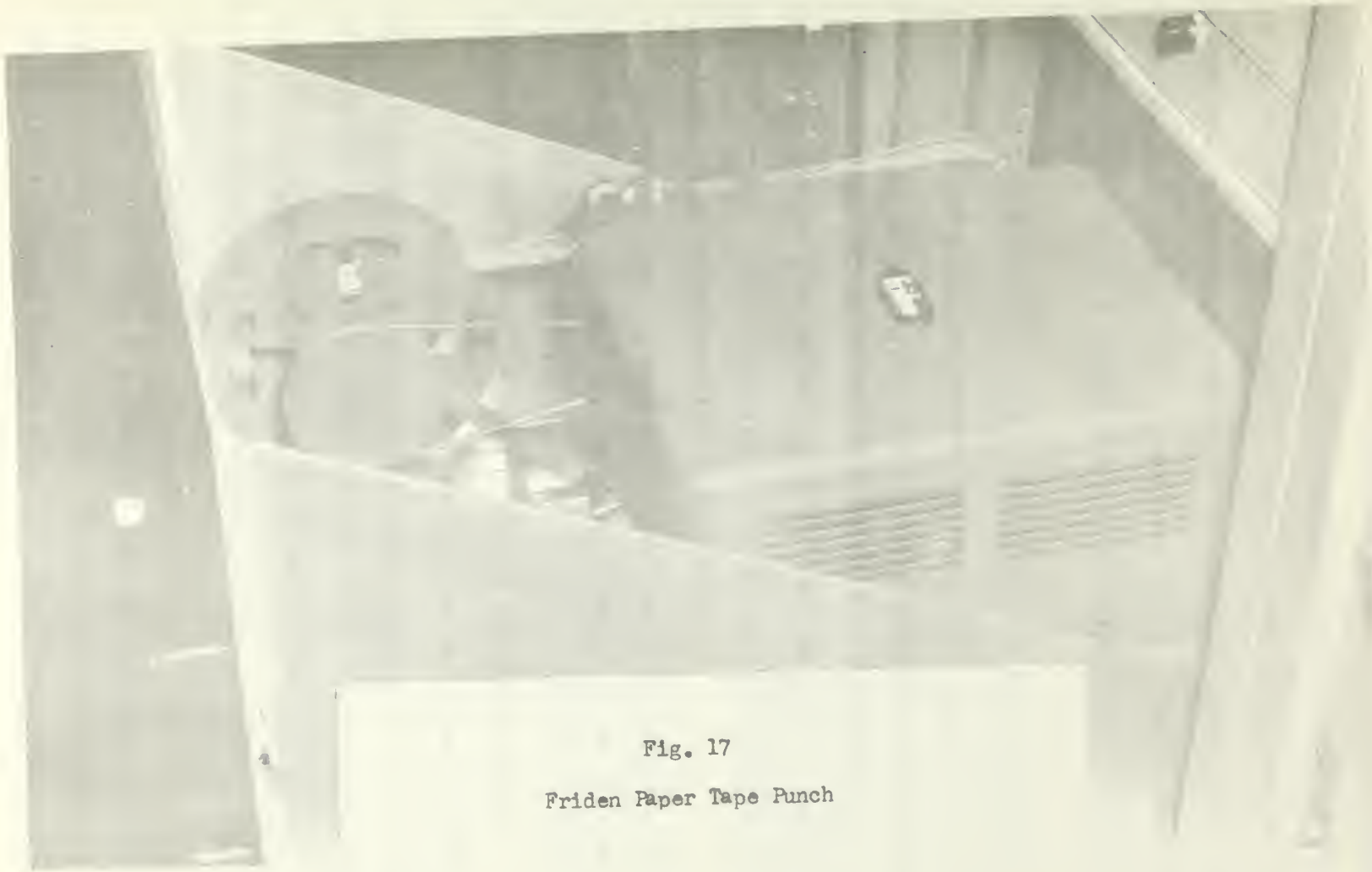

Fig. 17

Friden Paper Tape Punch

13.1 inches of water. The flow angle, Θ, is scaled so that a reading of 500 counts is zero degrees, 50 is 90 degrees clockwise (-) and 950 is 90 degrees counter-clockwise (+), as viewed from the console. Each count is therefore 0.2 of a degree. An example would be a count of 350. 350 - 500= -150 and 0.2 x -150= -30.0 degrees (CW). The y position is indicated to the hundredth of an inch from 0 to 9.99 inches.

The x position is also indicated to the hundredth of an inch (000-500). In order to have this accuracy it was necessary to recycle the measuring equipment every five inches. Thus after every five inches the counts go to zero and five inches are added to x in the computer program for the CDC 1604. This computer is made by the Control Data Corporation of Minneapolis, Minnesota.

Data can also be manually punched and printed on tape. Presently this is used for such information as plenum temperature, barometric pressure, run number, number of blade spacings, and a code to indicate end of input data.

Connected into the various pressure lines leading to the transducers are tubes which are connected to two manometer boards. One for each of the two probes (upper and lower). On these boards P, p, Δp and q are monitored. The main use of these manometers would be in calibrating the console readings.

Calibration of the console can be carried out between tests at arbitrary intervals. The procedures used to calibrate the pressure components are given as an example.

All of the pressure components can be calibrated at the same time by connecting their pressure leads to a manifold. With atmospheric pressure on the manifold, the component being calibrated is set to zero using the zero rheostat for that component. A known pressure is then put on the system and the gain control adjusted to give the counts required. The pressure must then be released and the zero rechecked. This procedure may have to be repeated several times. For more accurate readings the known pressure should be equal or greater than those expected during the tests. Checks on the calibration of each component can be made at any time by depressing the calibration switch for that component. The digitizer will then indicate the full scale deflection. This value will not change unless the component is no longer properly calibrated.

Total temperature is obtained from a temperature probe that extends into the plenum chamber. This information is manually punched on the paper tape.

4. Static Pressure Distribution

The momentum theorem, as discussed in Section 5, is used to determine the force exerted by the fluid on the test blades. This requires surveys of the flow conditions ahead of and behind the test blades. Theoretically the volume of fluid that is surveyed behind the blades should be the same as that surveyed ahead of the blades. Actually it is only necessary to survey a volume of air that has had the same

changes in momentum as that surveyed ahead. For that reason it is desired to have a wide regular flow profile entering the test section. A regular flow being defined as a steady-uniform flow except for wakes that are equal and evenly spaced. An accurate survey can then be conducted if the width of the regular flow profile entering the test section exceeds the length of the survey by one spacing. For these tests a static pressure gradient of less than two percent of the test section dynamic pressure was considered permissible.

The cascade was set up as shown in Fig. 6. The lower end walls were set at $+45^{\circ}$, the upper end walls at -49°, the test blade stagger angle was set at -25°, and the trailing edges of the inlet guide vanes were set at $+45^{\circ}$. The angle of the inlet guide vanes was determined from the relation:

$$\alpha_2^* = f(\mathrm{Cos}^{-1} o/s)$$

of Ref. 4, where o is the blade opening and s is the spacing or pitch. Fig. 5, of this reference indicates the relationship between gas outlet angles and $\mathrm{Cos}^{-1} o/s$ is linear for straight-backed blades operating at Mach numbers less than 0.5.

Ref. 4 limits this relationship to a Reynolds number of approximately 2×10^5 but there seems to be no reason why this relation should not be valid for higher values. Therefore this relation was used to initially position the inlet guide vanes.

Operation of the cascade under these conditions produced a pressure gradient in the x direction ahead of the test blades, Fig. 18. This pressure variation amounted to

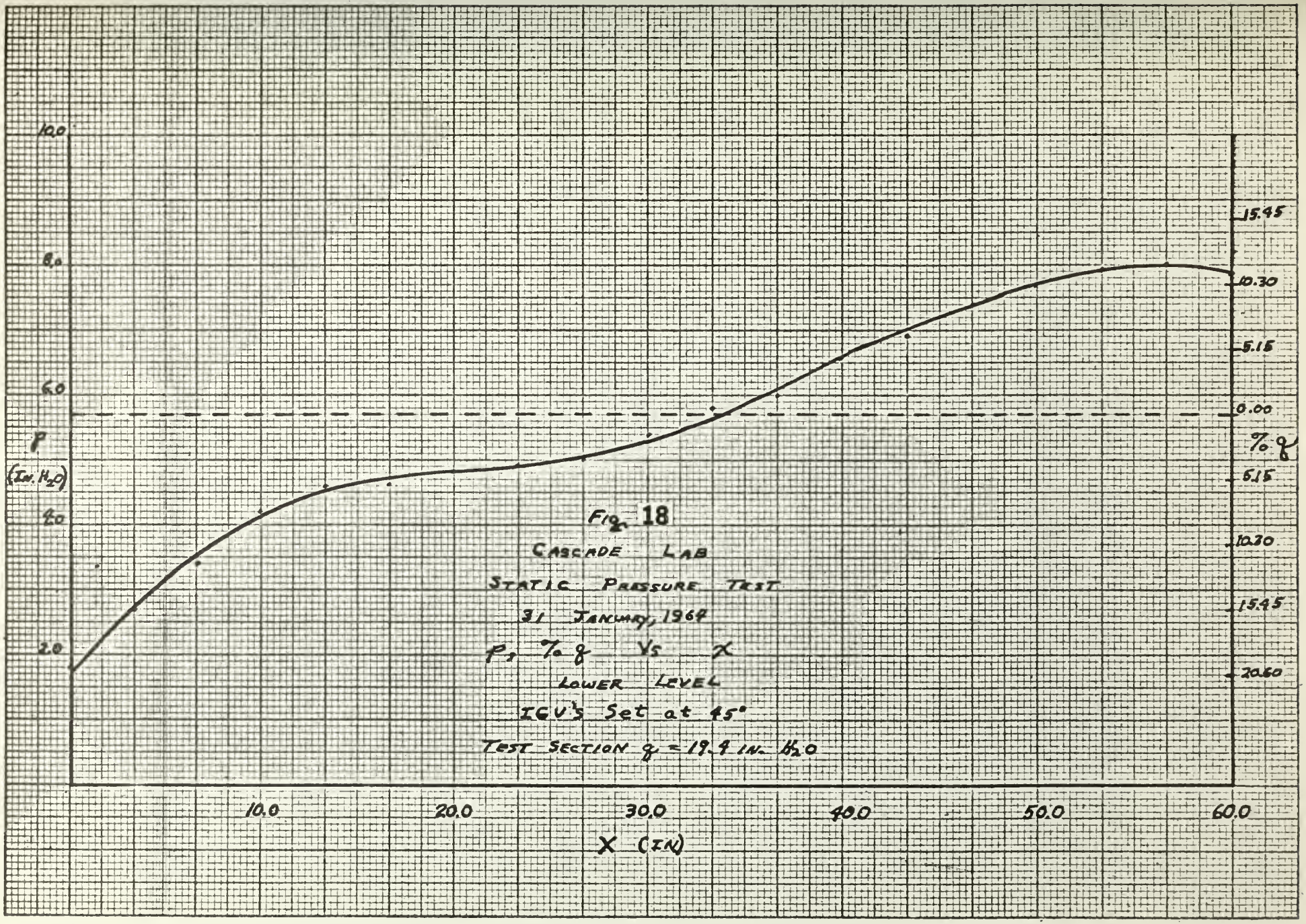

Fig. 18

CASCADE LAB

STATIC PRESSURE TEST

31 JANUARY, 1964

p_s % q Vs X

LOWER LEVEL

IGV's Set at 45°

TEST SECTION q = 19.9 IN. H_2O

20.6% of the test section dynamic pressure and therefore is not permissible.

To correct this situation the inlet guide vanes were set to 40°. In addition, gaskets were installed on the free end of each blade to prevent the passage of air between the blade tips and the wall. Prior to the installation of the gaskets a clearance of 3/32 inch existed between the removable side wall and the test blades. The gaskets eliminated this clearance and form a tight bond between the blade tips and the wall. As a result of the above alterations it was found that although a pressure gradient was still present, it had lessened to 12.9% of the test section dynamic pressure but had reversed its direction, Fig. 19.

The fact that the gradient had reversed indicated that the required inlet guide vane angle was between 40° and 45°. The guide vanes were reset to 42° and a fine mesh wire screen (20 holes/in., 0.016 in. wire diam.) was installed at the exit of the bell mouth immediately ahead of the guide vanes. Operation of the cascade in this configuration produced the pressure distribution as shown of Fig. 20. This figure indicates an undesirable pressure variation near the center of the cascade. It was also found from pressure readings that the total pressure had been reduced from 50 inches of water to 29 inches of water. This is a 42% reduction in total pressure caused by installing the screen just in front of the inlet guide vanes.

For the next run the fine mesh screen was removed. The

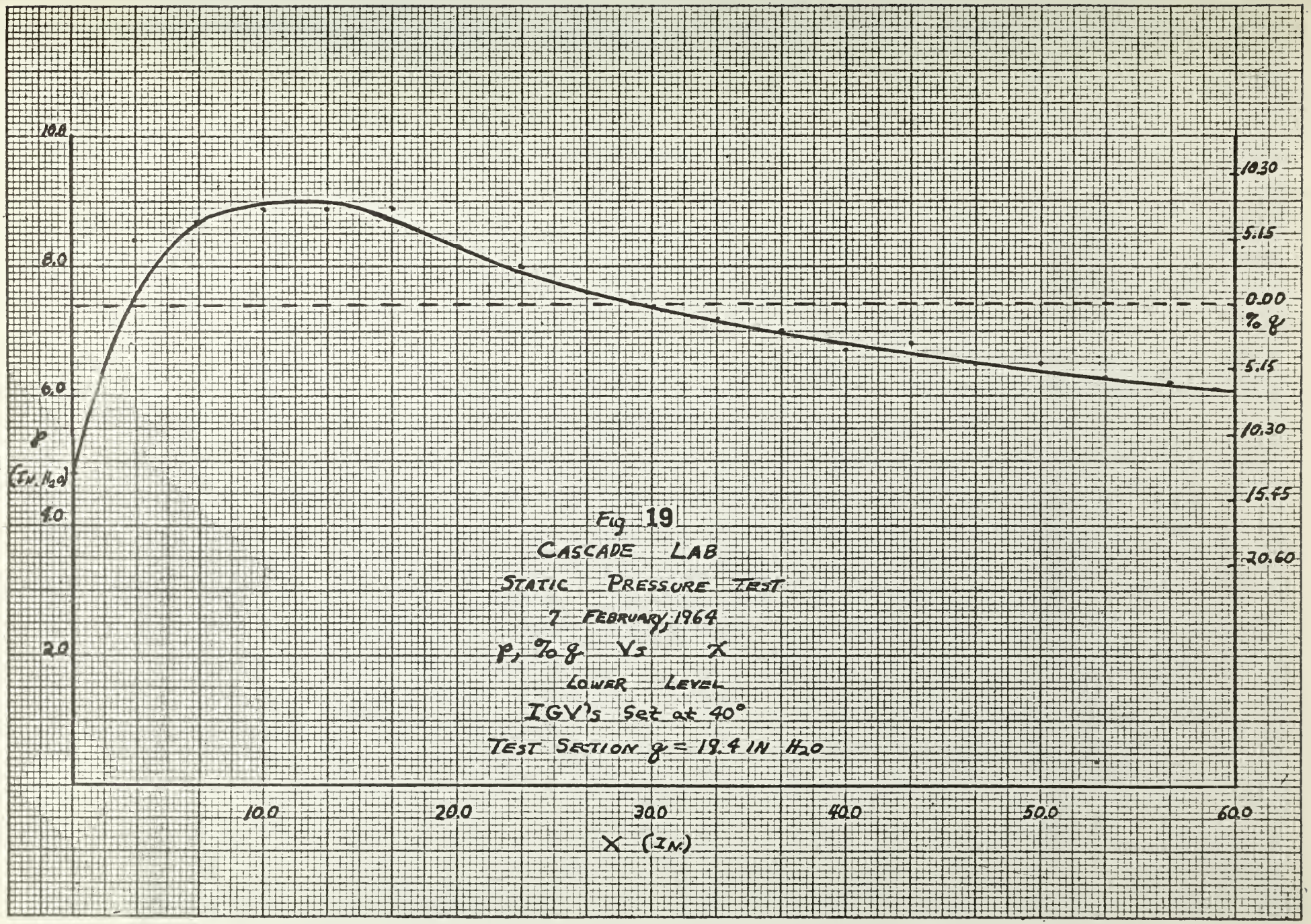

Fig 19

CASCADE LAB

STATIC PRESSURE TEST

7 FEBRUARY, 1964

P, % q Vs X

LOWER LEVEL

IGV's Set at 40°

TEST SECTION q = 19.4 IN H_2O

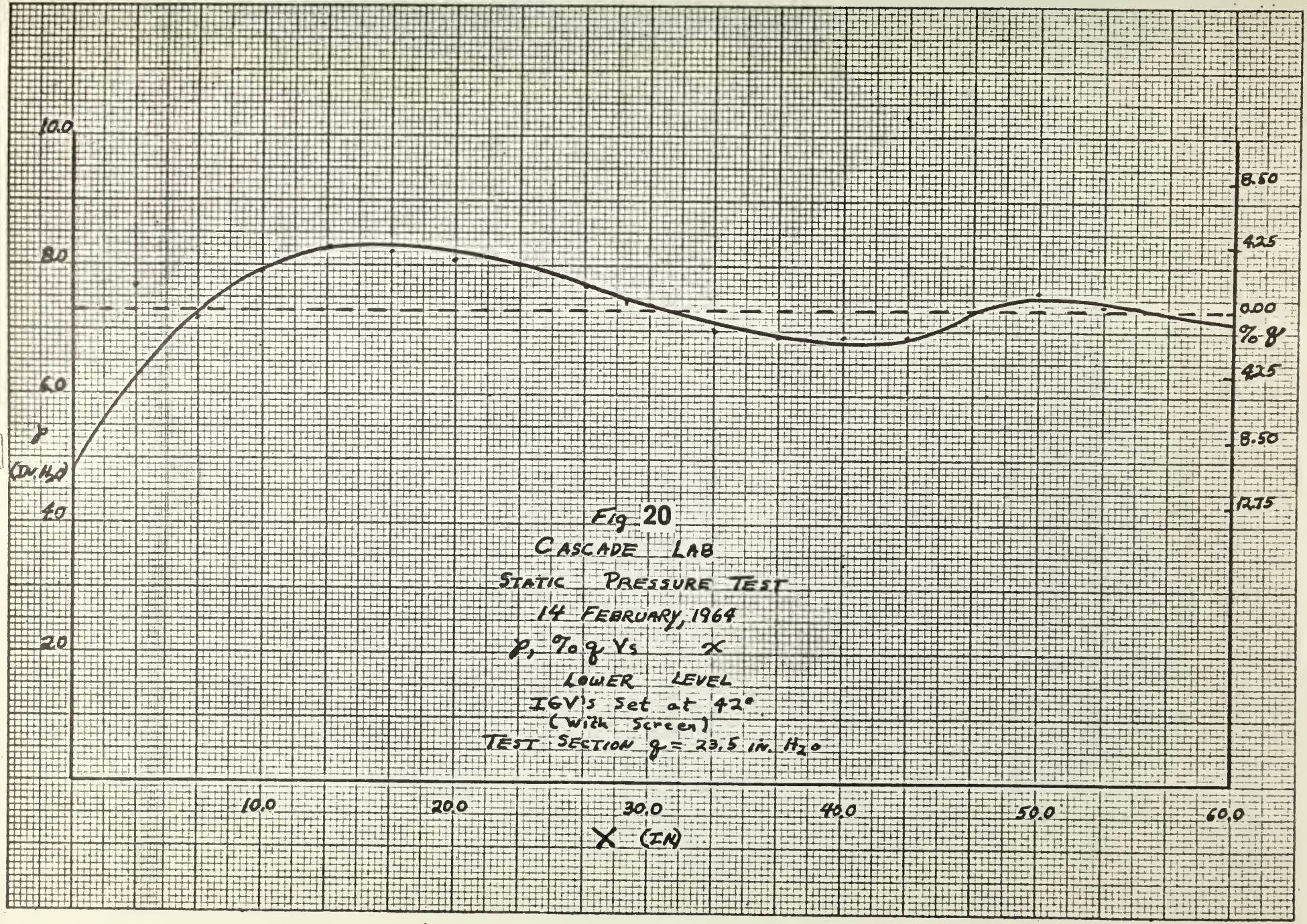

Fig. 20

CASCADE LAB

STATIC PRESSURE TEST

14 FEBRUARY, 1964

p, % q Vs X

LOWER LEVEL

IGV's set at 42°

(with screen)

TEST SECTION q = 23.5 IN. H_2O

guide vanes, test blades, and wall angles were maintained at the same position as in the preceding test. A comparison of Figs. 20 and 21 indicates the variation in operating with and without a fine mesh screen in front of the inlet guide vanes. These figures show that the general shape of the curve remains the same. The variation of the static pressure is 10.1% of the test section dynamic pressure with the screen and 15.2% without the screen.

Due to the excessive loss of total pressure caused by the location of fine mesh screen in this position, it was necessary to remove the screen. However, to reduce the static pressure variation to within 2% of the test section dynamic pressure the flow pattern had to be corrected.

Reference to Fig. 3 shows that the diffusor from the fan exits to a plenum chamber after passing through sound reducing baffles. To prevent the major portion of the air flow from proceeding out of the diffusor and through only the center part of the sound reducing system, a partial screen was installed on the upstream end of the sound reducers. This screen covers only the portion of the sound reducing baffles (described in section 2) that is directly in the flow from the diffusor. The purpose of the screen is to offer a greater resistance to air passing through the center portion of the sound attenuators and thereby forcing the flow to the edges. In this way the flow into the plenum would be more uniform.

Prior to the next run the inlet guide vanes and test blades were removed to eliminate any effects that the blading could have on the flow. The upper and lower end walls were positioned vertically. With this configuration the static pressure as indicated on the multitube manom-

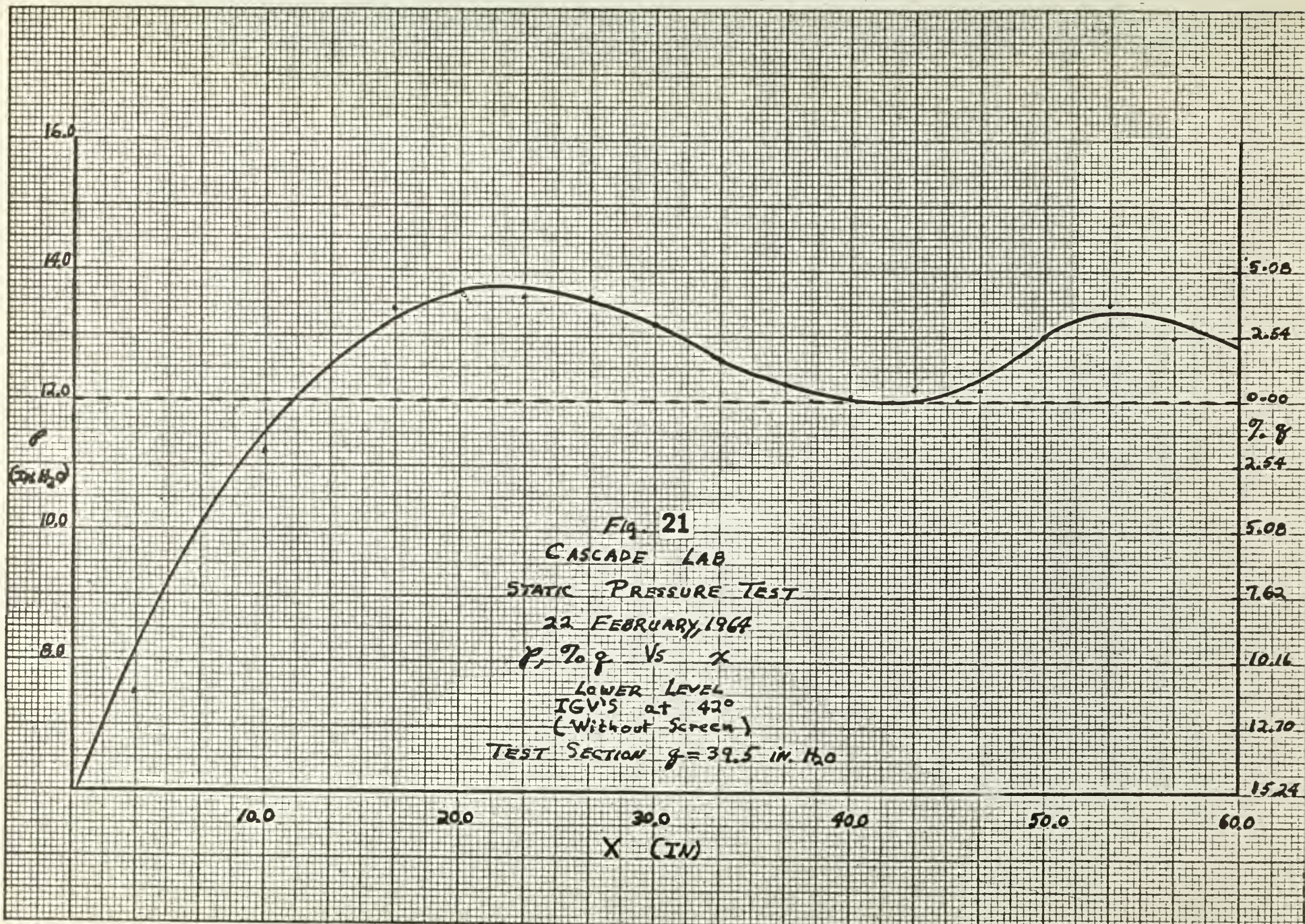

Fig. 21

CASCADE LAB

STATIC PRESSURE TEST

22 FEBRUARY, 1964

p, p_o & Vs x

LOWER LEVEL

IGV'S at 42°

(Without Screen)

TEST SECTION $p = 39.5$ IN. H_2O

eter boards were fluctuating by two inches of water. These fluctuations occurred at such a rapid rate that it was impossible to take readings. These pressure fluctuations could have been caused only by flow irregularities in the plenum chamber. Hence it was necessary to reduce the pressure fluctuations by installing additional screens.

At the entrance to the bell mouth from the plenum chamber a set of two screens were installed. The screens were both fine mesh (20 holes/in., 0.016 in. diam. wire) placed 3½ inches apart. This arrangement produced a symmetric static pressure distribution with a maximum static pressure variation of 0.35 inches of water, Fig. 22. This variation was 1.55% of the test section dynamic pressure and was within the desired limits stated previously.

Locating the screens at the entrance to the bell mouth produced an 8% total pressure drop from 50 to 46 inches of water. This is a considerable improvement over the 42% total pressure drop caused by placing one screen at the bell mouth exit. The reason for this improvement is that the air flow has a lower velocity at the bell mouth entrance, therefore the screens offer less resistance.

5. Evaluation of Test Data

Measurements of the air flow through the test section are taken just ahead of the test blades at station 1 and just behind the test blades at station 2. The data obtained at these stations must be used to find the conditions that would exist far ahead of the test blades at station 0 and far behind the blades at station 3. This must be done in order to account for the mixing loss.

Mixing loss is a nonreversible process in which fluids of

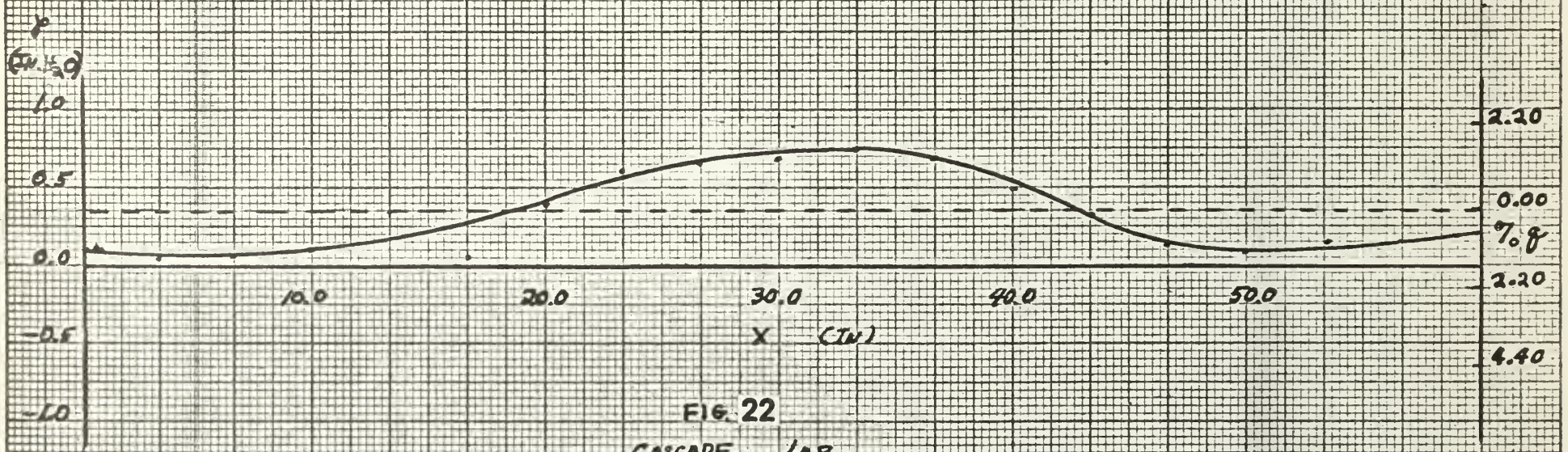

FIG. 22

CASCADE LAB

STATIC PRESSURE TEST

10 APRIL, 1964

p, % p VS X

LOWER LEVEL

TEST SECTION $\bar{p}$ = 22.5 IN. H_2O

different velocities are mixed, resulting in a loss of available energy. Therefore, there is a loss in total pressure due to the equalizing of the flow velocities after the air passes through the test blades. A velocity variation exists behind the test blades due to the blade wakes. The equalizing of the flow occurs because of viscous effects and turbulent mixing. These mixing losses are accounted for by analyzing the flow between stations 0 and 3 since uniform conditions are assumed to exist at these locations.

Appendix A shows how the total pressure, static pressure, the flow angle, and the flow velocity at stations 0 and 3 are determined from the measured data.

In order to find these values the momentum theorem is applied between stations 1 and 0 and between stations 2 and 3. The momentum theorem makes it possible to evaluate the force that the flow exerts on the test blades. This force is determined by equation 5(21) of Ref. 5 as:

$$\vec{R} = \int_{S_1} dm_{S_1} \vec{V}_1 - \int_{S_2} dm_{S_2} \vec{V}_2 + \int_{S_1} -\vec{n} \, p_1 \, dS_1$$

$$+ \int_{S_2} -\vec{n}_2 \, p_2 \, dS_2 + \int_{S_1} -\vec{\tau}_1 \tau_1 \, dS_1 + \int_{S_2} -\vec{\tau}_2 \tau_2 \, dS_2 \quad (1)$$

In the derivation of equations, Appendix A, the last two integrals of equation (1) are ignored. This does not introduce excessive errors as the velocity variations ahead of and after the test section are regular, Figs. 23 and 24. With a regular velocity variation the effects of shear stresses (τ) are small. It is for this reason the last two integrals of equation (1) may be omitted.

The elemental force vector $\vec{dR}$ of equation (1) may be represented by

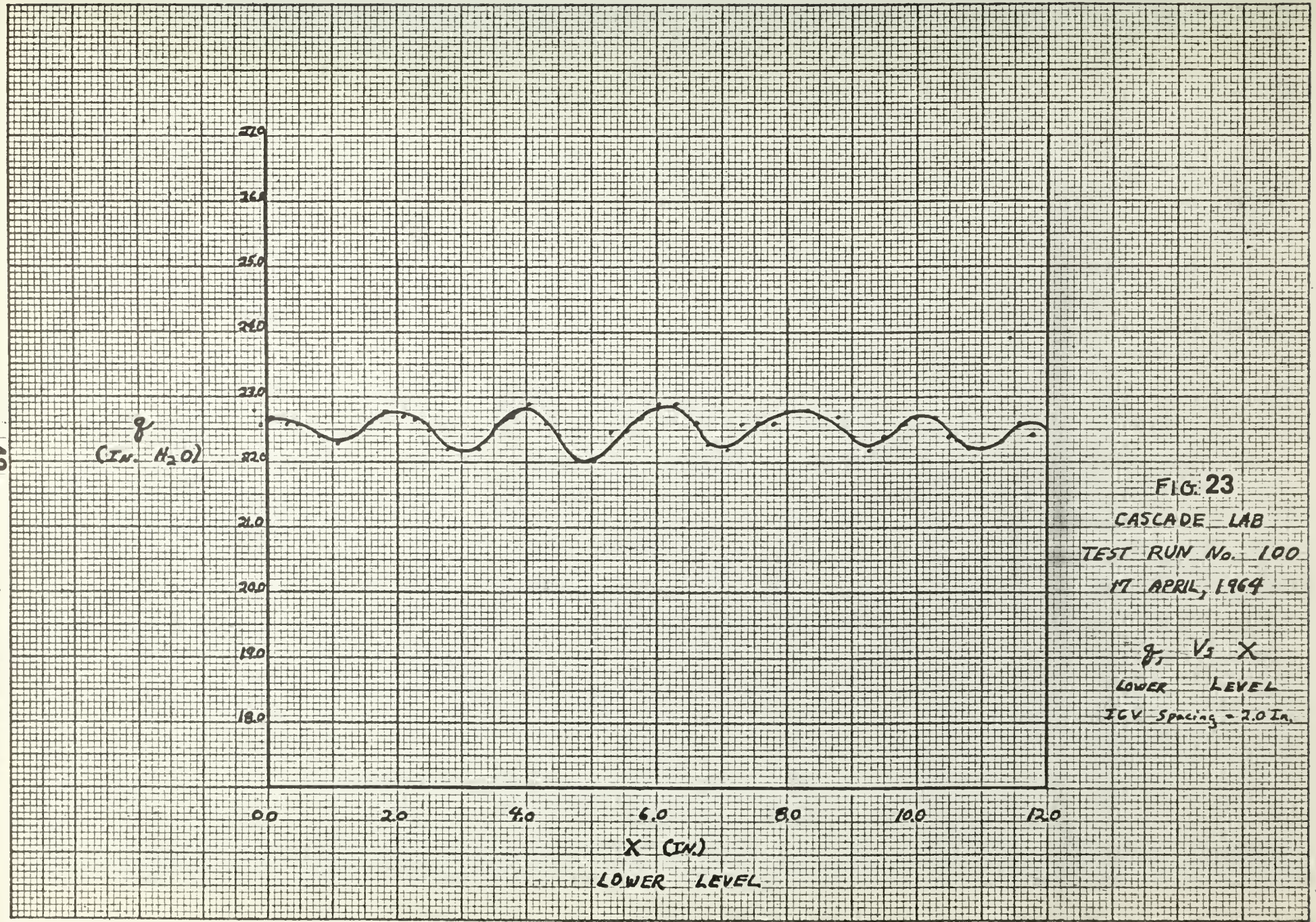

FIG. 23
CASCADE LAB
TEST RUN No. 100
17 APRIL, 1964

q_1 Vs X
LOWER LEVEL
IGV Spacing = 2.0 In.

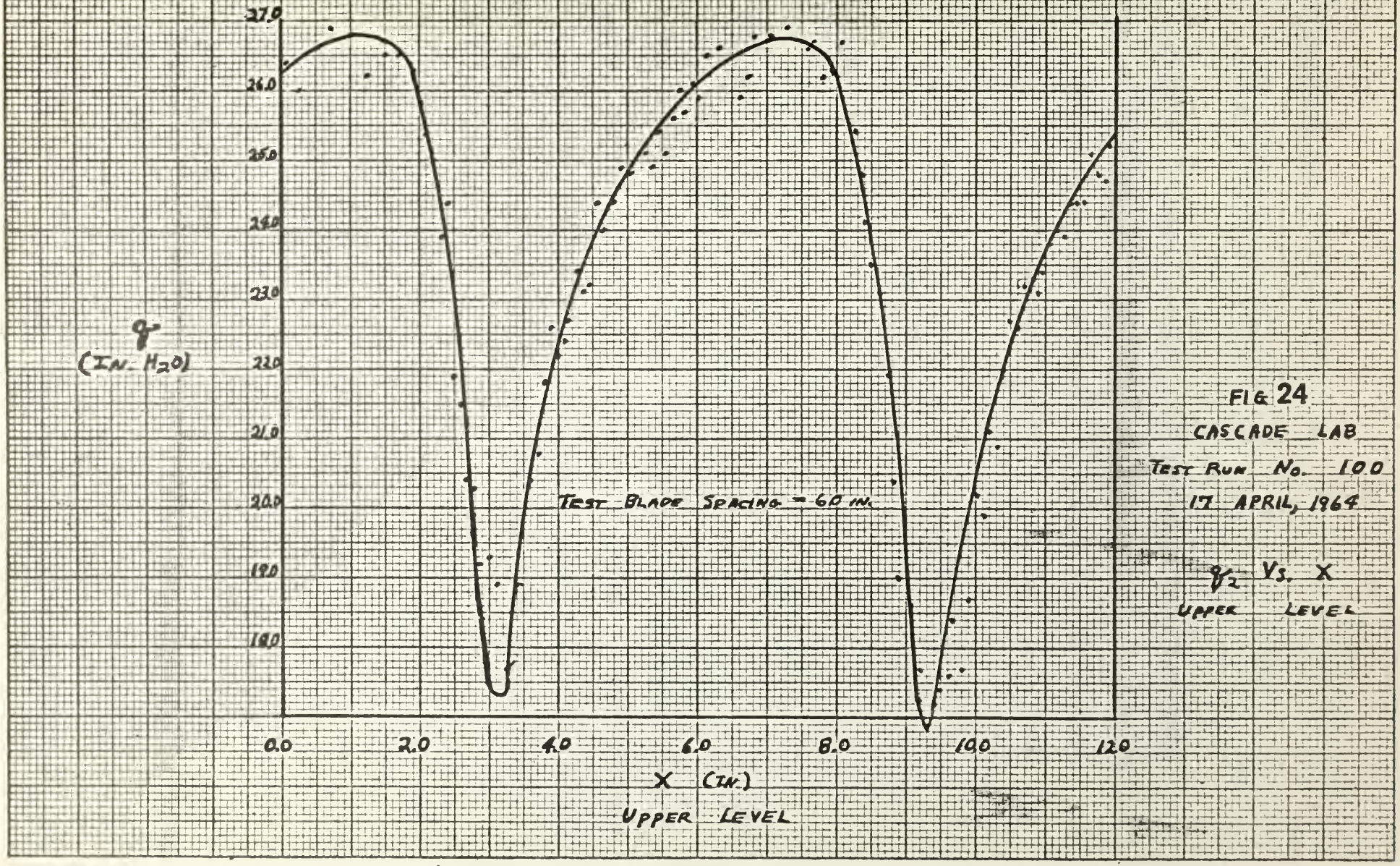

FIG 24
CASCADE LAB
TEST RUN No. 100
17 APRIL, 1964

q_2 VS. X
UPPER LEVEL

its components as:

$$\vec{dR} = \vec{i}\, dR_u + \vec{j}\, dR_a \tag{2}$$

Equation (2) shows the force in the tangential direction represented by the subscript u and in the axial direction by the subscript a. On the cascade the vertical direction $(\vec{j})$ is axial and the horizontal direction $(\vec{i})$ is tangential. The sign convention is as follows:

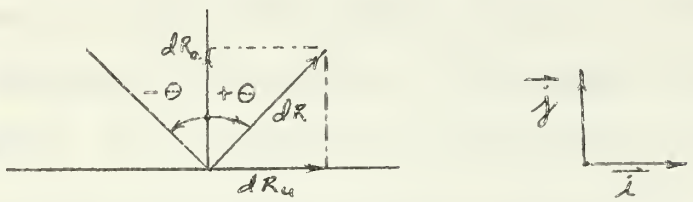

From this:

$$\theta = \tan^{-1}\left(dR_u / dR_a\right) \tag{3}$$

The measured values at stations 1 and 2 are total pressures, static pressures, and flow angles. To be found are the values of total pressures, static pressures, flow angles and velocities at stations 0 and 3. This is done in Appendix A by applying the momentum theorem (1) and the equation of continuity.

The equation of continuity is:

$$m_s = \int \rho_1\, dx\, V_1 \cos\theta_1 = \rho_0\, \Delta x\, V_0 \cos\theta_0$$

$$m_s = \int \rho_2\, dx\, V_2 \cos\theta_2 = \rho_3\, \Delta x\, V_3 \cos\theta_3 \tag{4}$$

Since a Mach number of 0.4 is obtained in the cascade rig, changes in density across the test section were taken into consideration.

The pressures and flow angles vary as a function of position in the x direction. At station 1 this is due to the presence of the wakes from the inlet guide vanes, Fig. 23. At station 2 this variation is caused by the test blade wakes, Fig. 24. Therefore it is necessary to integrate these values over the area tested. The trapezoidal area method of integration is used in the computer program to evaluate these integrals. The advantage of this method is that unequal intervals may be taken as required. In the blade wake a great number of readings must be taken as the velocity distribution changes rapidly with small changes in x. Between the blade wakes the flow velocity does not change as rapidly and a larger interval can be taken. In the blade wake it is necessary to take readings at intervals as small as 0.01 inch, whereas outside of the wakes it is necessary to take readings only every 0.10 inch.

The trapezoidal area method is as follows:

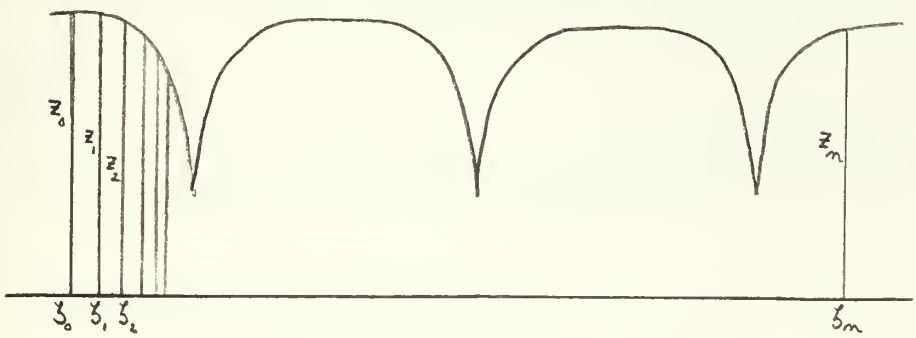

$$\text{AREA} = \tfrac{1}{2}(z_0+z_1)(\zeta_1-\zeta_0) + \tfrac{1}{2}(z_1+z_2)(\zeta_2-\zeta_1) + \cdots \tag{5}$$

$$\text{AREA} = \sum_{i=0}^{m} \tfrac{1}{2}(z_i+z_{i+1})(\zeta_{i+1}-\zeta_i)$$

The variable of integration may be made non-dimensional by :

$$\xi = \frac{x}{N_s} \quad ; \qquad N_s = \Delta x \tag{6}$$

Where: s = blade spacing; N = integer number of blade spacings.

The value for the density of air at stations 0 and 3 is found by:

$$\rho_0 = \int_0^1 \rho_1 \, d\xi \quad ; \qquad \rho_3 = \int_0^1 \rho_2 \, d\xi \tag{7}$$

where ρ_1 and ρ_2 are found by the following equation:

$$\rho = \frac{1}{a_p^2} \int_0^1 P\left(\gamma - \frac{\Delta P}{P}\right) d\xi \quad ; \quad a_p^2 = \gamma g R T_p \tag{8}$$

Equation (8) of Appendix A is as follows:

$$\rho_0 = \frac{1}{\Delta x} \int_{x_2}^{x_2} \rho_1 \, dx + \frac{1}{\Delta x} \int_{x_2}^{x_2} \rho_1 V_1^2 \cos^2\theta_1 \, dx - \frac{1}{\rho_0} \left[\frac{1}{\Delta x} \int_{x_2}^{x_2} \rho_1 V_1 \cos\theta_1 \, dx \right]^2 \tag{9}$$

This may be re-written by substitution in the last two integrals of:

$$\rho V^2 = 2 \Delta P \tag{10}$$

where: $\Delta P = P - p$

and:

$$\rho V = \sqrt{2 \rho \Delta P} = \sqrt{\frac{2 \Delta P}{a_p^2} (P\gamma - \Delta P)} \tag{11}$$

giving:

$$\rho_0 = \int_0^1 \rho_1 \, d\xi + 2 \int_0^1 \Delta P \cos^2\theta_1 \, d\xi - \frac{2}{\rho_0 a_p^2} \left[\int_0^1 \sqrt{\Delta P (\gamma P - \Delta P)} \cos\theta \, d\xi \right]^2 \tag{12}$$

Equation (10) of Appendix A is:

$$\tan\theta_0 = \frac{\rho_0 \Delta x}{2} \, \frac{\int_{x_2}^{x_2} \rho_1 V_1^2 \sin(2\theta_1) \, dx}{\left[\int_{x_2}^{x_2} \rho_1 V_1 \cos\theta_1 \, dx \right]^2} \tag{13}$$

Using (10) and (11) this may be re-written in the form:

$$\theta_0 = \tan^{-1} \frac{\rho_0 a_p^2}{2} \frac{\int_0^1 \Delta P_1 \sin(2\theta_1)\, d\xi}{\left[\int_0^1 \sqrt{\Delta P_1 (P_1\gamma - \Delta P_1)} \cos\theta_1\, d\xi\right]^2} \tag{14}$$

Equation (11) of appendix A is:

$$V_0^2 = \frac{1}{4} \frac{\left[\int_{x_\ell}^{x_e} \rho_1 V_1^2 \sin(2\theta_1)\, dx\right]^2}{\left[\int_{x_\ell}^{x_e} \rho_1 V_1 \cos\theta_1\, dx\right]^2} + \frac{1}{\rho_0^2 \Delta x^2}\left[\int_{x_\ell}^{x_e} \rho_1 V_1 \cos\theta_1\, dx\right]^2 \tag{15}$$

Again using (10) and (11) this gives:

$$V_0^2 = \frac{a_p^2}{2} \frac{\left[\int_0^1 \Delta P_1 \sin(2\theta_1)\, d\xi\right]^2}{\left[\int_0^1 \sqrt{\Delta P_1 (\gamma P_1 - \Delta P_1)} \cos\theta_1\, d\xi\right]^2} + \frac{2}{a_p^2 \rho_0^2}\left[\int_0^1 \sqrt{\Delta P_1 (\gamma P_1 - \Delta P_1)} \cos\theta_1\, d\xi\right]^2 \tag{16}$$

Total pressure at station 0 is found from:

$$P_0 = p_0 + \frac{\rho_0}{2} V_0^2 \tag{17}$$

The above procedure is repeated to find the conditions at station 3 by substituting the subscript 3 for 0 and 2 for 1.

These equations determine the total and static pressures, the angle and the velocity of flow at stations far upstream and downstream from the test section where uniform conditions exist.

The forces on the blades per unit blade height were found as follows:

From equation (1):

$$d\vec{R} = m_{s0}(\vec{i} V_0 \sin\theta_0 + \vec{j} V_0 \cos\theta_0) - m_{s3}(\vec{i} V_3 \sin\theta_3 + \vec{j} V_3 \cos\theta_3) + \vec{j}(p_0 - p_3) s \tag{18}$$

Resolving into components:

$$dR_a = m_{s0} V_0 \sin\theta_0 - m_{s3} V_3 \sin\theta_3 = \rho_0 s V_0^2 \cos\theta_0 \sin\theta_0 - \rho_3 s V_3^2 \cos\theta_3 \sin\theta_3 \tag{19}$$

$$dR_a = m_{s0} V_0 \cos\theta_0 - m_{s3} V_3 \cos\theta_3 + (p_0 - p_3) s$$

$$dR_a = \rho_0 s V_0^2 \cos^2\theta_0 - \rho_3 s V_3^2 \cos^2\theta_3 + (p_0 - p_3) s \tag{20}$$

Therefore:

$$d R_u = \tfrac{1}{2} S(\rho_0 V_0^2 \sin 2\theta_0 - \rho_3 V_3^2 \sin 2\theta_3) \tag{21}$$

$$d R_a = S(\rho_0 V_0^2 \cos^2\theta_0 - \rho_3 V_3^2 \cos^2\theta_3 + p_0 - p_3) \tag{22}$$

The lift and drag forces on the blade are determined from these values. This is accomplished by solving for $\vec{V}_\infty$.

For individual airfoils $\vec{V}_\infty$ is the velocity at an infinite distance from the airfoil. In a rectilinear cascade $\vec{V}_\infty$ is the mean vectorial velocity shown on Fig. 25 and represented by:

$$\vec{V}_\infty = \tfrac{1}{2}(\vec{V}_0 + \vec{V}_3); \quad V_a = V \sin\theta \; ; \quad V_u = V \cos\theta \tag{23}$$

$$V_\infty = \tfrac{1}{2}\sqrt{(V_{a0} + V_{a3})^2 + (V_{u0} + V_{u3})^2} \tag{24}$$

$$\theta_\infty = \tan^{-1} \frac{(V_{u0} + V_{u3})}{(V_{a0} + V_{a3})} \tag{25}$$

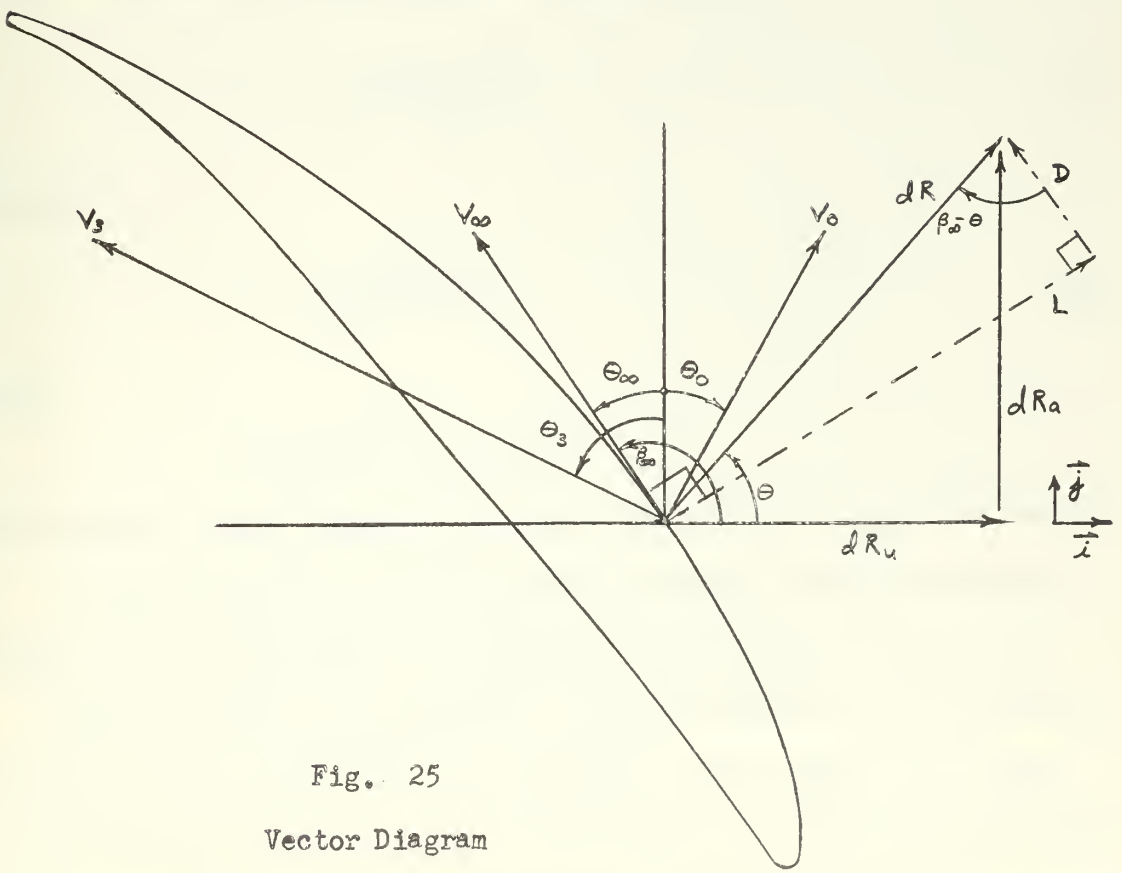

Fig. 25

Vector Diagram

Lift is the component of the force acting on the blades that is perpendicular to $\vec{V_\infty}$. Drag is the force component that is parallel to $\vec{V_\infty}$. From Fig. 25, β_∞ is defined as the angle from the horizontal to $\vec{V_\infty}$. The angle θ between $\vec{dR}$ and its horizontal component is known from equation (3). The sum of the lift and drag vectors must equal the force $\vec{dR}$ on the blade.

$$\vec{dR} = \vec{L} + \vec{D} \tag{26}$$
$$\vec{L} = \vec{dR} \sin(\beta_\infty - \theta)$$
$$\vec{D} = \vec{dR} \cos(\beta_\infty - \theta)$$

Therefore all of the vectors on Fig. 25 are known.

In order to non-dimensionalize lift and drag the coefficients of lift and drag are used. The coefficient of lift is defined as the lift force divided by the product of the test blade chord and dynamic pressure. The dynamic pressure is based on the velocity V_∞.

$$C_L = \frac{L}{\frac{1}{2}\rho V_\infty^2 c} \tag{27}$$

Likewise:

$$C_D = \frac{D}{\frac{1}{2}\rho V_\infty^2 c} \tag{28}$$

where:

$$\rho = \frac{1}{2}(\rho_0 + \rho_3)$$

NACA in Ref. 3 bases dynamic pressure on the velocity V_0 and the density ρ_0. However, since V_∞ is the factor that fixes the lift and drag vectors it is more logical to define the coefficients by this value.

The total loss in the cascade is the difference in total pressures far upstream and downstream of the cascade. This total loss is given by the loss coefficient ζ. The coefficient ζ includes the mixing and

frictional losses in stationary cascades for both accelerated and decelerated flows. Therefore the total loss of the cascade, as developed in Appendix A, is defined as:

$$\zeta = \frac{(p_0 + \frac{1}{2}\rho_0 V_0^2) - (p_3 + \frac{1}{2}\rho_0 V_3^2)}{(p_0 + \frac{1}{2}\rho_0 V_0^2) - p_3} \tag{29}$$

6. Discussion of Results

The results calculated from the test run are listed in Table II. These results are compared with NACA TN 3802 results, Ref. 3, in Table III.

Table II is the output of the computer program for the test run. The computer program is included in Appendix B. Table II indicates that the flow accelerates slightly from 312.49 ft./sec. ahead of the test blades to 322.32 ft./sec. after the test blades. The inlet flow angle was 43.63 deg. and the outlet flow angle was -46.18 deg. The value for V_∞ was 224.86 ft./sec. at an angle of -2.16 deg. These vectors are shown on Fig. 25.

The total force per test blade is 120.58 lb./ft. This total force is composed of a lift force of 120.07 lb./ft. and a drag force of 11.10 lb./ft.

The coefficient of lift is 2.8223 and the coefficient of drag is 0.2609. These coefficients are based on V_∞ and the average of the fluid densities at stations 0 and 3.

The flow deflection is the difference between the inlet flow angle and the outlet flow angle. For the test run this value was 43.63 deg. minus -46.18 deg. or 89.81 deg.

Fig. 15(5) of Ref. 5 is a plot of the variation of velocity

TABLE II

CASCADE LABORATORY
U.S. NAVAL POSTGRADUATE SCHOOL

TEST RUN NO. 100

BAROMETRIC PRESS. 29.98 IN. HG.

AMBIENT TEMP. 66.5 DEG. F.

VO (FT/SEC)	THETA 0 (DEG)	V3 (FT/SEC)	THETA 3 (DEG)	V INF (FT/SEC)	THETA INF (DEG)	BETA (DEG)
312.49	43.63	322.32	-46.18	224.86	-2.16	92.17

AXIAL FORCE (LB/FT)	TANGENTIAL FORCE (LB/FT)	TOTAL FORCE (LB/FT)	THETA (DEG)	LIFT (LB/FT)	DRAG (LB/FT)
15.62	119.56	120.58	7.44	120.07	11.10

NON-DIMENSIONAL COEFFICIENTS

LIFT	DRAG	LOSS
2.8223	.2609	.1334

LEGEND

VO = V_0, velocity at station 0
THETA 0 = θ_0, angle between $\vec{j}$ and $\vec{V}_0$
V3 = V_3, velocity at station 3
V INF = V_∞, vectorial mean of $\vec{V}_0$ and $\vec{V}_3$
THETA INF = θ_∞, angle between $\vec{j}$ and $\vec{V}_\infty$
BETA = β_∞, angle between $\vec{i}$ and $\vec{V}_\infty$
AXIAL FORCE = $d\vec{R}_a$, $\vec{j}$ component of force per blade
TANGENTIAL FORCE = $d\vec{R}_u$, $\vec{i}$ component of force per blade
TOTAL FORCE = $d\vec{R}$, force per blade
THETA = θ, angle between $\vec{i}$ and $d\vec{R}$
THETA 3 = θ_3, angle between $\vec{j}$ and $\vec{V}_3$

TABLE III

COMPARISON OF RESULTS

	TN 3802	TN 3802	USNPGS
σ	1.8	1.5	1.415
θ_1	45°	45°	43.63°
θ_c	95°	95°	95°
θ	94.4°	93.0°	89.81°
C_{Lo}	1.239	1.362	1.453
C_{Do}	.0236	.0227	.1343
Re	0.5×10^6	0.5×10^6	1.4×10^6

LEGEND

θ = Turning angle of air

θ_c = Angle between tangents to camber line at leading and trailing edges

coefficient with respect to flow deflection. Velocity coefficient ψ is related to the loss coefficient ζ by:

$$\zeta = 1 - \psi^2$$

Using this relation Ref. 5 gives a loss coefficient of 0.1338 for wide blades. Table II indicates a loss coefficient of 0.1334.

In the comparison on Table III it must be taken into consideration that slightly different test conditions existed between the present cascade and the cascade of Ref. 3. The solidity of the present cascade was 1.415 whereas 1.5 is the closest value with which a comparison could be made with TN 3802. The 1.8 solidity values of TN 3802 are included to show the effect of solidity on the various parameters.

From Table III the inlet flow angle of the present cascade was 43.63 deg. This is 1.37 deg. less than the inlet angle of TN 3802. A lower inlet angle indicates a lower angle of attack on the blades. The turning angle of the flow was also found to be 3.19 deg. less than the 1.5 solidity case and 4.59 deg. less than the 1.8 solidity case. For a given inlet angle, cascades of high solidity have greater turning angles than low solidity cascades as the flow is guided more exactly. Fig. 51 of Ref. 3 indicates the deviation of the leaving flow direction for this blade profile at 1.5 and 1.8 solidity. A greater angle between leaving flow direction and trailing-edge meanline direction exists for the lower solidity. For a leaving flow angle of 46.18 deg. this reference gives a deviation of 5.5 deg. for solidity of 1.5. This indicates that the actual turning angle of the TN 3802 blade should be 89.5 deg. The turning angle for a cascade of 1.415 solidity should be less than 89.5 deg. However, a turning angle of 89.81 deg. was obtained. This discrepancy may be due to the interpolation error in reading Fig. 51 of Ref. 3.

The lift and drag coefficients are based on the upstream dynamic

pressure in order to compare them with values from TN 3802.

The lift coefficients of TN 3802 are 1.239 for a solidity of 1.8 and 1.362 for a solidity of 1.5. A lift coefficient of 1.453 for a solidity of 1.415 was obtained for the present cascade.

At given inlet flow angles and solidities, the flow deflection is a measure of blade loading. Table III indicates that with decreasing solidity there is a decrease in turning angle and an increase in the lift coefficient. This increase in the lift coefficient appears to be a discrepancy as a smaller turning angle should produce less lift. However, separation must occur at the higher turning angles and thus reduce the lift coefficient.

The coefficients of drag from Table III are 0.0236 for 1.8 solidity and 0.0227 for 1.5 solidity of the NACA cascade. The coefficient of drag for the present cascade is 0.1343.

A cascade with a large number of blades will have large frictional effects on the surfaces of these blades. In other words, skin friction drag increases as solidity increases. This is shown on Table III where the drag coefficient increases from 0.0227 to 0.0236 as solidity increases from 1.5 to 1.8. However, the drag coefficient for the present cascade is 0.1343 for a solidity of 1.415.

To analyze these results it is necessary to examine the two cascade rigs involved. In the NACA cascade the boundary layer was removed for reasons stated in Section 2. In the present cascade the boundary layer was not removed.

The removal of the boundary layer makes the flow more nearly ideal and reduces the secondary losses. Secondary losses are caused by the interaction of the blade ends with the boundary layer on the walls. The

secondary losses predominate over all other losses at large angles of deflection.

Fig. 24 is a plot of $1/2\, \rho_2 V_2^2$. This figure shows the large velocity deficit that is present after the test blades. This velocity deficit is included in the loss coefficient ζ of Table II. The loss coefficient is related to the drag coefficient by equation 13(11) of Ref. 5. This equation is for compressor blades but is also applicable to turbine blades. Equation 13(11) is rewritten as:

$$C_D = \frac{\zeta}{\sigma} \frac{\cos^3 \theta_\infty}{\cos^2 \theta_3}$$

Using this equation with the results of Table II gives a coefficient of drag of 0.1926.

The test Reynolds number for NACA TN 3802 was 0.5×10^6. The test Reynolds number for the present cascade was 1.4×10^6. This is a small variation in Reynolds number and could not be a factor in the comparison of results.

Fig. 23 is a graph showing the variation of dynamic pressure (P_1-p_1) with respect to x. These measurements were taken on the lower traverse (station 1). The curve passes through a maximum and minimum dynamic pressure at two inch intervals. The minimum q values represent the wakes of the inlet guide vanes which are spaced two inches apart.

Fig. 24 is a graph of dynamic pressure (P_2-p_2) variation with respect to distance in the x direction for the upper traverse. On this figure the minimum and maximum values of q occur at six inch intervals. The minimum dynamic pressure is the center of a wake from the test blades which are spaced six inches apart. The spread of the points on Fig. 24 is an indication of the non-uniformity of the flow after passing

through the test blades. This non-uniformity is more pronounced on Fig. 24 than on Fig. 23 as the measurements are taken closer to the blades. Fig. 23 then shows how the flow tends to become more uniform as it progresses downstream.

Fig. 26 is a plot of static pressure variation with respect to the x distance. This figure shows the variation for both the upper and lower traverses. The readings of the static pressure by the measuring equipment are accurate to $\pm$0.1 inch of water pressure. The maximum variation of static pressure on the lower level was 0.2 inch of water from 2.2 to 2.4 inches. In other words the possible error is 50% of the maximum variation. For this reason the curve does not present a good picture of the static pressure distribution. However it does show that there is no static pressure gradient throughout the test section.

The upper level curve of Fig. 26 indicates two areas of high static pressures at 4.5 inches and 10.5 inches. These peaks indicate the wakes of the test blades or areas of reduced dynamic pressure. The peaks occur at the test blade spacing of six inches. The variations on the pressure side of the wake are due to the wakes of the inlet guide vanes.

Fig. 27 is a graph of flow angle variation with respect to x distance. The lower graph on this figure shows the variation of flow angle as measured by the lower traverse. The accuracy of the measuring equipment for flow angle is $\pm$0.2 deg. The maximum variation of the flow angle was 1.2 deg. from 44.4 to 43.2. This is a 16.7% error and reduces the value of the graph to a point where no definite statements may be made.

The upper level indicates maximum flow angles at a six inch

FIG. 26

STATIC PRESSURE VARIATIONS

Test Run No. 100

17 April, 1964

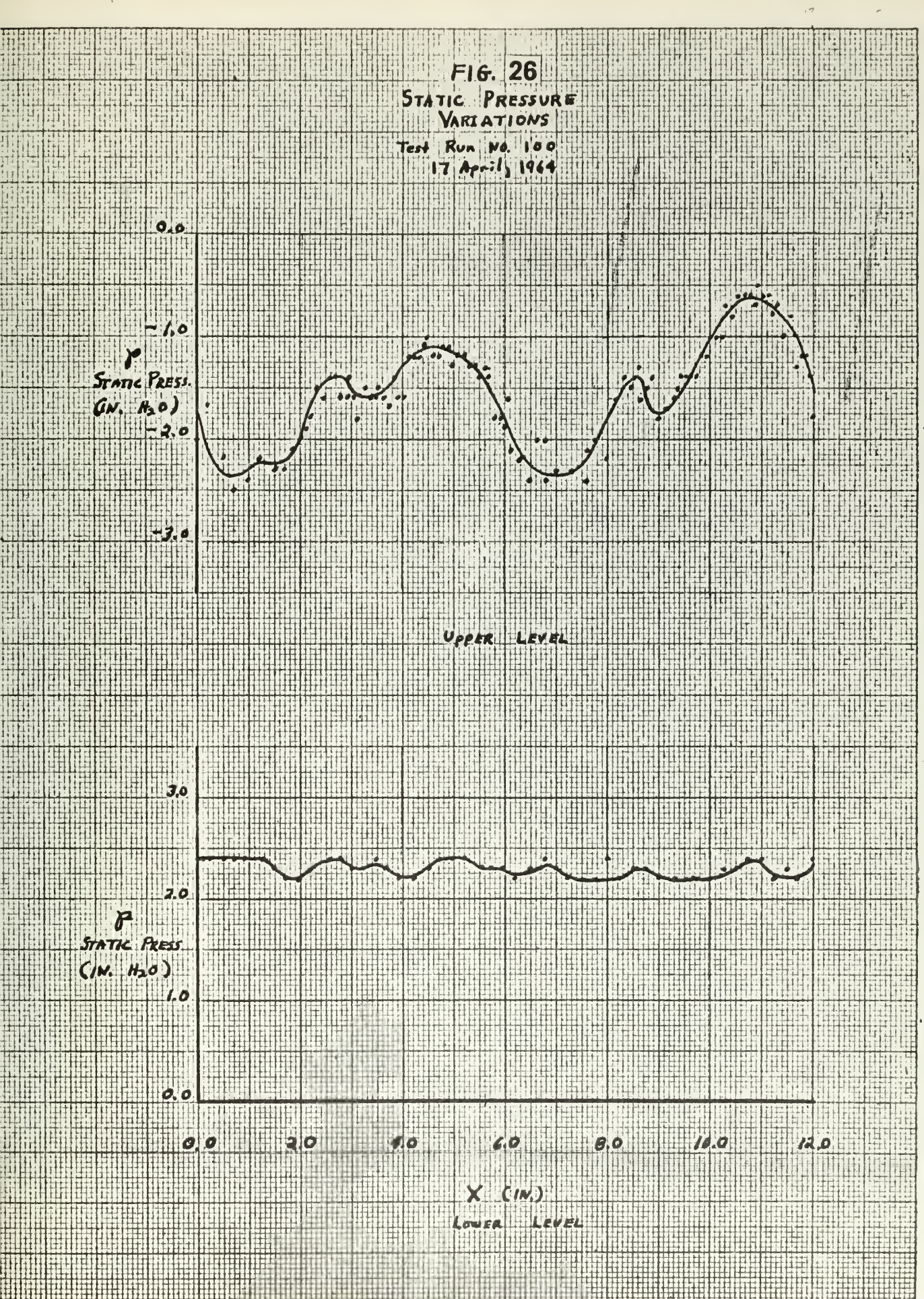

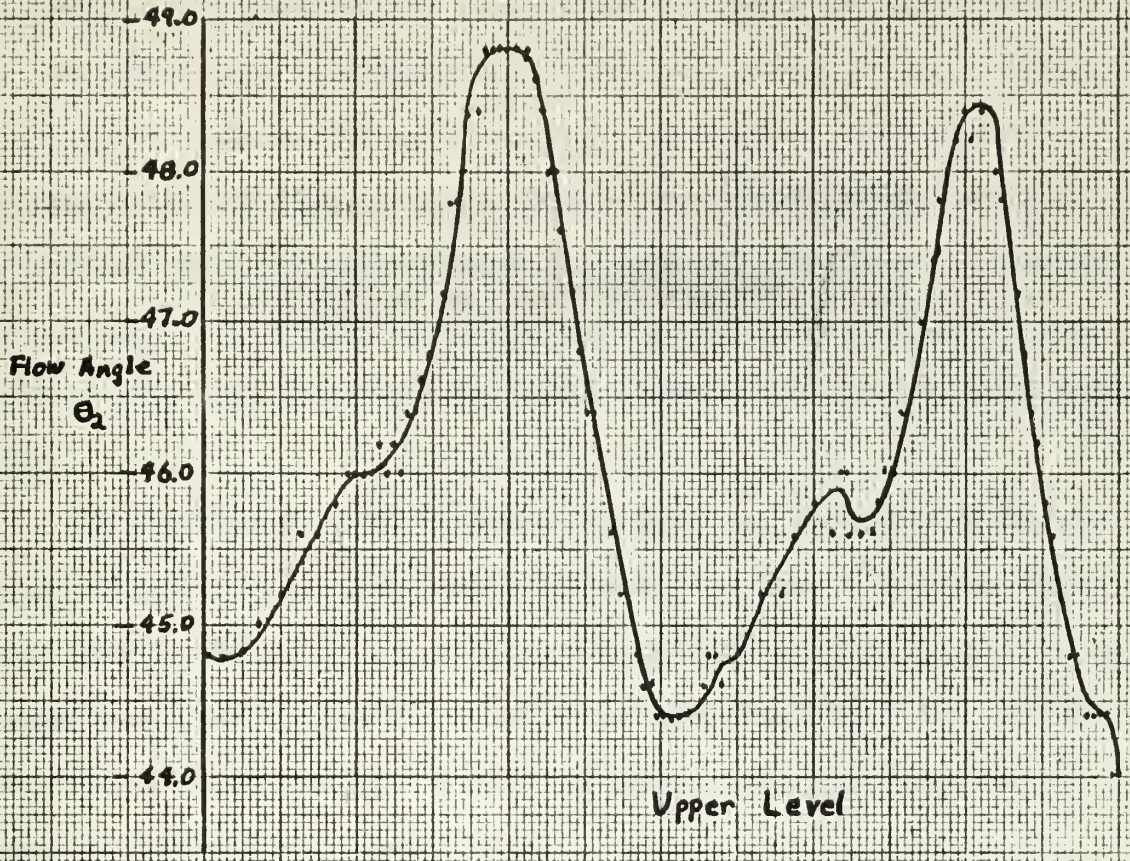

FIG. 27
FLOW ANGLE
VARIATIONS
Test Run No. 100
17 April, 1964

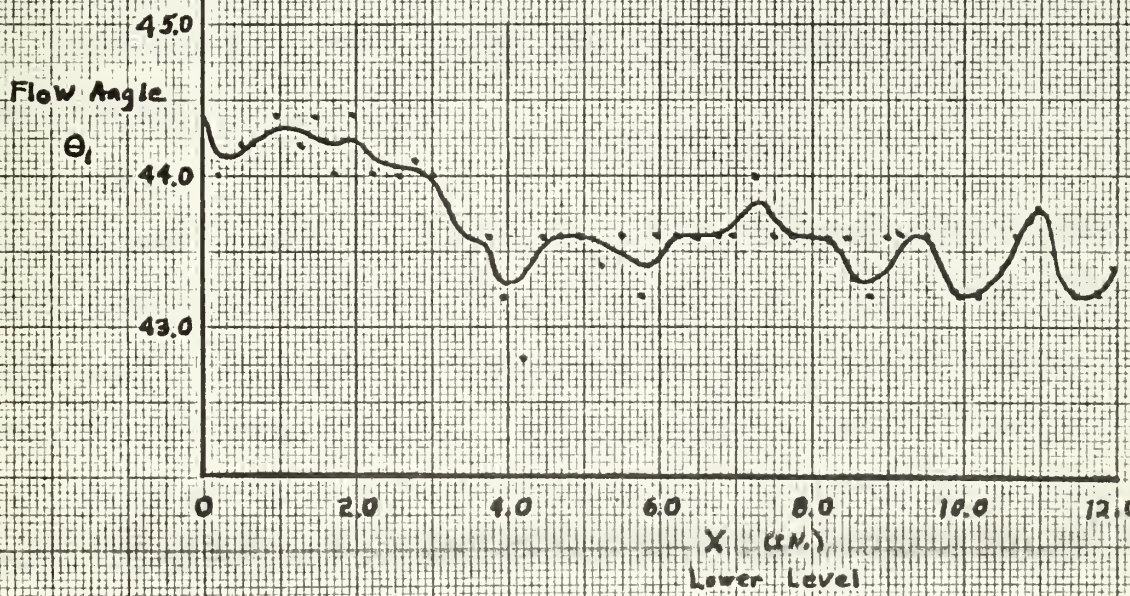

interval. This again is due to the wakes following the test blades. As the value for x increases the flow angles are read from the pressure side of the blade to the suction side. The slope of the flow angle curve is symmetric with respect to the peak. This indicates that the flow experiences the same angle change with respect to distance on each side of the wake. The slight variations in the flow angle on the pressure side of each peak at 2.0 and 8.0 inches are due to the inlet guide vane wakes.

The variations in the outlet flow angles and the static pressures behind the test blades show the effects of the inlet guide vane wakes. This also is the cause of the scatter of points in Fig. 24, the plot of downstream dynamic pressure. This shows the advantage of this unique test rig in approximating the flow obtained in turbomachinery as compared to conventional cascade rigs.

In section 4, Static Pressure Distribution, it is indicated that the inlet guide vanes were set at 42 deg. in order to obtain the acceptable static pressure distribution.

With the vanes set at 42 deg. the inlet flow angle was found to be 43.63 deg. The relation:

$$\alpha_a^* = \cos^{-1} \sigma_s$$

as mentioned in section 4 indicated that the guide vanes should be set at 45 deg. This relation can be used to find a first approximation for inlet guide vane settings. However, the position of the inlet guide vanes must be adjusted to give a static pressure variation of less than 2.0% of the test section dynamic pressure and the required inlet flow angle. Therefore, the above equation must be used only as an approximation. The inlet flow angle and static pressure distribution are

factors that must be considered in positioning the inlet guide vanes.

7. General Discussion

During the earlier tests adverse pressure gradients were present in the test section. It was determined that these gradients were caused by flow irregularities that entered the bell mouth from the plenum. The main contributor to the irregularities was the sound attenuating baffles shown in Fig. 4. The size and shape of these baffles are completely unsatisfactory. The blunt upstream end of each baffle is $8\frac{1}{2}$ inches in width, extends from the floor to the ceiling, and is $3\frac{1}{2}$ inches horizontally from the next baffle. The downstream end of each baffle is slightly less blunt but this is not considered sufficient to prevent separation. Also the area reduction caused by the baffles (3.4:1) accelerates the air at a position where deceleration is desired.

These baffles create large turbulent wakes which prevent the velocity from being equal over the cross section of the plenum. They were installed without regard to the aerodynamic conditions as an afterthought which proved to have bad consequences. These baffles are not needed as the noise is produced by the Mach 0.4 air passing through the cascade rig and not by the blower.

During the installation of the screen on the sound reducing baffles it was discovered that the diffusor was warped. This was caused when the outer frames were welded onto the diffusor walls. These frames are located about every three feet along the diffusor. The walls have deflections of about one inch between each pair of frames. This warping causes additional irregularities in the air flow.

The original design included a bell mouth at the exit of the diffusor.

In addition, screen attachments were to be installed on the walls at the bell mouth exit. The installation of several screens at this position would have ensured an equal velocity distribution over the cross section of the plenum. The installation of the sound baffles eliminated the space available for this arrangement.

Installing two wire screens at the entrance of the cascade rig bell mouth gave the best results in smoothing out the flow irregularities. This configuration produced a static pressure variation of only 1.55% of test section dynamic pressure and a total pressure loss of only 8%.

There was some difficulty in setting the inlet guide vanes to the proper angles. This was due to the fact that the vanes are not identical. Some fixture is required to determine which blades have the proper shape and alignment. A similar fixture is required for each test blade shape.

The automatic data logging system performed as desired.

The Friden paper tape punch used in the automatic data logging system uses one inch, 8 level paper tape. This tape has eight bits per frame, i.e. eight holes per line. Standard systems use 7/8 inch, 7 level tape which has seven bits per frame. This was the system used by the Control Data Corporation 1604 computer located at the U. S. Naval Postgraduate School. The computer was modified by the Computer Center to be able to read 8 level tapes.

The computer program used for the data reduction was written in Fortran 60 language. A difficult part of the program was the coding for the reading of the punched paper tape. This part of the program was written in Symbolic Fortran by Mrs. Carol Hayworth, a programer for the

Computer Center. The computer program is listed and explained in Appendix B.

The paper tape supplied with the Friden punch was pink, oiled tape. This proved too transparent for the photo-electric reader to properly decode. To solve this problem the punched paper tape was colored black with a quick drying marker ink. Future data will be punched on black paper tape.

8. Conclusions

The results obtained in this work indicated that the cascade rig will perform its function properly but modifications are necessary. It can be expected, therefore, that the rectilinear cascade test rig will become a valuable research toolwhich can be used to establish more precise design data for existing and future cascades. Such data will make it possible to design axial-flow machines more accurately and save considerable development time.

The data logging system proved to be a labor and time conserving device. For example, an average test run would cover at least three blade spacings. The x distance involved would vary depending on the blade spacing. Measurements of distances, flow angles, and total and static pressures must be taken on an average every 0.05 inch. This would require roughly 700 readings of each value for the six inch blade spacing on each plane in the y direction. Without the punched paper tape this data must be transcribed to punched cards for the computer input. This would involve about 30 man hours of labor to do what can be accomplished in two man hours with the data logging system.

9. Recommendations

It is recommended that additional modifications be made to the cascade rig in order to improve the flow in the test section. Static pressure variation of less than one percent should be obtained with a zero pressure gradient.

The following are the steps required to obtain this improved flow:

Eliminate the effects of the warped diffusor. This could be accomplished by lining the diffusor with plywood walls. These wooden walls could be attached to the metal walls with countersunk bolts.

Then the diffusor should be modified with an addition of a hyperbolic divergence bell mouth. This was in the original design but was eliminated in the latter stages of planning when it was decided to install the sound baffles.

At the exit of the bell mouth a large number of screens could be attached to the side walls of the chamber. These screens would offer greater resistance to the higher velocities and thus smooth out disturbances in the flow. With these modifications the air would leave the modified diffusor section at a lower velocity and more uniformly.

These modifications require the removal of the sound baffles in the plenum chamber. Diffusors of the type described have been used with success in wind tunnels. Since the sound baffles have a very unfavorable aerodynamic shape, their removal would produce a considerable improvement of the flow conditions ahead of the cascade. These baffles are not required as the noise is created by the Mach 0.4 air passing through the cascade rig and not by the blower.

To measure the total pressure in the plenum chamber it is recommended that a copper tube of 1/8 in. inner diameter be installed in

the conduit which is used for the total temperature probe.

Fixtures should be constructed to check the profiles and alignments of the test blades and the inlet guide vanes. In each case the profile should be checked at several positions along the blade height.

For low and medium speed tests, the data logging system should be recalibrated to measure the static pressures to 0.01 inches of water. This will provide more accurate results and better plots of the static pressure distribution.

REFERENCES

1. Fahland, F. R. and L. L. Hawkins, An Electrical Analogy for Analysis of Flow Through Cascades, 1958, U. S. Naval Postgraduate School, Monterey, Calif.

2. Eshman, J. R., Investigation of a Two-Dimensional Low-Speed Cascade, 1959, U. S. Naval Postgraduate School, Monterey, Calif.

3. Dunavant, J. C. and J. R. Erwin, Investigation of a Related Series of Turbine-Blade Profiles in Cascade, NACA TN 3802, October, 1956.

4. Ainley, D. G. and G. C. R. Mathieson, A Method of Performance Estimation for Axial-Flow Turbines, Reports and Memoranda No. 2974, December, 1951.

5. Vavra, M. H., Aero-Thermodynamics and Flow in Turbomachines, 1960, 1st ed., John Wiley & Sons, Inc., New York.

Appendix A

DERIVATION OF EQUATIONS

1. SYMBOLS

p = static pressure

P = total pressure

$q = \frac{1}{2}\rho V^2$

V = velocity

ρ = mass density

x = distance along cascade axis

Θ = flow angle

Indices:

(0) far ahead of cascade

(1) measuring plane ahead of cascade

(2) " " after cascade

(3) far aft of cascade

2. CONDITIONS FAR AHEAD OF CASCADE

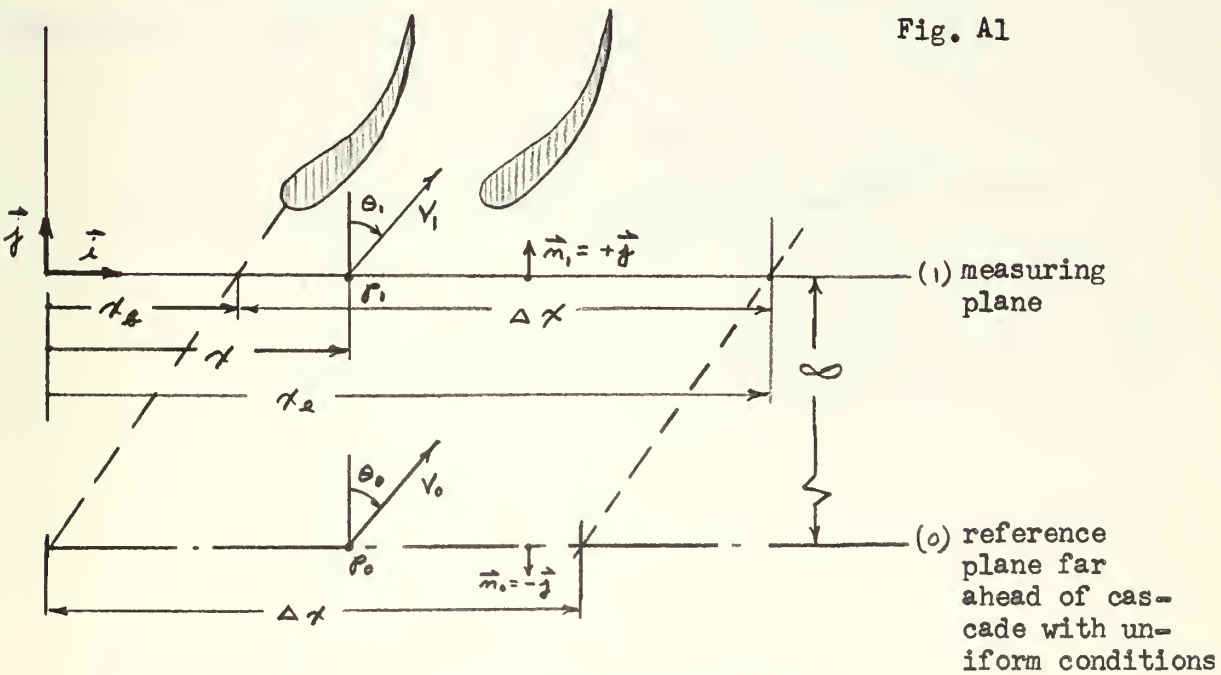

Fig. A1

Measured Values: P_1 ; p_1 ; Θ_1 as functions of x

To be determined: P_0, p_0, Θ_0, V_0

From Eq. 5(21) Ref. 5 for $\vec{R} = o$, ignoring shear stress integrals τ

$$\int_{(o)} dm_s \vec{V}_o - \int_{(1)} dm_s \vec{V}_1 + \vec{j} \int_{(o)} p_o \, dS - \vec{j} \int_{(1)} p_1 \, dS = 0 \tag{1}$$

for Δh = unity perpendicular to plane of Fig. 1

$$m_s \vec{V}_o - \int_{x_b}^{x_a} \rho_1 \, dx \, V_1^2 \cos\theta_1 = \vec{j} \int_{x_b}^{x_a} p_1 \, dx - \vec{j} \, p_o \, \Delta x \tag{2}$$

From continuity

$$m_s = \int_{x_b}^{x_a} \rho_1 \, dx \, V_1 \cos\theta_1 = \rho_o \, \Delta x \, V_o \cos\theta_o \tag{3}$$

From Fig. A1

$$\vec{V}_o = \vec{i} \, V_o \sin\theta_o + \vec{j} \, V_o \cos\theta_o \tag{4}$$

$$\vec{V}_1 = \vec{i} \, V_1 \sin\theta_1 + \vec{j} \, V_1 \cos\theta_1 \tag{5}$$

From Eqs. 2, 4, and 5

$$m_s (\vec{i} \, V_o \sin\theta_o + \vec{j} \, V_o \cos\theta_o) - \int_{x_b}^{x_a} \rho_1 \, dx \, V_1 \cos\theta_1 (\vec{i} \, V_1 \sin\theta_1 + \vec{j} \, V_1 \cos\theta_1) = \vec{j} \int_{x_b}^{x_a} p_1 \, dx - \vec{j} \, p_o \, \Delta x \tag{6}$$

From equality of $\vec{i}$ components of Eq. 6

$$m_s V_0 \sin\theta_0 = \int_{x_1}^{x_2} \rho_1 \, dx \, V_1^2 \sin\theta_1 \cos\theta_1$$

$$m_s V_0 \sin\theta_0 = \frac{1}{2} \int_{x_1}^{x_2} \rho_1 \, dx \, V_1^2 \sin(2\theta_1)$$

With Eq. 3

$$V_0 \sin\theta_0 = \frac{1}{2} \frac{\int_{x_1}^{x_2} \rho_1 V_1^2 \sin(2\theta_1) \, dx}{\int_{x_1}^{x_2} \rho_1 V_1 \cos\theta_1 \, dx} \tag{7a}$$

From equality of $\vec{j}$ components of Eq. 6

$$m_s V_0 \cos\theta_0 = \int_{x_1}^{x_2} \rho_1 \, dx \, V_1^2 \cos^2\theta_1 + \int_{x_1}^{x_2} p_1 \, dx - p_0 \, \Delta x$$

or, with Eq. 3

$$V_0 \cos\theta_0 = \frac{\int_{x_1}^{x_2} \rho_1 V_1^2 \cos^2\theta_1 \, dx + \int_{x_1}^{x_2} p_1 \, dx - p_0 \, \Delta x}{\int_{x_1}^{x_2} \rho_1 V_1 \cos\theta_1 \, dx} \tag{7b}$$

Eqs. 7b and 3 give

$$\frac{\frac{1}{\rho_0}\int_{x_e}^{x_t} \rho_1 V_1 \cos\theta_1 \, dy}{\Delta x} = \frac{\int_{x_e}^{x_t} \rho_1 V_1^2 \cos^2\theta_1 \, dy + \int_{x_e}^{x_t} p_1 \, dy - p_0 \Delta x}{\int_{x_e}^{x_t} \rho_1 V_1 \cos\theta_1 \, dy}$$

or

$$\frac{1}{\rho_0}\left[\int_{x_e}^{x_t} \rho_1 V_1 \cos\theta_1 \, dy\right]\frac{1}{\Delta x} = \int_{x_e}^{x_t} \rho_1 V_1^2 \cos^2\theta_1 \, dy + \int_{x_e}^{x_t} p_1 \, dy - p_0 \Delta x$$

Thus

$$p_0 = -\frac{1}{\rho_0}\left[\frac{1}{\Delta x}\int_{x_e}^{x_t} \rho_1 V_1 \cos\theta_1 \, dy\right]^2 + \frac{1}{\Delta x}\int_{x_e}^{x_t} \rho_1 V_1^2 \cos^2\theta_1 \, dy + \frac{1}{\Delta x}\int_{x_e}^{x_t} p_1 \, dy$$

or

$$p_0 = \frac{1}{\Delta x}\int_{x_e}^{x_t} p_1 \, dy + \frac{1}{\Delta x}\int_{x_e}^{x_t} \rho_1 V_1^2 \cos^2\theta_1 \, dy - \frac{1}{\rho_0}\left[\frac{1}{\Delta x}\int_{x_e}^{x_t} \rho_1 V_1 \cos\theta_1 \, dy\right]^2 \qquad (8)$$

From Eq. 3

$$V_0 \cos\theta_0 = \frac{1}{\rho_0 \Delta x} \int_{x_l}^{x_e} \rho_1 V_1 \cos\theta_1 \, dx \tag{9}$$

From Eqs. 7a and 9

$$\tan\theta_0 = \frac{\rho_0 \Delta x}{2} \frac{\int_{x_l}^{x_e} \rho_1 V_1^2 \sin(2\theta_1) \, dx}{\left[\int_{x_l}^{x_e} \rho_1 V_1 \cos\theta_1 \, dx\right]^2} \tag{10}$$

Since

$$V_0^2 = V_0^2 \sin^2\theta_0 + V_0^2 \cos^2\theta_0$$

From Eqs. 7a and 9

$$V_0^2 = \frac{1}{4} \frac{\left[\int_{x_l}^{x_e} \rho_1 V_1^2 \sin(2\theta_1) \, dx\right]^2}{\left[\int_{x_l}^{x_e} \rho_1 V_1 \cos\theta_1 \, dx\right]^2} + \frac{1}{\rho_0^2 \Delta x^2} \left[\int_{x_l}^{x_e} \rho_1 V_1 \cos\theta_1 \, dx\right]^2 \tag{11}$$

3. CONDITIONS FAR DOWNSTREAM OF CASCADE

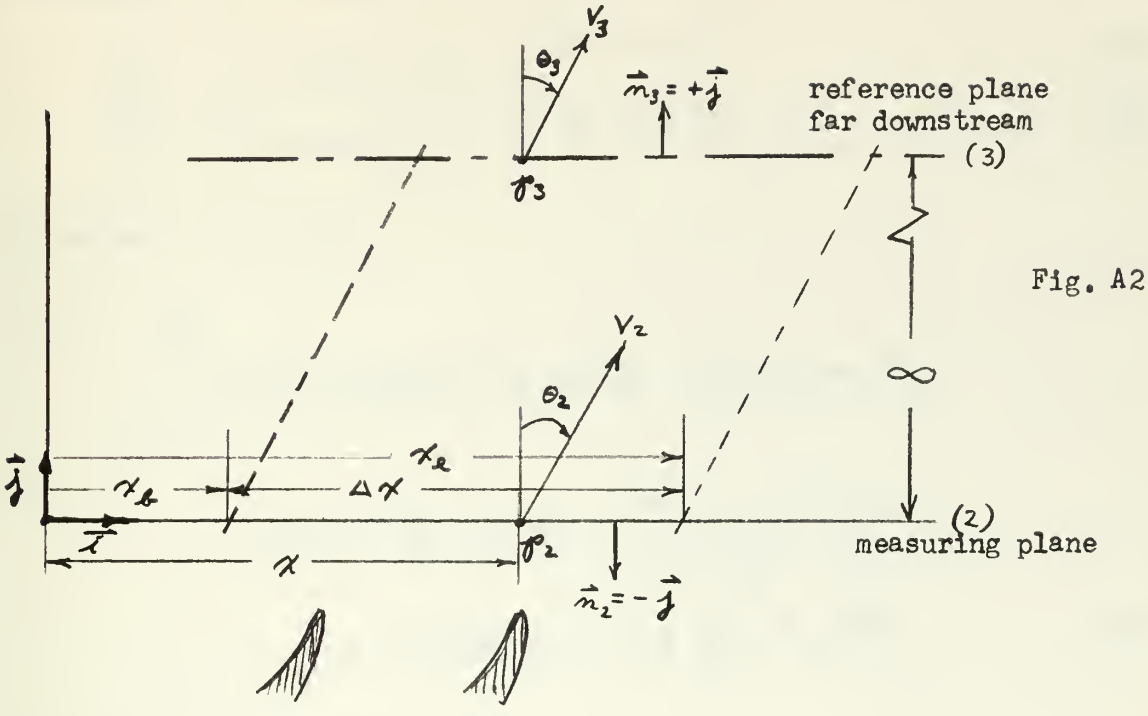

Fig. A2

From Eq. 5(21) similar to Eq. 1

$$\int_{(2)} dm_s\, V_2 - \int_{(3)} dm_s V_3 + \vec{j}\int_{(2)} p_2\, dS - \vec{j}\int_{(3)} p_3\, dS = 0$$

$$\int_{(2)} dm_s\, V_2 - m_s V_3 + \vec{j}\int_{(2)} p_2\, dx - \vec{j}\, p_3\, \Delta x = 0 \qquad (12)$$

From continuity

$$m_s = \int_{x_b}^{x_e} \rho_2 V_2 \cos\theta_2\, dx = \rho_3\, \Delta x\, V_3 \cos\theta_3 \qquad (13)$$

From Fig. A2

$$\vec{V}_2 = \vec{i}\, V_2 \sin\theta_2 + \vec{j}\, V_2 \cos\theta_2 \tag{14}$$

$$\vec{V}_3 = \vec{i}\, V_3 \sin\theta_3 + \vec{j}\, V_3 \cos\theta_3 \tag{15}$$

From Eqs. 12, 14, 15

$$\int_{x_b}^{x_e} \rho_2\, dx\, V_2 \cos\theta_2 \left(\vec{i}\, V_2 \sin\theta_2 + \vec{j}\, V_2 \cos\theta_2\right)$$

$$- m_s \left(\vec{i}\, V_3 \sin\theta_3 + \vec{j}\, V_3 \cos\theta_3\right)$$

$$= +\vec{j}\, \rho_3 \Delta x - \vec{j} \int_{x_b}^{x_e} \rho_2\, dx \tag{16}$$

For the $\vec{i}$ components of Eq. 16

$$\frac{1}{2} \int_{x_b}^{x_e} \rho_2\, V_2^2 \sin(2\theta_2)\, dx = m_s V_3 \sin\theta_3$$

With Eq. 13

$$V_3 \sin\theta_3 = \frac{1}{2} \frac{\int_{x_b}^{x_e} \rho_2 V_2^2 \sin(2\theta_2)\, dx}{\int_{x_b}^{x_e} \rho_2 V_2 \cos\theta_2\, dx} \tag{17}$$

From the $\vec{j}$ components of Eq. 16 and with Eq. 13

$$\int_{x_b}^{x_e} \rho_2 V_2^2 \cos^2\theta_2\, dx - m_s V_3 \cos\theta_3 = \rho_3 \Delta x - \int_{x_b}^{x_e} \rho_2\, dx$$

$$V_3 \cos\theta_3 = \frac{\int_{x_b}^{x_e} \rho_2 V_2^2 \cos^2\theta_2\, dx + \int_{x_b}^{x_e} \rho_2\, dx - \rho_3 \Delta x}{\int_{x_b}^{x_e} \rho_2 V_2 \cos\theta_2\, dx} \tag{18}$$

From Eq. 13

$$V_3 \cos\theta_3 = \frac{1}{\rho_3 \Delta x} \int_{x_b}^{x_e} \rho_2 V_2 \cos\theta_2 \, dx \tag{19}$$

Similar to Eq. 8

$$\rho_3 = \frac{1}{\Delta x} \int_{x_b}^{x_e} \rho_2 \, dx + \frac{1}{\Delta x} \int_{x_b}^{x_e} \rho_2 V_2^2 \cos^2\theta_2 \, dx - \frac{1}{\rho_3} \left[\frac{1}{\Delta x} \int_{x_b}^{x_e} \rho_2 V_2 \cos\theta_2 \, dx \right]^2 \tag{20}$$

Similar to Eq. 10, from Eqs. 17 and 19

$$\tan\theta_3 = \frac{\rho_3 \Delta x}{2} \frac{\int_{x_b}^{x_e} \rho_2 V_2^2 \sin(2\theta_2) \, dx}{\left[\int_{x_b}^{x_e} \rho_2 V_2 \cos\theta_2 \, dx \right]^2} \tag{21}$$

From Eqs. 17 and 19

$$V_3^2 = \frac{1}{4} \frac{\left[\int_{x_b}^{x_e} \rho_2 V_2^2 \sin(2\theta_2) \, dx \right]^2}{\left[\int_{x_b}^{x_e} \rho_2 V_2 \cos\theta_2 \, dx \right]^2} + \frac{1}{\rho_3^2 \Delta x^2} \left[\int_{x_b}^{x_e} \rho_2 V_2 \cos\theta_2 \, dx \right]^2 \tag{22}$$

4. THERMODYNAMIC RELATIONS AT MODERATE MACH NUMBERS.

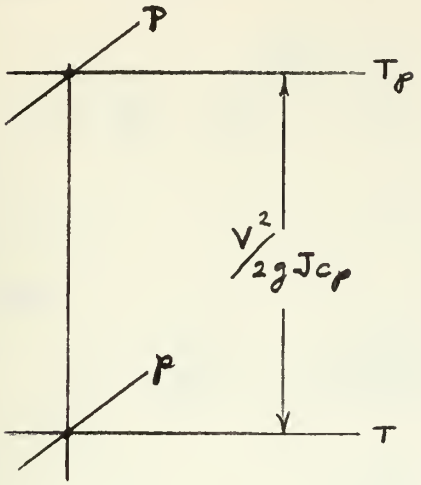

Fig. A3

P= measured total pressure (psia)

p= measured static pressure (psia)

V= actual velocity (ft./sec)

$C_p = \frac{R}{J}\frac{\gamma}{\gamma-1}$

T_p= constant total temperature

= plenum temperature ($^{\circ}R$)

T= static temperature ($^{\circ}R$)

$$\frac{V^2}{2gJc_p} = T_p - T = T_p\left[1 - \left(\frac{p}{P}\right)^{\frac{\gamma-1}{\gamma}}\right] \tag{23}$$

Let

$$\Delta P = P - p \tag{24}$$

With

$$p = P - \Delta P$$

$$V^2 = 2gR\frac{\gamma}{\gamma-1}\,T_p\left[1 - \left(1 - \frac{\Delta P}{P}\right)^{\frac{\gamma-1}{\gamma}}\right]$$

Let

$$a_p^2 = g\,R\,\gamma\,T_p = \text{velocity of sound squared in plenum}$$

Then

$$V^2 = \frac{2}{\gamma-1}\, a_p^2 \left[1 - \left(1 - \frac{\Delta P}{P}\right)^{\frac{\gamma-1}{\gamma}}\right] \tag{25}$$

With

$$(1-y)^{\frac{\gamma-1}{\gamma}} = 1 - \frac{\gamma-1}{\gamma}\, y + \left(\frac{\gamma-1}{\gamma}\right)\left(\frac{\gamma-1}{\gamma} - 1\right)\frac{y^2}{2}$$

$$= 1 - \frac{\gamma-1}{\gamma}\, y - \left(\frac{\gamma-1}{\gamma}\right)\left(\frac{1}{2\gamma}\right) y^2$$

$$= 1 - \frac{\gamma-1}{\gamma}\, y \left(1 + \frac{1}{2\gamma}\, y\right) \tag{25'}$$

Eq. 25 becomes

$$V^2 = \frac{2}{\gamma-1}\, a_p^2 \left[1 - 1 + \frac{\gamma-1}{\gamma}\,\frac{\Delta P}{P}\left(1 + \frac{1}{2\gamma}\,\frac{\Delta P}{P}\right)\right]$$

With

$$K_v = 1 + \frac{1}{2\gamma}\,\frac{\Delta P}{P} = 1 + \frac{1}{2\gamma}\,\frac{P - p}{P} \tag{26}$$

there is

$$V^2 = \frac{2}{\gamma-1}\, a_p^2 \left[\frac{\gamma-1}{\gamma}\,\frac{\Delta P}{P}\, K_v\right] = \frac{2}{\gamma}\, a_p^2\,\frac{\Delta P}{P}\, K_v$$

$$= \frac{2}{\gamma}\, a_p^2 \left(\frac{P - p}{P}\right) K_v \tag{27}$$

The density ρ_t at P, T_p is

$$\rho_t = \frac{P}{R T_p g}$$

From $pv^\gamma = \text{const}$ or $\rho \propto p^{1/\gamma}$, the density ρ at the static temperature T and the static pressure p is

$$\rho = \rho_t \left(\frac{p}{P}\right)^{1/\gamma}$$

With Eq. 24

$$\rho = \rho_t \left(\frac{P-\Delta P}{P}\right)^{1/\gamma} = \rho_t \left(1 - \frac{\Delta P}{P}\right)^{1/\gamma}$$

From

$$\begin{aligned}(1-y)^{1/\gamma} &= 1 - \frac{1}{\gamma} y + \left(\frac{1}{\gamma}\right)\left(\frac{1}{\gamma}-1\right)\frac{y^2}{2} \\ &= 1 - \frac{1}{\gamma} y - \frac{1}{\gamma}\left(\frac{\gamma-1}{2\gamma}\right) y^2 \\ &= 1 - \frac{1}{\gamma} y \left(1 + \frac{\gamma-1}{2\gamma} y\right)\end{aligned}$$

Then

$$\rho = \frac{P}{R T_p g}\left[1 - \frac{1}{\gamma}\frac{\Delta P}{P}\left(1 + \frac{\gamma-1}{2\gamma}\frac{\Delta P}{P}\right)\right]$$

$$= \frac{P}{R T_p g \gamma}\left[\gamma - \frac{\Delta P}{P}\left(1 + \frac{\gamma-1}{2\gamma}\frac{\Delta P}{P}\right)\right]$$

Let

$$K_D = 1 + \frac{\gamma-1}{2\gamma}\frac{\Delta P}{P} = 1 + \frac{\gamma-1}{2\gamma}\frac{P-p}{P} \tag{28}$$

Then

$$\rho = \frac{P}{a_p^2}\left[\gamma - \frac{P-p}{P} K_D\right] \tag{29}$$

For measured values of P and p the velocity V, corresponding to P and p is therefore obtained from Eqs. 27 and 26. The value of ρ that has to be introduced in the equations of paragraphs 2 and 3 is given by Eqs. 28 and 29. To be determined are also the densities ρ_0 and ρ_3 . They can be determined with small error with the relations

$$\rho_0 = \frac{\int_{x_1}^{x_2} \rho_1 \, dx}{\Delta x} \tag{30}$$

$$\rho_3 = \frac{\int_{x_1}^{x_2} \rho_2 \, dx}{\Delta x} \tag{31}$$

A more accurate way or check of these values could be carried out by using Eqs. 30 or 31 for the determination of, say, V_0, p_0, θ_0 and then checking Eq. 3 to see whether continuity is satisfied. This can be followed up by a method of successive approximations. A similar procedure could be used for ρ_3.

Assume now that p_0, V_0, ρ_0 and p_3, V_3, ρ_3 have been determined by the equations of paragraphs 2 and 3. To be established is now the loss

coefficient ζ of the cascade.

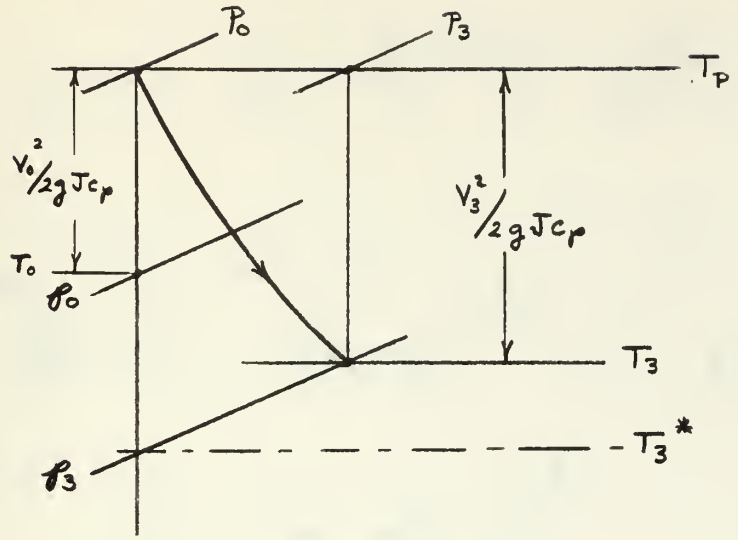

Fig. A4

By definition, for turbine cascades,

$$\zeta = \frac{T_3 - T_3^*}{T_P - T_3^*} = \frac{T_P - V_3^2/2gJc_p - T_3^*}{T_P - T_3^*}$$

or

$$\zeta = 1 - \frac{V_3^2}{2gJc_p(T_P - T_3^*)} \qquad (32)$$

There is

$$T_P - T_3^* = T_P\left[1 - \left(\frac{p_3}{P_0}\right)^{\frac{\gamma-1}{\gamma}}\right]$$

Further

$$T_p - T_0 = T_p \left[1 - \left(\frac{p_0}{p_0} \right)^{\frac{\gamma-1}{\gamma}} \right] = \frac{V_0^2}{2gJc_p}$$

hence

$$\frac{p_0}{p_0} = \left[1 - \frac{V_0^2}{2gJc_p T_p} \right]^{\frac{\gamma}{\gamma-1}} = \left[1 - \frac{V_0^2}{2g R \frac{\gamma}{\gamma-1} T_p} \right]^{\frac{\gamma}{\gamma-1}}$$

$$= \left[1 - \frac{\gamma-1}{2} \frac{V_0^2}{a_p^2} \right]^{\frac{\gamma}{\gamma-1}}$$

Thus

$$P_0 = p_0 \left[1 - \frac{\gamma-1}{2} \frac{V_0^2}{a_p^2} \right]^{-\frac{\gamma}{\gamma-1}} \tag{33}$$

With

$$(1-z)^{-\frac{\gamma}{\gamma-1}} = 1 + z\frac{\gamma}{\gamma-1} + \left(-\frac{\gamma}{\gamma-1}\right)\left(-\frac{\gamma}{\gamma-1} - 1\right)\frac{z^2}{2}$$

$$= 1 + z\frac{\gamma}{\gamma-1} + \left(\frac{\gamma}{\gamma-1}\right)\left(\frac{2\gamma-1}{\gamma-1}\right)\frac{z^2}{2}$$

$$= 1 + z\frac{\gamma}{\gamma-1}\left(1 + \frac{2\gamma-1}{2(\gamma-1)}z\right)$$

there is

$$P_0 = p_0\left[1 + \frac{\gamma-1}{2}\frac{V_0^2}{a_p^2}\frac{\gamma}{\gamma-1}\left(1 + \frac{2\gamma-1}{2(\gamma-1)}\ \frac{\gamma-1}{2}\ \frac{V_0^2}{a_p^2}\right)\right]$$

$$= p_0\left[1 + \frac{\gamma}{2}\frac{V_0^2}{a_p^2}\left(1 + \frac{2\gamma-1}{4}\ \frac{V_0^2}{a_p^2}\right)\right]$$

With

$$K_p = 1 + \frac{2\gamma-1}{4}\ \frac{V_0^2}{a_p^2} \tag{34}$$

$$P_0 = p_0\left[1 + \frac{\gamma}{2}\frac{V_0^2}{a_p^2}\ K_p\right] \tag{35}$$

Eq. 32 rewritten

$$1 - \zeta = \frac{V_3^2}{2gR\frac{\gamma}{\gamma-1}T_p\left(1 - T_3^*/T_p\right)} = \frac{\frac{\gamma-1}{2}\ \frac{V_3^2}{a_p^2}}{1 - T_3^*/T_p} \tag{36}$$

$$\frac{T_3^*}{T_p} = \left(\frac{p_3}{P_0}\right)^{\frac{\gamma-1}{\gamma}} = \left(\frac{p_3}{p_0}\ \frac{p_0}{P_0}\right)^{\frac{\gamma-1}{\gamma}} = \left(\frac{p_3}{p_0}\right)^{\frac{\gamma-1}{\gamma}}\left[\left(\frac{T_0}{T_p}\right)^{\frac{\gamma}{\gamma-1}}\right]^{\frac{\gamma-1}{\gamma}}$$

$$= \left(\frac{p_3}{p_0}\right)^{\frac{\gamma-1}{\gamma}}\frac{T_0}{T_p} = \left(\frac{p_3}{p_0}\right)^{\frac{\gamma-1}{\gamma}}\ \frac{T_p - V_0^2/2gJc_p}{T_p}$$

$$= \left(\frac{p_3}{p_0}\right)^{\frac{\gamma-1}{\gamma}}\left[1 - \frac{\gamma-1}{2}\ \frac{V_0^2}{a_p^2}\right] \tag{37}$$

Let

$$p_0 - p_3 = \Delta p_s \tag{38}$$

$$p_3 = p_0 - \Delta p_s$$

$$\frac{p_3}{p_0} = 1 - \frac{\Delta p_s}{p_0}$$

From Eq. 25

$$\left(\frac{p_3}{p_0}\right)^{\frac{\gamma-1}{\gamma}} = \left(1 - \frac{\Delta p_s}{p_0}\right)^{\frac{\gamma-1}{\gamma}} = 1 - \frac{\gamma-1}{\gamma}\,\frac{\Delta p_s}{p_0}\left(1 + \frac{1}{2\gamma}\,\frac{\Delta p_s}{p_0}\right)$$

With

$$K_s = 1 + \frac{1}{2\gamma}\,\frac{\Delta p_s}{p_0} = 1 + \frac{1}{2\gamma}\left(\frac{p_0 - p_3}{p_0}\right) \tag{39}$$

$$\left(\frac{p_3}{p_0}\right)^{\frac{\gamma-1}{\gamma}} = 1 - \frac{\gamma-1}{\gamma}\,\frac{\Delta p_s}{p_0}\,K_s = 1 - \frac{\gamma-1}{\gamma}\left(\frac{p_0 - p_3}{p_0}\right)K_s \tag{40}$$

Then, from Eqs. 36, 37, and 40

$$1 - \zeta = \frac{\frac{\gamma-1}{2}\,\frac{V_3^2}{a_p^2}}{1 - \left[1 - \frac{\gamma-1}{\gamma}\,\frac{\Delta p_s}{p_0}\,K_s\right]\left[1 - \frac{\gamma-1}{2}\,\frac{V_0^2}{a_p^2}\right]}$$

$$= \frac{\frac{\gamma-1}{2}\,\frac{V_3^2}{a_p^2}}{1 - 1 + \frac{\gamma-1}{\gamma}\,\frac{\Delta p_s}{p_0}\,K_s + \frac{\gamma-1}{2}\,\frac{V_0^2}{a_p^2} - \frac{(\gamma-1)^2}{2\gamma}\,\frac{\Delta p_s}{p_0}\,K_s\,\frac{V_0^2}{a_p^2}}$$

$$\zeta = 1 - \frac{\frac{\gamma-1}{2} V_3^2/a_p^2}{\frac{\gamma-1}{\gamma}\frac{\Delta p_s}{p_0} K_s + \frac{\gamma-1}{2}\frac{V_0^2}{a_p^2} - \frac{(\gamma-1)^2}{2\gamma}\frac{\Delta p_s}{p_0} K_s \frac{V_0^2}{a_p^2}}$$

$$= 1 - \frac{\frac{\gamma-1}{2} V_3^2/a_p^2}{\frac{\gamma-1}{\gamma}\frac{\Delta p_s}{p_0} K_s \left(1 - \frac{\gamma-1}{2}\frac{V_0^2}{a_p^2}\right) + \frac{\gamma-1}{2}\frac{V_0^2}{a_p^2}}$$

or

$$\zeta = \frac{\frac{\gamma-1}{\gamma}\frac{\Delta p_s}{p_0} K_s \left(1 - \frac{\gamma-1}{2}\frac{V_0^2}{a_p^2}\right) + \frac{\gamma-1}{2}\frac{1}{a_p^2}\left(V_0^2 - V_3^2\right)}{\frac{\gamma-1}{\gamma}\frac{\Delta p_s}{p_0} K_s \left(1 - \frac{\gamma-1}{2}\frac{V_0^2}{a_p^2}\right) + \frac{\gamma-1}{2}\frac{V_0^2}{a_p^2}}$$

or

$$\zeta = \frac{\frac{p_0 - p_3}{p_0} K_s \left(1 - \frac{\gamma-1}{2}\frac{V_0^2}{a_p^2}\right) + \frac{\gamma}{2}\frac{1}{a_p^2}\left(V_0^2 - V_3^2\right)}{\frac{p_0 - p_3}{p_0} K_s \left(1 - \frac{\gamma-1}{2}\frac{V_0^2}{a_p^2}\right) + \frac{\gamma}{2}\frac{V_0^2}{a_p^2}} \qquad (41)$$

where K_s is given by Eq. 39. It can be noted that in this expression there occur only p_0, p_3, V_0, and V_3.

5. RELATIONS FOR INCOMPRESSIBLE FLOWS

From Eqs. 26 and 27 for $K_v = 1$

$$V^2 = 2 g R T_p \left(\frac{P - p}{P}\right) = \frac{2}{\rho_t}(P - p) \qquad (42)$$

$$= \frac{2 g R T_p \gamma}{\gamma P}(P - p) = \frac{2}{\gamma} a_p^2 \frac{(P - p)}{P}$$

where

$$\rho_t = \frac{P}{g R T_p} \tag{43}$$

In this equation P is the total pressure at a station and T_p the plenum temperature.

From Eq. 28 and 29 for K_D 1, with Eq. 43

$$\rho = \frac{P}{a_\rho^2}\left[\gamma - \frac{P-\rho}{P}\right] \tag{44}$$

From Eqs. 34 and 35, with $K_p = 1$

$$P_o = \rho_o + \rho_o \frac{\gamma}{2} \frac{V_o^2}{g\gamma R T_p} = \rho_o + \frac{V_o^2}{2} \frac{\rho_o}{g R T_p}$$

It is seen that the total pressure P_o is obtained from p_o and V_o by

$$P_o = \rho_{so} \frac{V_o^2}{2} + \rho_o \tag{45}$$

where

$$\rho_{so} = \frac{\rho_o}{g R T_p} \tag{46}$$

Hence it is more accurate to take the static density ρ_{so} for the determination of the total pressure.

From Eqs. 39 and 41 for $K_s = 1$

$$\zeta = \frac{\frac{p_o - p_3}{p_o}\left(1 - \frac{\gamma-1}{2}\frac{V_o^2}{g\gamma R T_p}\right) + \frac{\gamma}{2}\frac{1}{g\gamma R T_p}\left(V_o^2 - V_3^2\right)}{\frac{p_o - p_3}{p_o}\left(1 - \frac{\gamma-1}{2}\frac{V_o^2}{g\gamma R T_p}\right) + \frac{\gamma}{2}\frac{V_o^2}{g\gamma R T_p}}$$

$$= \frac{(p_o - p_3)\left(1 - \frac{\gamma-1}{2}\frac{V_o^2}{g\gamma R T_p}\right) + \frac{p_o}{2g R T_p}\left(V_o^2 - V_3^2\right)}{(p_o - p_3)\left(1 - \frac{\gamma-1}{2}\frac{V_o^2}{g\gamma R T_p}\right) + \frac{p_o}{2g R T_p} V_o^2}$$

On page 80 it is seen that

$$\frac{T_o}{T_p} = 1 - \frac{\gamma-1}{2}\frac{V_o^2}{a_p^2} = 1 - \frac{\gamma-1}{2}\frac{V_o^2}{g\gamma R T_p}$$

Hence

$$\zeta = \frac{(p_o - p_3)\frac{T_o}{T_p} + \frac{p_o}{2g R T_p}\left(V_o^2 - V_3^2\right)}{(p_o - p_3)\frac{T_o}{T_p} + \frac{p_o}{2g R T_p}\left(V_o^2\right)}$$

With

$$\rho_0 = \frac{p_0}{g R T_0} \tag{47}$$

$$\zeta = \frac{\left(p_0 + \frac{1}{2}\rho_0 V_0^2\right) - \left(p_3 + \frac{1}{2}\rho_0 V_3^2\right)}{\left(p_0 + \frac{1}{2}\rho_0 V_0^2\right) - p_3} \tag{48}$$

Hence to be consistent the static density of Eq. 47 should be introduced here as well as in the relations of paragraphs 2 and 3.

APPENDIX B

COMPUTER PROGRAM

Introduction

Program sheets B-1 through B-6 list the computer program which was used in conjunction with the CDC 1604 computer to reduce the test data. This program utilizes Fortran 60 language for the main program and Symbolic Fortran for the subroutine.

The main program consists of two parts. The subroutine sends integers read from the punched paper tape to the first part of the main program. In this part of the program the integers are identified and stored in the proper arrays of the computer memory. The second part of the program then evaluates the input data and computes the lift, drag, and loss coefficients.

Input Procedures

Manual inputs to the punch paper tape include the run number, barometric pressure, plenum temperature, number of blade spacings surveyed, and length of blade spacing. In addition, a code is manually punched to indicate the end of the input data. A five digit number is available for manual entry. The left most digit is used as a code to identify the manual input data. The remaining four digits are available for the value of the data. The coding of the manual input data is as follows:

1 Run Number (3 digit number)

2 Barometric Pressure (in. Hg. to 0.01 in.)

3 Plenum Temperature (deg. F. to 0.1 deg.)

4 Number of Spacings Surveyed (1 digit number)

5 Length of Spacing (1 or 2 digit number)

9 End of Input Data

Manual information is punched by depressing the manual Data record button after rotating the dials of the manual control to the proper code and value. In the case where less than all four digits are required the value must be inserted to the extreme right. For example, a temperature of 66.5 degrees is inserted as 30665.

The data collected automatically by the data logging system is recorded whenever the scan button is depressed. A six digit number is used for this automatic data. The left three integers identify the information and the right three integers indicate the value of the data.

Listed below is the coding used by the data logging system to identify the automatic input data:

300 x, lower

400 y, lower

500 θ, lower

610 P, total pressure, lower

620 p, positive static pressure, lower

060 -p, negative static pressure, lower

A one in the third column indicates values for the upper traverse.

The paper tape is one inch wide and uses an eight level frame to indicate an integer. The levels are numbered from the right. The first four levels use binary to indicate a decimal integer. The values of the levels are 1, 2, 4, and 8. Punches in the first and third levels would be the integer five (1+4). The fifth and six levels are always punched. A punch in the seventh level indicates the first digit of a five digit manual input. The eighth level is used to indicate the first digit

of a six digit automatic input.

Discussion of Program

In discussing the program, the term "sequence number" will refer to the identification number in the right hand six columns of the program. The term "statement number" will refer to the assigned number in the left five columns.

Subroutine Paper starts at sequence number 002600 and continues through the end cards. This routine first determines whether the first frame it reads is that of a manual or automatic input. It sets INDIC to one if manual input or to zero if automatic input. If the seventh level is punched (manual input) the subroutine reads that frame and the next four frames. After setting INDIC to one, a return is made to statement number 1 of the main program. At the next statement INDIC is tested to determine if the data is manual input. If manual it goes to statement number 7 where the manual operations start. The code (first integer) is checked at the "Assigned Go To" statement where the value formed by the four other integers is assigned to the proper constant.

If the input is automatic the first three integers must be checked to determine which array the value is to be assigned. This value is formed with the last three integers.

After the punched tape has been completely read the main program continues at statement number 19. At this point the program must add five inches to the values of x where the counters of the data logging system recycled to zero. This is done within the two outer "DO" loops between statements 19 and 950.

Between statements 950 and 101 the values of x are adjusted so that

the first x value is set equal to zero. This is done as an aid in the plotting of the input data.

While the punch tape is being read, the values read are printed as shown in Fig. B-1. This provides a format which is easy to check with the printed paper tape of the data logging system. At sequence number 001140 the input data is again printed but this time in the proper units as shown in Tables B-I and B-II. These tables contain the actual input data used to obtain the results listed in Table II.

One restriction on the program is that the value for M must always be equal to, or greater than, the value for L. This means that more data points must be taken on the upper traverse than on the lower. This is the normal situation due to the wakes at the upper station and therefore is not a problem.

After converting the pressures into pounds per square foot and angles into radians, the program performs the required integrations starting after statement 100.

The integrals of the lower traverse are defined as follows:

$$\text{SUML1} = \int_0^1 P_1 \, d\xi$$

$$\text{SUML12} = \int_0^1 \Delta P_1 \, d\xi$$

$$\text{SUML2} = \int_0^1 p_1 \, d\xi$$

$$\text{SUML3} = 2\int_0^1 \Delta P_1 \cos^2\theta_1 \, d\xi$$

$$\text{SUML4} = \int_0^1 \sqrt{\Delta P_1 P_1 \gamma - \Delta P_1^2} \cos\theta_1 \, d\xi$$

$$SUML5 = \int_0^1 2 \, \Delta P_1 \sin 2\theta_1 \, d\xi$$

The integrals for the upper traverse are obtained by substituting U for L on the left side of the above equations and 2 for 1 on the right side.

The remainder of the program computes the lift, drag, and loss coefficients as indicated in Section 4 of this thesis. Starting at sequence number 002290 a table of results is printed as shown in Table B-III. This table is the same as Table II.

Definitions

The following symbols are followed by L to indicate lower traverse or U to indicate upper traverse:

FORTRAN SYMBOLS	DEFINITION
DELP	total pressure minus static pressure (P-p)
PS	static pressure (p)
PSN	negative values of static pressure (-p)
PSP	positive values of static pressure (+p)
PT	total pressure (P)
THETA	angle of flow (θ)
X	distance in tangential direction
Y	distance along blade height

The following symbols are followed by A to indicate station 0 and B to indicate station 3:

FORTRAN SYMBOLS	DEFINITION
PS	static pressure (p)
PT	total pressure (P)
RHO	fluid density (ρ)
THETA	angle of flow (θ)
V	velocity of fluid
VCT	product of velocity and cosine theta
VST	product of velocity and sine theta

The following symbols are used without a suffix:

FORTRAN SYMBOLS	DEFINITION
A	conversion unit, 5.2022,$(lb/ft^2)/(in\ H_2O)$
AP2	speed of sound squared, γgRT_p,(ft^2/sec^2)
B	conversion unit, $2gJc_p$,$(ft^2/{}^oR\ sec^2)$
BETAIN	angle from $\vec{i}$ to $\vec{V}_\infty$, (deg)
BN	integer number of blades, (dimensionless)
BP	barometric pressure, (in Hg)
C	test blade chord, (ft)
CD	coefficient of drag based on V_∞ and RHO, (dimensionless)
CL	coefficient of lift based on V_∞ and RHO, (dimensionless)
CD1	coefficient of drag based on V_0 and RHOA, (dimensionless)
CL1	coefficient of lift based on V_0 and RHOA, (dimensionless)

FORTRAN SYMBOLS	DEFINITION
DR	total force per test blade, (lb/ft)
DRA	axial component of total force per test blade, (lb/ft)
DRAG	drag per test blade, (lb/ft)
DRU	tangential component of total force per test blade, (lb/ft)
G	gravitational constant, (ft/sec^2)
GAMMA	ratio of specific heats, (dimensionless)
K	run number, (dimensionless)
L	number of lower data points, (dimensionless)
M	number of upper data points, (dimensionless)
R	product of gas constant and gravitational constant, ($ft^2/^oR\ sec^2$)
RHO	average of fluid density at stations 0 and 3, ($lb\ sec^2/ft^4$)
S	blade spacing, (in)
TA	ambient temperature, (^oR)
TF	ambient temperature, (^oF)
TLIFT	lift per test blade, (lb/ft)
THETAIN	angle from $\vec{j}$ to $\vec{V}_\infty$, (deg)
VA2	velocity at station 0 squared, (ft^2/sec^2)
VB2	velocity at station 3 squared, (ft^2/sec^2)
VIN	velocity at station ∞, (ft/sec)
XLO	initial lower traverse value of x, (in)
XUO	initial upper traverse value of x, (in)
ZETA	loss coefficient, (dimensionless)

```
..JOB*ROSE-GUTTORMSON     BOX 3C                                                000000
      PROGRAM CASCADE                                                          000010
      DIMENSION  XL(200), XU(200),YL(200),YU(200),THETAL(200),                 000020
     1PTL(200),PTU(200),PSPL(200),PSPU(200),PSNL(200),PSNU(200),DELPL          000030
     2(200),DELPU(200),THETAU(200),PSU(200),PSL(200),IN(6)                     000040
      L=0                                                                      000050
      M=0                                                                      000060
    1 CALL PAPER (  IN,INDIC)                                                  000070
      IF(INDIC) 7,8,7                                                          000080
    7 I1 = IN(1)                                                               000090
      NO = IN(2)*1000+IN(3)*100+IN(4)*10+IN(5)                                 000100
      PRINT 2,  IN(1), NO                                                      000110
    2 FORMAT (  I5,I20)                                                        000120
      GO TO (11,12,13,14,15,16,17,18,19),I1                                    000130
   11 K = NO                                                                   000140
      GO TO 1                                                                  000150
   12 BP = NO                                                                  000160
      BP = .01*BP                                                              000170
      GO TO 1                                                                  000180
   13 TF = NO                                                                  000190
      TF = .1 * TF                                                             000200
      GO TO 1                                                                  000210
   14 BN=IN(5)                                                                 000220
      GO TO 1                                                                  000230
   15 S =   NO                                                                 000240
      GO TO 1                                                                  000250
   16 GO TO 99                                                                 000260
   17 GO TO 99                                                                 000270
   18 GO TO 99                                                                 000280
   99 PRINT 199, IN(1) , NO                                                    000290
      GO TO 1                                                                  000300
    8 NO = IN(4)*100+IN(5)*10+IN(6)                                            000310
      PRINT 3,IN(1), IN(2), IN(3), NO                                          000320
    3 FORMAT (  3I5,I10)                                                       000330
      I1 =  IN(1)+1                                                            000340
      I2 =   IN(2)-1                                                           000350
      I3 =  IN(3)                                                              000360
      IF (  IN(1)-7) 20,1,1                                                    000370
   20 GO TO (21,22,22,23,24,25,26),I1                                          000380
   21 IF (  I2 - 6  ) 210,22,22                                                000390
  210 IF (I3) 122,121,122                                                      000400
  121 PSNL(L)=NO                                                               000410
      IF(PSNL(L)-950.)33,34,34                                                 000420
   34 PSNL(L)=0.                                                               000430
   33 PSNL(L)=-.1*PSNL(L)                                                      000440
   22 GO TO 1                                                                  000450
  122 PSNU(M)=NO                                                               000460
      IF(PSNU(M)-950.)53,54,54                                                 000470
```

```
   54 PSNU(M)=0.                                                        000480
   53 PSNU(M)=-.1*PSNU(M)                                               000490
      GO TO 1                                                           000500
   23 IF (I3) 232,231,232                                               000510
  231 L=L+1                                                             000520
      XL(L)=NO                                                          000530
      XL(L)=XL(L)*.01                                                   000540
      GO TO 1                                                           000550
  232 M=M+1                                                             000560
      XU(M)=NO                                                          000570
      XU(M)=XU(M)*.01                                                   000580
      GO TO 1                                                           000590
   24 IF (I3) 242,241,242                                               000600
  241 YL(L)=NO                                                          000610
      YL(L)=YL(L)*.01                                                   000620
      GO TO 1                                                           000630
  242 YU(M)=NO                                                          000640
      YU(M)=YU(M)*.01                                                   000650
      GO TO 1                                                           000660
   25 IF (I3)252,251,252                                                000670
  251 THETAL(L)=NO-500                                                  000680
      THETAL(L)=.2*THETAL(L)                                            000690
      GO TO 1                                                           000700
  252 THETAU(M)=NO-500                                                  000710
      THETAU(M)=.2*THETAU(M)                                            000720
      GO TO 1                                                           000730
   26 IF (I2) 262, 261,262                                              000740
  261 IF(I3) 2612, 2611,2612                                            000750
 2611 PTL(L)=NO                                                         000760
      PTL(L)=PTL(L)*.1                                                  000770
      GO TO 1                                                           000780
 2612 PTU(M)=NO                                                         000790
      PTU(M)=PTU(M)*.1                                                  000800
      GO TO 1                                                           000810
  262 IF (I3) 2622,2621,2622                                            000820
 2621 PSPL(L)=NO                                                        000830
      IF(PSPL(L)-950.)31,32,32                                          000840
   32 PSPL(L)=0.                                                        000850
   31 PSPL(L)=PSPL(L)*.1                                                000860
      GO TO 1                                                           000870
 2622 PSPU(M)=NO                                                        000880
      IF(PSPU(M)-950.)51,52,52                                          000890
   52 PSPU(M)=0.                                                        000900
   51 PSPU(M)=PSPU(M)*.1                                                000910
      GO TO 1                                                           000920
   19 CONTINUE                                                          000930
      DO 900 I = 1,L                                                    000940
      IF ( XL(I+1) - XL(I)) 42,900,900                                  000950
```

```
   42 I1 = I + 1                                                                000960
      IF (I1 - L) 43,43,900                                                     000970
   43 DO 44 KK = I1,L                                                           000980
   44 XL(KK) = XL(KK) + 5.                                                      000990
  900 CONTINUE                                                                  001000
      DO 950 I = 1,M                                                            001010
      IF ( XU(I+1) - XU(I)) 62,950,950                                          001020
   62 I1 = I + 1                                                                001030
      IF ( I1 - M) 63,63,950                                                    001040
   63 DO 64 KK = I1,M                                                           001050
   64 XU(KK) = XU(KK) + 5.                                                      001060
  950 CONTINUE                                                                  001070
      XLO = XL(1)                                                               001080
      XUO = XU(1)                                                               001090
      DO 101 I = 1,M                                                            001100
      XL(I) = XL(I) - XLO                                                       001110
      XU(I) = XU(I) - XUO                                                       001120
  101 CONTINUE                                                                  001130
      PRINT 800                                                                 001140
      PRINT 801, K, BP, TF, BN, S                                               001150
      PRINT 802                                                                 001160
      PRINT 803,(I,XL(I),YL(I),THETAL(I),PTL(I),PSPL(I),PSNL(I),I=1,L)          001170
      PRINT 804                                                                 001180
      PRINT 803,(I,XU(I),YU(I),THETAU(I),PTU(I),PSPU(I),PSNU(I),I=1,M)          001190
C     CONVERT BP(IN HG) TO LB/SQUARE FOOT                                       001200
      BP = BP*70.727                                                            001210
C     CONVERT PM(IN H2O) TO LB/SQUARE FOOT                                      001220
      A=5.2022                                                                  001230
      TA=TF + 459.69                                                            001240
      G= 32.174                                                                 001250
      B = 2. * G * 778.26 * .24                                                 001260
      R = 53.35 * G                                                             001270
      GAMMA = 1.4                                                               001280
      AP2 = GAMMA* R * TA                                                       001290
      S = S / 12.                                                               001300
      DO 100 I=1,M                                                              001310
      XL(I)=XL(I)/12.                                                           001320
      XU(I)=XU(I)/12.                                                           001330
      PTL(I)=PTL(I)*A + BP                                                      001340
      PTU(I)=PTU(I)*A + BP                                                      001350
      PSU(I)=PSPU(I)+PSNU(I)                                                    001360
      PSU(I)=PSU(I)*A + BP                                                      001370
      PSL(I)=PSPL(I)+PSNL(I)                                                    001380
      PSL(I)=PSL(I)*A + BP                                                      001390
      DELPL(I)=PTL(I)-PSL(I)                                                    001400
      DELPU(I)=PTU(I)-PSU(I)                                                    001410
      THETAL(I)=THETAL(I)/57.2958                                               001420
      THETAU(I)=THETAU(I)/57.2958                                               001430
  100 CONTINUE                                                                  001440
      LL=L-1                                                                    001450
      SUML1 = 0.0                                                               001460
```

```
      SUML12 = 0.0                                                          001470
      SUML2 = 0.0                                                           001480
      SUML3=0.0                                                             001490
      SUML4 = 0.                                                            001500
      SUML5 = 0.                                                            001510
      DO 200 I=1,LL                                                         001520
      SUML1 = SUML1 + ( PTL(I) + PTL(I+1))/2. * (XL(I+1) - XL(I))/(BN*S)    001530
      SUML12 = SUML12 + (DELPL(I) + DELPL(I+1))/2. * (XL(I+1) - XL(I))      001540
     1/(BN * S)                                                             001550
      SUML2 = SUML2 + ( PSL(I) + PSL(I+1))/2. * (XL(I+1)- XL(I))/(BN*S)     001560
      SUML3 = SUML3 + ( DELPL(I)*COSF(THETAL(I))**2+ DELPL(I+1) * COSF      001570
     1(THETAL(I+1))**2)*(XL(I+1) - XL(I))/ ( BN * S)                        001580
      DPP = SQRTF(DELPL(I) * PTL(I) * GAMMA - DELPL(I)**2)                  001590
      DPP1 = SQRTF(DELPL(I+1)* PTL(I+1)* GAMMA - DELPL(I+1)**2)             001600
      SUML4 = SUML4 + (DPP * COSF(THETAL(I)) + DPP1 * COSF(THETAL(I+1)))    001610
     1/2.* (XL(I+1) - XL(I))/(BN * S)                                       001620
      SUML5 = SUML5 + ( DELPL(I) * SINF(2. * THETAL(I))+ DELPL(I+1) *       001630
     1SINF(2. * THETAL(I+1)))* (XL(I+1) - XL(I)) / ( BN * S)                001640
  200 CONTINUE                                                              001650
      MM=M-1                                                                001660
      SUMU1=0.0                                                             001670
      SUMU12 = 0.0                                                          001680
      SUMU2=0.0                                                             001690
      SUMU3=0.0                                                             001700
      SUMU4 = 0.                                                            001710
      SUMU5 = 0.                                                            001720
      DO 300 I=1,MM                                                         001730
      SUMU1 = SUMU1 + ( PTU(I) + PTU(I+1))/2. * (XU(I+1) - XU(I))/(BN*S)    001740
      SUMU12 = SUMU12 + (DELPU(I) + DELPU(I+1))/2. * (XU(I+1) - XU(I))      001750
     1/(BN * S)                                                             001760
      SUMU2 = SUMU2 + ( PSU(I) + PSU(I+1))/2. * (XU(I+1)- XU(I))/(BN*S)     001770
      SUMU3 = SUMU3 + ( DELPU(I)*COSF(THETAU(I))**2+ DELPU(I+1) * COSF      001780
     1(THETAU(I+1))**2)*(XU(I+1) - XU(I))/ ( BN * S)                        001790
      DPP = SQRTF(DELPU(I) * PTU(I) * GAMMA - DELPU(I)**2)                  001800
      DPP1 = SQRTF(DELPU(I+1)* PTU(I+1)* GAMMA - DELPU (I+1)** 2)           001810
      SUMU4 = SUMU4 + (DPP * COSF(THETAU(I)) + DPP1 * COSF(THETAU(I+1)))    001820
     1/2.* (XU(I+1) - XU(I))/(BN * S)                                       001830
      SUMU5 = SUMU5 + ( DELPU(I) * SINF(2. * THETAU(I)) + DELPU(I+1) *      001840
     1SINF(2. * THETAU(I+1)))* (XU(I+1) - XU(I))/ ( BN * S)                 001850
  300 CONTINUE                                                              001860
      RHOA = (GAMMA * SUML1 -SUML12)/AP2                                    001870
      RHOB = (GAMMA * SUMU1 -SUMU12)/AP2                                    001880
      SL42 = 2./AP2 * SUML4 * SUML4                                         001890
      SU42 = 2./AP2 * SUMU4 * SUML4                                         001900
      PSA = SUML2 + SUML3 - SL42/RHOA                                       001910
      PSB = SUMU2 + SUMU3 - SU42/RHOB                                       001920
      VA2 = SUML5 * SUML5 / (4.* SL42) + SL42/(RHOA * RHOA)                 001930
      VB2 = SUMU5 * SUMU5 /( 4.* SU42)+ SJ42/(RHOB * RHOB)                  001940
      VA = SQRTF(VA2)                                                       001950
```

```
      VB = SQRTF(VB2)                                                          001960
      THETAA = ATANF( RHOA/2. * SUML5/ SL42)                                   001970
      THETAB = ATANF( RHOB/2. * SUMU5/ SU42)                                   001980
      VSTA = VA * SINF(THETAA)                                                 001990
      VCTA = VA * COSF(THETAA)                                                 002000
      VSTB = VB * SINF(THETAB)                                                 002010
      VCTB = VB * COSF(THETAB)                                                 002020
      VIN=SQRTF(.25*(VSTA+VSTB)*(VSTA+VSTB)+.25*(VCTA+VCTB)*(VCTA+VCTB))       002030
      THETAIN=ATANF((VSTA+VSTB)/(VCTA+VCTB))                                   002040
      BETAIN=3.14159/2.-THETAIN                                                002050
      PTA = PSA + .5 * RHOA * VA2                                              002060
      PTB = PSB + .5 * RHOA * VB2                                              002070
      DRA = S*(RHOA * VA2 *COSF(THETAA)**2-RHOB*VB2*COSF(THETAB)**2 +PSA       002080
     1-PSB)                                                                    002090
      DRU = .5 *S*(RHOA*VA2*SINF(2. *THETAA) -RHOB*VB2*SINF(2.*THETAB))        002100
      THETA=ATANF(DRA/DRU)                                                     002110
      DR=SQRTF(DRA*DRA+DRU*DRU)                                                002120
      TLIFT=DR*SINF(BETAIN-THETA)                                              002130
      DRAG=DR*COSF(BETAIN-THETA)                                               002140
      C=8.5/12.                                                                002150
      RHO = .5 *(RHOA + RHOB)                                                  002160
      CL = 2. * TLIFT / ( RHO * C * VIN * VIN )                                002170
      CD = 2. * DRAG / ( RHO * C * VIN * VIN )                                 002180
      ZETA = (PTA - PTB) / ( PTA - PSB)                                        002190
      CL1 = CL * RHO *VIN *VIN/ ( RHOA * VA2)                                  002200
      CD1 = CD * RHO *VIN *VIN/ ( RHOA * VA2)                                  002210
      THETAA=THETAA*57.3                                                       002220
      THETAB=THETAB*57.3                                                       002230
      THETAIN=THETAIN*57.3                                                     002240
      THETA=THETA*57.3                                                         002250
      BETAIN=BETAIN * 57.3                                                     002260
      BP = BP/70.727                                                           002270
C     CONVERT BP(LB/SQ FT) TO IN. HG.                                          002280
      PRINT 400, K, BP, TF                                                     002290
  400 FORMAT(1H1////////////34X18HCASCADE LABORATORY/28X30HU.S. NAVAL PO       002300
     1STGRADUATE SCHOCL///35X13HTEST RUN NO. I3,//27X18HBAROMETRIC PRES.       002310
     2 =F6.2,8H IN. HG.//29X16HAMBIENT TEMP. = F4.1,8H DEG. F.////16X2HV       002320
     305X7HTHETA 04X2HV34X7HTHETA 33X5HV INF3X9HTHETA INF2X4HBETA/13X8H(       002330
     4FT/SEC)3X5H(DEG)2X8H(FT/SEC)2X5H(DEG)3X8H(FT/SEC)3X5H(DEG)4X5H(DEG       002340
     5)//)                                                                     002350
      PRINT 401, VA,THETAA, VB, THETAB, VIN, THETAIN, BETAIN                   002360
  401 FORMAT(11X6F9.2, F8.2////)                                               002370
      PRINT 402                                                                002380
  402 FORMAT (17X5HAXIAL2X10HTANGENTIAL3X5HTOTAL/17X5HFORCE5X5HFORCE5X5H       002390
     1FORCE3X5HTHETA5X4HLIFT6X4HDRAG/16X7H(LB/FT)3X7H(LB/FT)3X7H(LB/FT)2       002400
     2X5H(DEG)4X7H(LB/FT)3X7H(LB/FT)//)                                        002410
      PRINT 403, DRA, DRU, DR, THETA, TLIFT, DRAG                              002420
  403 FORMAT(12X3F10.2, F8.2, 2F10.2////)                                      002430
      PRINT 404                                                                002440
```

```
404 FORMAT(29X28HNON-DIMENSIONAL COEFFICIENTS/29X4HLIFT8X4HDRAG8X4HLCS   002450
   1S//)                                                                 002460
    PRINT 405, CL, CD, ZETA                                              002470
405 FORMAT(22X3F12.4)                                                    002480
    PRINT 910, CL1,CD1                                                   002490
800 FORMAT (8H1RUN NO. 5X 2HBP 5X 4HTEMP 5X 2HBN 5X 1HS / )              002500
801 FORMAT ( I5, F11.2, F8.1, F7.0, F7.1)                                002510
802 FORMAT(6HOPOINT6X2HXL8X2HYL6X6HTHETAL5X3HPTL7X4HPSPL6X4HPSNL  /)     002520
803 FORMAT ( I5, 6F10.2)                                                 002530
804 FORMAT(6HOPOINT6X2HXU8X2HYU6X6HTHETAU5X3HPTU7X4HPSPU6X4HPSNU  /)     002540
910 FORMAT ( 6H1CL1 = F10.5, 5X 5HCD1 = F10.5  )                         002550
199 FORMAT (52H1UNIDENTIFIED MANUAL INPUT CODE USED IN PUNCH TAPE        002560
   1I4,I10   )                                                           002570
    STOP                                                                 002580
    END                                                                  002590
    SUBROUTINE PAPER ( IN1, INDIC)                                       002600
    DIMENSION IN1(6)                                                     002610
    RSV (ICHAR = 5, XRSAV = 1, IN = 7)                                   002620
    CON(MASK1=777777777777577B,MASK2=777777777777677B,MASK3=77777777    002630
   177777760B)                                                           002640
1A1 SIU1(XRSAV)                                                          002650
    EXF(11200B),-EXF7(11B).          SELECT PT READER                    002660
1A2 EXF7(11211B),SLJ(2ERR).          EXIT ON CHAR. MODE                  002670
    ENA(1),SAL(1A21),SAL(1A31),SAL(1A41).    ADDR. OF BUFFER WORD        002680
1A21 ENA(ICHAR+1),STA(N).            SET LAST ADDR. IN BUFF. WORD        002690
1A3 EXF1(ICHAR),-EXF7(11B).          READ IN 1ST CHAR.                   002700
    LDA(ICHAR),AJP(1A3).                                                 002710
    LDA(ICHAR).                                                          002720
    STA(IN+1),SCL(MASK1).            CLEAR ALL BUT 8 PUNCH               002730
    AJP(1A4), ENI1(4).               IF NO 8 PUNCH, GO TEST 7 PUNCH      002740
 10 INDIC = 0                                                            002750
1A31 ENA(ICHAR+5), STA(N).           READ IN 5 CHARACTERS                002760
1A5 EXF1(ICHAR),-EXF7(11B).                                              002770
    LDA(IN+1),SCL(MASK3).            CLEAR THE 5,6,7,8 PUNCHES           002780
    STA(IN+1)                                                            002790
1A6 LDA1(ICHAR),SCL(MASK3)                                               002800
    STA1(IN+2),IJP1(1A6).                                                002810
    DO 110 I = 1,6                                                       002820
110 IN1(I) = IN(I)                                                       002830
    LIU1(XRSAV)                                                          002840
  8 RETURN                                                               002850
1A4 LDA(ICHAR),SCL(MASK2).           CLEAR ALL BUT 7 PUNCH               002860
    AJP( 1A3 ).                      JUMP IF NOT 7 PUNCH                 002870
1A41 ENA(ICHAR+4),STA(N).                                                002880
  9 INDIC = 1                                                            002890
    ENI1(3), SLJ(1A5).                                                   002900
2ERR SLS(1A1 ).                      .  PAPER TAPE READER NOT CHAR. MODE 002910
    END                                                                  002920
    END                                                                  002930
```

Fig. B-1

Initial Print Out

of Input Data

```
1                                   101
2                                  2999
3                                   690
3                                   690
4                                     2
3          0        0               192
4          0        0               482
5          0        0               715
6          1        0               250
6          2        0                24
0          6        0               991
0          7        0               997
0          8        0               998
0          9        0               999
1          0        0               999
3          0        0               241
4          0        0               481
5          0        0               714
6          1        0               251
6          2        0                24
0          6        0               991
0          7        0               996
0          8        0               998
0          9        0                 0
1          0        0                 0
3          0        0               290
4          0        0               482
5          0        0               714
6          1        0               252
6          2        0                22
0          6        0               992
0          7        0               997
0          8        0               996
0          9        0               998
1          0        0               998
3          0        0               337
4          0        0               480
5          0        0               714
6          1        0               253
6          2        0                23
0          6        0               992
0          7        0               996
0          8        0               998
0          9        0               996
1          0        0               996
3          0        0               388
4          0        0               480
5          0        0               794
6          1        0               249
6          2        0                24
0          6        0               992
0          7        0               996
0          9        0               997
1          0        0               998
```

Table B-I

Input Data

Lower Traverse

RUN NO.	BP	TEMP	BN	S
100	29.98	66.5	2.	6.0

POINT	XL	YL	THETAL	PTL	PSPL	PSNL
1	.00	5.00	44.40	25.20	2.40	.00
2	.10	5.00	44.20	25.00	2.40	.00
3	.20	5.00	44.00	25.10	2.40	.00
4	.47	5.00	44.20	25.00	2.40	.00
5	.66	5.00	44.20	25.00	2.40	.00
6	.96	5.00	44.40	24.80	2.40	.00
7	1.24	5.00	44.20	24.70	2.40	.00
8	1.46	5.00	44.40	24.70	2.30	.00
9	1.71	5.00	44.00	24.80	2.20	.00
10	1.96	5.00	44.40	25.00	2.20	.00
11	2.22	5.00	44.00	25.00	2.30	.00
12	2.48	5.00	44.00	25.10	2.40	.00
13	2.74	5.00	44.20	24.90	2.40	.00
14	3.00	5.00	44.00	24.50	2.30	.00
15	3.20	5.00	41.80	24.50	2.30	.00
16	3.48	5.00	43.60	24.60	2.40	.00
17	3.72	5.00	43.60	24.90	2.30	.00
18	3.96	5.00	43.20	24.90	2.20	.00
19	4.19	5.00	42.60	25.10	2.20	.00
20	4.48	5.00	43.60	24.90	2.30	.00
21	4.68	5.00	43.60	24.80	2.40	.00
22	4.94	5.00	43.60	24.40	2.40	.00
23	5.23	5.00	43.40	24.40	2.40	.00
24	5.50	5.00	43.60	24.80	2.30	.00
25	5.72	5.00	43.20	24.80	2.30	.00
26	5.96	5.00	43.60	25.00	2.30	.00
27	6.21	5.00	43.60	25.10	2.20	.00
28	6.47	5.00	43.60	25.20	2.30	.00
29	6.75	5.00	43.60	25.00	2.40	.00
30	6.98	5.00	43.60	24.60	2.30	.00
31	7.24	5.00	44.00	24.40	2.20	.00
32	7.48	5.00	43.60	24.80	2.20	.00
33	7.72	5.00	43.60	24.80	2.20	.00
34	7.98	5.00	43.60	25.00	2.40	.00
35	8.20	5.00	43.60	25.00	2.20	.00
36	8.48	5.00	43.60	25.10	2.30	.00
37	8.72	5.00	43.20	25.00	2.30	.00
38	8.97	5.00	43.60	24.90	2.20	.00
39	9.20	5.00	43.60	24.60	2.20	.00
40	9.48	5.00	43.60	24.40	2.20	.00
41	9.70	5.00	43.40	24.60	2.20	.00
42	9.95	5.00	43.20	24.80	2.20	.00
43	10.21	5.00	43.20	24.80	2.30	.00
44	10.50	5.00	43.40	25.00	2.30	.00
45	10.66	5.00	43.60	24.80	2.40	.00
46	10.97	5.00	43.80	24.60	2.40	.00
47	11.22	5.00	43.20	24.40	2.20	.00
48	11.46	5.00	43.20	24.60	2.30	.00
49	11.73	5.00	43.20	24.80	2.20	.00
50	11.96	5.00	43.40	24.80	2.40	.00

Table B-II

Input Data

Upper Traverse

POINT	XU	YU	THETAU	PTU	PSPU	PSNU
1	.00	5.00	-44.80	24.40	.00	-2.00
2	.22	5.00	-44.80	24.30	.00	-1.70
3	.45	5.00	-44.80	24.40	.00	-2.20
4	.68	5.00	-45.00	24.40	.00	-2.50
5	.96	5.00	-45.20	24.40	.00	-2.40
6	1.22	5.00	-45.60	24.00	.00	-2.20
7	1.44	5.00	-45.60	24.20	.00	-2.30
8	1.66	5.00	-45.80	24.20	.00	-2.30
9	1.85	5.00	-46.00	24.20	.00	-2.10
10	1.96	5.00	-46.00	23.80	.00	-2.00
11	2.04	5.00	-46.00	23.50	.00	-1.90
12	2.15	5.00	-46.00	23.20	.00	-1.80
13	2.26	5.00	-46.20	22.40	.00	-1.50
14	2.34	5.00	-46.00	22.80	.00	-1.60
15	2.44	5.00	-46.20	20.50	.00	-1.40
16	2.54	5.00	-46.00	20.10	.00	-1.40
17	2.62	5.00	-46.40	18.80	.00	-1.60
18	2.73	5.00	-46.40	18.70	.00	-1.60
19	2.82	5.00	-46.60	17.80	.00	-1.40
20	2.94	5.00	-46.80	17.70	.00	-1.60
21	3.08	5.00	-47.20	17.10	.00	-1.80
22	3.20	5.00	-47.80	16.20	.00	-1.50
23	3.26	5.00	-47.80	17.00	.00	-1.60
24	3.34	5.00	-48.00	17.30	.00	-1.60
25	3.42	5.00	-48.40	17.40	.00	-1.50
26	3.57	5.00	-48.40	18.80	.00	-1.60
27	3.66	5.00	-48.80	19.10	.00	-1.70
28	3.77	5.00	-48.80	20.40	.00	-1.40
29	3.84	5.00	-48.80	21.00	.00	-1.60
30	3.95	5.00	-48.80	20.60	.00	-1.60
31	4.04	5.00	-48.80	21.20	.00	-1.20
32	4.11	5.00	-49.20	21.50	.00	-1.20
33	4.22	5.00	-48.80	22.20	.00	-1.20
34	4.30	5.00	-48.60	22.00	.00	-1.10
35	4.40	5.00	-48.40	22.20	.00	-1.00
36	4.49	5.00	-48.00	23.20	.00	-1.20
37	4.59	5.00	-47.60	22.80	.00	-1.20
38	4.68	5.00	-47.60	23.20	.00	-1.10
39	4.77	5.00	-47.20	23.30	.00	-1.10
40	4.87	5.00	-46.80	23.60	.00	-1.30
41	5.00	5.00	-46.40	23.60	.00	-1.20
42	5.09	5.00	-46.40	23.90	.00	-1.20
43	5.19	5.00	-45.80	23.80	.00	-1.30
44	5.30	5.00	-45.60	23.60	.00	-1.30
45	5.40	5.00	-45.20	24.00	.00	-1.40
46	5.47	5.00	-45.20	23.80	.00	-1.30
47	5.60	5.00	-44.80	24.20	.00	-1.40
48	5.68	5.00	-44.60	24.20	.00	-1.80
49	5.78	5.00	-44.60	23.90	.00	-1.80
50	5.90	5.00	-44.40	24.20	.00	-1.90
51	5.97	5.00	-44.40	24.30	.00	-1.60
52	6.07	5.00	-44.40	24.40	.00	-2.10

Table B-II (Continued)

53	6.29	5.00	-44.40	24.40	.00	-2.20
54	6.50	5.00	-44.60	24.00	.00	-2.40
55	6.58	5.00	-44.80	23.90	.00	-2.00
56	6.67	5.00	-44.80	24.20	.00	-2.00
57	6.78	5.00	-44.60	24.40	.00	-2.40
58	7.00	5.00	-44.80	24.50	.00	-2.30
59	7.27	5.00	-45.20	24.60	.00	-2.30
60	7.54	5.00	-45.20	24.20	.00	-2.40
61	7.58	5.00	-45.60	24.60	.00	-2.10
62	7.75	5.00	-45.60	24.20	.00	-2.00
63	8.00	5.00	-45.80	24.50	.00	-2.20
64	8.22	5.00	-45.60	23.80	.00	-1.60
65	8.30	5.00	-46.00	23.40	.00	-1.40
66	8.39	5.00	-46.00	22.60	.00	-1.50
67	8.44	5.00	-45.60	22.10	.00	-1.40
68	8.59	5.00	-45.60	21.80	.00	-1.30
69	8.70	5.00	-45.60	20.30	.00	-1.60
70	8.79	5.00	-45.80	18.90	.00	-1.50
71	8.88	5.00	-46.00	17.60	.00	-1.40
72	9.01	5.00	-46.00	16.80	.00	-1.80
73	9.10	5.00	-46.40	15.80	.00	-1.70
74	9.18	5.00	-46.40	16.10	.00	-1.60
75	9.27	5.00	-46.60	15.30	.00	-1.50
76	9.36	5.00	-47.00	15.80	.00	-1.40
77	9.44	5.00	-47.00	16.00	.00	-1.40
78	9.55	5.00	-47.40	16.20	.00	-1.40
79	9.62	5.00	-47.80	17.00	.00	-1.40
80	9.75	5.00	-48.00	16.50	.00	-1.20
81	9.84	5.00	-48.20	17.50	.00	-1.20
82	9.94	5.00	-48.40	19.20	.00	-1.00
83	10.04	5.00	-48.20	18.90	.00	-1.00
84	10.18	5.00	-48.40	20.10	.00	-1.00
85	10.27	5.00	-48.40	20.20	.00	-.70
86	10.35	5.00	-48.00	21.20	.00	-.80
87	10.44	5.00	-47.80	22.10	.00	-.60
88	10.56	5.00	-47.40	22.00	.00	-.60
89	10.66	5.00	-47.20	22.60	.00	-.60
90	10.76	5.00	-46.80	22.60	.00	-.70
91	10.82	5.00	-46.40	22.60	.00	-.50
92	10.92	5.00	-46.20	22.80	.00	-.60
93	11.02	5.00	-45.80	23.20	.00	-.60
94	11.10	5.00	-45.60	23.20	.00	-.80
95	11.20	5.00	-45.20	23.20	.00	-.70
96	11.32	5.00	-44.80	23.40	.00	-1.00
97	11.40	5.00	-44.80	23.60	.00	-.80
98	11.52	5.00	-44.40	23.40	.00	-1.00
99	11.62	5.00	-44.40	23.80	.00	-1.30
100	11.70	5.00	-44.40	23.60	.00	-1.20
101	11.80	5.00	-44.40	23.50	.00	-1.20
102	11.88	5.00	-44.00	23.80	.00	-1.40
103	11.92	5.00	-44.00	23.80	.00	-1.80

Table B-III

CASCADE LABORATORY
U.S. NAVAL POSTGRADUATE SCHOOL

TEST RUN NO. 100

BARCMETRIC PRES. = 29.98 IN. HG.

AMBIENT TEMP. = 66.5 DEG. F.

VO (FT/SEC)	THETA O (DEG)	V3 (FT/SEC)	THETA 3 (DEG)	V INF (FT/SEC)	THETA INF (DEG)	BETA (DEG)
312.49	43.63	322.32	-46.18	224.86	-2.16	92.17

AXIAL FORCE (LB/FT)	TANGENTIAL FORCE (LB/FT)	TOTAL FORCE (LB/FT)	THETA (DEG)	LIFT (LB/FT)	DRAG (LB/FT)
15.62	119.56	120.58	7.44	120.07	11.10

NON-DIMENSIONAL COEFFICIENTS

LIFT	DRAG	LOSS
2.8223	.2609	.1334